SID
SOCIETY FOR INFORMATION DISPLAY

BOOK OF ABSTRACTS

International conference "EuroDisplay 2019"

September 16–20, 2019, Minsk, Belarus

Sponsored by

SID INTEGRAL DISPLAY PROTECTING THE FUTURE IZOVAC DISPLAY CITY ELDIM

Society for Information Display (США)
Министерство образования Республики Беларусь
Учреждение образования «Белорусский государственный университет информатики и радиоэлектроники»

EURODISPLAY 2019

Сборник тезисов докладов международной конференции

(Республика Беларусь, г. Минск, 16–20 сентября 2019 года)

Book of abstracts of International Conference

(Belarus, Minsk, September 16–20, 2019)

Минск БГУИР 2019

УДК 004.51(4)
ББК 32.973.26-04
Е24

Е24 **EURODISPLAY** 2019 : тез. докл. междунар. конф. (Республика Беларусь, г. Минск, 16–20 сентября 2019 года) / редкол. : В. А. Богуш [и др.]. – Минск : БГУИР, 2019. – 102 с.
ISBN 978-985-543-531-1.

В сборник включены тезисы докладов, отобранные программным комитетом конференции.

УДК 004.51(4)
ББК 32.973.26-04

ISBN 978-985-543-531-1

PROGRAM COMMITTEE

Kristiaan Neyts, **General Chair** (Ghent, Belgium)

Dear participants to Eurodisplay 2019,
Welcome to Minsk!

I hope you are prepared for an exciting week, in which you will learn more about novel results in the field of display research and development. Researchers and engineers from Europe and from all over the world are gathering in Minsk to exchange their work and ideas.

The program committee has selected a wide variety of keynote talks, invited talks, oral presentation and posters. Due to the large numbers of presentations, we have usually two sessions in parallel. This makes it possible for you to attend the sessions with your favorite subjects. There are sessions on liquid crystals, organic LEDs, thin film transistors and display materials, but there are also sessions about micro-LEDs, augmented reality devices, and production methods.

The venue of the conference is on the right bank of the Svisloch river, a few km northwest of the city center. It is pleasant to go out onto the terrace of the Marriott and to make a small a walk in the park along the river. The organizing committee has prepared an excursion on Thursday afternoon to bring you in closer contact with the beautiful city of Minsk. The city has suffered a lot during the second world war and many historic building had to be rebuilt. Now it has become a pleasant and modern city. I hope you will be able to enjoy it.

In name of the organizing committee and the program committee, I would like to thank the people and the organizations that have contributed to setting up Eurodisplay 2019. The conference is organized by the Society for Information Display and the Belarusian State University of Informatics and Radioelectronics. In particular I would like all the sponsors for their contributions.

Thank you for your attendance to Eurodisplay 2019. May I ask you to contribute to the interactive aspect to help us make Eurodisplay 2019 a successful event? Feel free to ask questions not only after the talks or during the poster session, but throughout the conference. Feel free to contact participants and start a conversation, and to share interests and ideas.

I sincerely hope that Eurodisplay 2019 in Minks will be interesting and enjoyable, and will bring you inspiration for your future activities.

Kristiaan Neyts,
General Chair

Program Committee

François Templier (Paris, France)
Herbert De Smet (Ghent, Belgium)
Ian Sage (London, UK)
Jose Manuel Oton (Madrid, Spain)
Jyrki Kimmel (Tampere, Finland)
Norbert Fruehauf (Stuttgart, Germany)
Karlheinz Blankenbach (Pforzheim, Germany)
Uwe Vogel (Dresden, Germany)
Valeri Lapanik (Minsk, Belarus)
Victor Belayev (Moscow, Russia)
Vladimir Chigrinov (Hong Kong, China)
Wiktor Piecek (Warsaw, Poland)
Xiao Wei Sun (Shenzen, China)
Seunghyup Yoo (Daejon, Korea)

ORGANIZING COMMITTEE

Vadim Bogush, Organizing Committee Chair
D.Sc., Professor,
Rector of Education Establishment "Belarusian State University of Informatics and Radioelectronics"

Welcome to the EuroDisplay 2019!

I am very glad to welcome you at the 34th International Conference "EuroDisplay 2019" that is held in Minsk, Belarus and co-organized by the Society for Information Display and Belarusian State University of Informatics and Radioelectronics.
The program of this four-days event keeps the traditions of previous EuroDisplay Conferences (former International Display Research Conferences IDRC) in Strasbourg (1993), Birmingham (1996), Berlin (1999), Nice (2002), Edinburgh (2005), Moscow (2007), Rome (2009), Arcashon (2011), London (2013), Ghent (2015) and Berlin (2017).
At the EuroDisplay 2019 one can see the tremendous progress made in display research during the last decade in a broad range of fields ranging from basic principles and display devices to manufacturing and image quality. Looking back over the past years, nobody could forecast the dramatic changes we have seen in the availability of very advanced flat-panel displays and other modern devices for broad areas of applications. I guess that the worldwide display community has made a great job and can be proud of what it has achieved.
The Conference Program includes 6 keynote addresses, 13 invited talks, more than a hundred oral and poster presentations from all over the world. The Conference Program is structured around a number of topics with Liquid Crystal-, microLED- and OLED technologies being especially prominent.
All camera-ready submissions are published in the Conference Book of Abstracts mainly in their original form.
I especially acknowledge a very efficient contribution of the Program Committee members who carefully reviewed all proposals in a short time. Thanks to all of them, the number and quality of papers is very high. I sincerely thank also all the authors for their contributions.
The Sponsors who kindly provided the financial support for the Conference enjoy our deep appreciation.
On behalf of the Organizing Committee members, I hope you will enjoy your staying in Minsk and of course find the Conference of enormous benefit.

Many thanks for attending and have a great time!

Prof. Vadim Bogush,
Organizing Committee Chairman

Vladimir Labunov, Honorary Organizing Committee Chair
Academician of NASB,
Acting foreign member of Russian Academy of Sciencies,
D.Sc., Professor,
Head of the R&D Laboratory "Integrated micro- and nanosystems",
Education Establishment "Belarusian State University of Informatics and Radioelectronics"

Anatoly Osipov, Co-Chairman Organizing Committee
Ph.D., Associate Professor,
Member of the Belarusian Engineering Academy,
Vice-rector for R&D, Education Establishment "Belarusian State University of Informatics and Radioelectronics"

Alexander Smirnov, Co-Chairman Organizing Committee
D.Sc., Professor,
Head of the R&D Laboratory "Information display and processing units", Education Establishment "Belarusian State University of Informatics and Radioelectronics"

Organizing committee

Victor Belyaev (Moscow, Russia)
Alexander Voytenkov (Vitebsk, Belarus)
Vladimir Vysotski (Minsk, Belarus)
Victor Sorokin (Kiev, Ukraine)
Yaroslav Solovjov *(Minsk, Belarus)*
Vladimir Shiripov (Minsk, Belarus)
Vladimir Bezborodov (Minsk, Belarus)
Ludmila Shichko (Minsk, Belarus)
Valeria Makeeva (Minsk, Belarus)
Elena Bakunova (Minsk, Belarus)
Svetlana Belan (Minsk, Belarus)
Galina Ivanova (Minsk, Belarus)
Olga Atroshkina *(Minsk, Belarus)*
Andrei Stepanov (Minsk, Belarus)
Yauhen Mukha (Minsk, Belarus)

PLENARY SPEAKERS

Philippe Coni
Avionics Displays Expert, THALES AVONICS ELECTRICAL SYSTEMS SAS, Display Technologies Teacher, Institut d'Optique European Committee Chair, Society for Information Display

Short Course Title: Display in Europe

Speaker Biography
Philippe Coni graduated from ENISE in 1986 (National Engineer School of St Etienne, France), is specialized in avionics display and he works as Display Expert at the Cockpit Centre of Competence at THALES Avionics / Mérignac – France.
Since 1988, he joined THOMSON (Now THALES) and he was in charge of the development more than 20 avionics displays and system (Including RAFALE Cockpit Displays, Airbus Helicopter Cockpit Displays). He is the author of 18 international publications (SAE, IEEE, SID) in the frame of touchscreen, displays technologies and optics and he is the inventor of more than 30 patents.
He is teaching Displays technology at the Optical Institute Graduate School (Also known as Sup Optique).
He gets one Distinguished paper from the Society of Information Display (SID) in 2017. He is reviewer for the Journal of SID (JSID), and member of the technical committee of the SID.
Since 2018, he is the Chairman of the European Program Committee of the SID and member of the Executive Committee of the SID. His skill domains are Touchscreen technologies, Interaction means, Haptics displays, 3D head up displays.

Zine Bouhamri, Ph.D.
Member of the Photonics, Sensing and Display division at Yole Développement

Short Course Title: MicroLEDs and other emerging display technologies: a technology, industry and market landscape

Speaker Biography
As a technology and market analyst for the display industry, Dr. Zine Bouhamri is a member of the Photonics, Sensing and Display division at Yole Développement. Zine manages the day-to-day production of technology and market reports, as well as custom consulting projects. He is also deeply involved in business development activities for the Displays unit at Yole. Previously, Zine was in charge of numerous R&D programs at Aledia. In his time there he developed strong technical expertise as well as a detailed understanding of the display industry. Zine is the author and co-author of several papers and patents.
Dr. Bouhamri holds a degree in Electronic Engineering from the National Polytechnic Institute of Grenoble (France), one from the Politecnico di Torino (Italy), and a PhD in Radio Frequency and Optoelectronics from Grenoble University (France).

Bart Maximus, Ph.D.
Director of Technology and Innovation in the Projection Division of Barco, Member of the Society for Information Display

Short Course Title: New illumination technologies for projection applications

Speaker Biography
Bart Maximus has graduated as an engineer in electronics at the University of Ghent, Belgium, in 1991. In 1996, he achieved his PhD at the same university, on the topic of LCDs. In the same year, he started working for the company Barco as R&D manager leading project groups involved in the development of LCD, LCoS, and DLP® projectors for multiple applications.
In 2013, he became Director of Technology and Innovation in the Projection Division of Barco. The focus of his work Is mainly on finding and assessign new technologies to improve the image quality of projected images for these different applications, ranging from simulation over business projection to digital cinema. He is member of the Society for Information Display.

Michael D. McCreary, Ph.D.
Chief Innovation Officer, E Ink Corporation

Short Course Title: Reflective Electrophoretic Displays: A dramatically different technology and application space from LCDs and OLEDs

Speaker Biography
Michael McCreary is a veteran of the imaging industry with a 46 year career ranging from chemical photographic image capture, to digital CCD image capture, to digital display imaging. Dr. McCreary has been at E Ink since 2000 where he is responsible for expanding the portfolio of novel electronic paper and other related technologies. During this period of time, E Ink has grown from a modest MIT Media Laboratory spin-out startup company to a mature $500M per year corporation. He also currently serves as the Chairman of the SEMI FlexTech Governing Council.
Prior to joining E Ink in 2000, McCreary held a number of leadership positions with the Eastman Kodak Company including the development of the Kodak instant photography developer chemistry and later as General Manager of the Microelectronics Technology Division, which developed world record high performance solid-state image sensors in the 1980s and 1990s.
McCreary earned his B.S. degree in Chemistry from Principia College, a Ph.D. in Physical Organic Chemistry from the Massachusetts Institute of Technology, and completed further studies in solid state and device physics at the Rochester Institute of Technology as well as business training at the University of Pennsylvania Wharton School. Dr. McCreary is co-inventor on 92 patents worldwide.

Mingjong Jou, M.Sc.
China Star Optoelectronics Technology Co., Ltd (CSOT)

Short Course Title: Big Challenges and Great Opportunities: All in Displays

Speaker Biography

Ming-Jong Jou joined Shenzhen China Star Optoelectronics since 2014 as the R&D director for system technology development division in charging of hardware/software development and various advance display driving architecture research.

Ming-Jong Jou received the B.E. and M.E. degree in electronics engineering from National Cheng Kung University, Taiwan, R.O.C, in 2000 and 2004, respectively. In 2004, he joined AU-Optronics LTD, Taiwan, and was dedicated in image enhancement processor development and also research in electronic paper displays. He serves as technical committee member of the SID Beijing Chapter.

INVITED SPEAKERS

Prof. Hoi-Sing Kwok, Ph.D.
Hong Kong University of Science and Technology, Hong Kong
Short Course Title: Photoaligned polarizers

Prof. Xiao Wei Sun, Ph.D.
Southern University of Science and Technology, China
Short Course Title: The Color Revolution: Towards Ultra-Wide Color Gamut

Prof. Qun Yan, Ph.D.
SID China Chairman, Fuzhou University, China
Short Course Title: High Resolution Active-Matrix GaN μ-LED Micro Displays

Dr. Vitaly Bondarenko, Ph.D.
Belarusian State University of Informatics and Radioelectronics, Belarus
Short Course Title: Nanocomposits based on porous silicon: from idea to implementation

Prof. Yong-Seog Kim, Ph.D.
SID Past President
Short Course Title: Theoretical analysis of charge carrier injection and transport in OLED layers

Prof. Vladimir Chigrinov, Ph.D.
Foshan University, China
Short Course Title: Liquid Crystal Display and Photonics Devices based on Photoalignment

Prof. Karlheinz Blankenbach, Ph.D.
Pforzheim University, Germany
Short Course Title: Augmented Reality Head-up Displays: from requirements to solutions

Prof. Martin D. Dawson, Ph.D.
Institute of Photonics, University of Strathclyde, UK
Short Course Title: Gallium nitride micro-LEDs: a novel, multi-mode, high-brightness and fast response display technology

Dr. Gunter Haas, Ph.D.
Microled S.A.S., France
Short Course Title: OLED microdisplays for augmented Reality Applications

Dr. Xabier Quintana Arregui, Ph.D.
Universidad Politécnica de Madrid, Spain
Short Course Title: Liquid Crystals in Focus

Prof. Victor Belayev, Ph.D.
Moscow Region State University, Russia
Short Course Title: Photoinduced optical anisotropy (PIA) in condensed media – nature, properties, applications. 100 anniversary of Weigert effect

Dr. Chenggong Wang, Ph.D
Visionox Technology Inc., China
Short Course Title: The R&D progress and future of microLED display technology

Academician V. Labunov, D.Sc.
Belarusian State University of Informatics and Radioelectronics, Belarus
Short Course Title: Vertically oriented graphene based walls and columns obtained by ICP CVD method on moving substrates as prior stage of the roll-to-roll technology

SPONSORED BY

Society for Information Display (SID), https://www.sid.org/
Society for Information Display is comprised of the top scientists, engineers, corporate researchers, and business people of the display industry, valued at over US$100B annually. SID was formed in 1962 to promulgate display technology, and that work continues today, publishing a monthly Journal of SID, Information Display magazine, and our annual Digest of Technical Papers, which is presented at our annual spring Display Week Symposium and Exhibition. These publications are available online without additional charge for members.

Ministry of Education of the Republic of Belarus, http://edu.gov.by/en-uk/
The Republican administrative body implementing public policy in education, regulating and controlling the quality of education and coordinating the activities of other Republican administrative bodies and public organizations in this sector.

Holding "INTEGRAL", https://integral.by/en
Holding "INTEGRAL" today:
– One of the largest scientific and industrial complexes in the CIS and Eastern Europe, specializing in microelectronics.
– Complete cycle of design/development and manufacture of integrated circuits and semiconductor devices: from silicon ingots to a finished product.
– Highly skilled personnel.
According to generally accepted international classification of holding "INTEGRAL" refers to a class of IDM – because it implements a full range of activities, including design, production, marketing and maintenance of the final product by the consumer Almost all ICs produced by the Corporation as well as semiconductor devices and technologies for their manufacturing have been designed at the Belmicrosystems possessing both advanced design methods and up-to-date technological processes.
The most promising sales markets in the long term are the Russian Federation, as well as traditional foreign markets of South-East Asia (China, Korea, Singapore, Taiwan), India.
Range of holding "INTEGRAL" production totals: more than 2000 types of ICs; 500 types of semiconductor devices; 200 types of liquid crystal displays and modules; 150 electronic products.

"Display" Design office", JSC, https://kbdisplay.com/
Display" Design office", JSC is placed in Vitebsk, the Republic of Belarus. It was founded in 1987. The enterprise has been specializing in engineering and production of display devices for harsh service conditions based on LCD panels with the screens of 0.6" - 98" size. Our high-tech solutions:
– LCD matrix cutting.
– Deep LCD ruggedization by bonding of AR, EMI, ITO.
– High-performance LED-lighting (incl. multicolor).
– Operation at low temperatures (up to minus 60°C) with warm-up time from 2 up to 15 minutes.

IZOVAC Group of Companies, http://www.izovac.com/en/
Founded in 1992.
Main competence: thin-film technologies and vacuum coating systems for displays, optics, lasers, hybrid microelectronics and photovoltaics.
Main products for displays: In-line Vacuum Systems for mass-production of coatings: AR, AF, AR+AF (in one process), ITO, index match + ITO, dielectric protective, metal conductive, multicolor on glass and plastic, AR+AF multilayer on curved surfaces, etc.
Headquarter and R&D center – Minsk, Belarus.
Partnership company and manufacturing – Taiwan.

ELDIM, http://www.eldim.fr/
ELDIM is a French company located near Caen in Normandy. Since 1992, we are experts on display technologies and metrology.
The company develops and manufactures Fourier Optics viewing angle systems for visible and Near InfraRed range, video photometers, colorimeters, temporal analysis systems, turn-key inspection systems.
We are proud to provide competitive advantages to our customers, as ELDIM's products are used by most of the display manufacturers around the world. Thanks to our technical knowledges in cross technologies (Optics, software and hardware design), our engineering team develops efficient and cost-effective solutions for your inline tests.

Sponsored by

DISPLAY CITY

CONTENT

Session 1. LC materials

Chairman: Prof. Herbert De Smet

Invited I-1

Liquid crystals in focus

X.Quintana[1], Morten A.Geday[1], M.Caño-García[2], M.García De Bias[1], J.M.Otón[1]

[1]CEMDATIC, ETSI Telecomunicación, Universidad Politécnica de Madrid, Spain
[2]Department of Nanophotonics, Ultrafast Bio- and Nanophotonics Group, INL-International Iberian Nanotechnology Laboratory, Portugal

1. Introduction

Liquid Crystal (LC) lenses may be used for imaging or projection systems, in portable devices and vision correction in head-mounted devices. There are many types of LC lenses with tunable focal length, but only few have achieved practical importance, due to their small size or due to their limited focusing capability. The three most important classes of LC lenses with variable focus are lenses with curved surfaces, flat gradient index lenses and composite lenses [1]. Fresnel lenses, included in flat gradient lenses, achieve better aperture size (1-2 cm) in thin cells and fast response, but they are on-off lenses or they have a complicated multilevel electrode structures to achieve different focal power.

In this work we present a novel approach to make tunable LC Fresnel lenses, with a very simple electrode structure.

2. Liquid Cristal spiral plates (SPP): liquid crystal vortices with tunable topological charge

An optical vortex is a wavefront in which the phase of the light varies spatially with the angular position in the beam. A special case of the spiral phase plate is the integer spiral phase plate, where the phase retardation variation per revolution about the beam centre is an integer number, l, times 2π. l is the so-called topological charge (Figure 1). Integer spiral phase plates converts planar light waves into continuous helical wavefronts with a singular point in the middle, where no light can exist. The power distribution around the singular point depends on the topological charge.

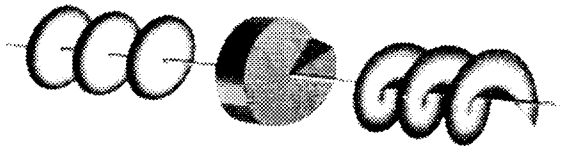

Figure 1: Generation of helical beam shape

One way to generate a LC vortex is alluringly simple. A device with electrodes cut in forms of portions of cheese can be used to generate a tunable topological charge device [2]. The device only has electrical contacts in the periphery.

3. The trick: Combining SPP and Fresnel lens

Adding the phase change introduced by an SPP to the phase change introduced by a Fresnel lens and removing the constant phase change in all the area (phase wrapping) we obtain a spiral fresnel lens with a singularity in the middle. This can be made tunable with LCs, and still the connection diagram is very easy, because all contacts are in the periphery (Figure 2).

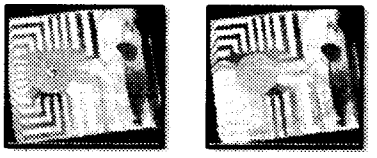

Figure 2: Tunable LC lenses with topologies 1 & 2

4. Conclusions

In this work we present inch-sized tunable LC Fresnel lenses with a simple electrical driving and easy manufacture. Lenses and driving electronics have been fabricated and lenses have been characterized for imaging. Future works will remove the topological charge and polarization dependence.

5. Acknowledgements

Authors are indebted for financial help received from the "Programa RETOS" from the Ministerio de Economía y Competitividad (TEC2016-77242-C3-2-R), the "Programa Regional de I+D SINFOTON 2" from the Comunidad de Madrid and European Structural funds (P2018/NMT-4326 SINFOTON2-CM) (FEDER) and to ATTRACT Program (European Union's Horizon 2020 programme). Manuel Caño García wants to express his gratitude to the Ministerio de Economía y Competitividad for his postdoctoral grant (FPI (POP) research fellowship Ref. BES-2014-070964) & postdoctoral research fellow program NanoTRAINforGrowth II (MSCA-COFUND H2020 framework).

6. References

[1] Yi-Hsin Lin, Yu-Jen Wang, Victor Reshetnyak "Liquid crystal lenses with tunable focal length", Liquid Crystals Reviews, 5:2, 111-143, (2017) DOI: 10.1080/21680396.2018.1440256

[2] M. Caño-García, X. Quintana, J.M. Otón, M.A. Geday; "Dynamic Multilevel Spiral Phase Plate Generator" Sci. Reports 8, 15804 (2018). doi: 10.1038/s41598-018-34041-2

Bistable switching of a polymer-walled liquid crystal phase grating cell

Su-Min Do, Tae-Hoon Choi, Byoung-Gyu Jeon, Tae-Hoon Yoon
Department of Electronics Engineering, Pusan National University, Korea

Abstract

We report bistable switching of a liquid crystal (LC) phase grating cell. Polymer walls are formed in an LC cell by phase separation of an LC mixture, induced by the spatial difference of the elastic energy and electric field intensity. Bistable switching of a polymer-walled liquid crystal phase grating cell could be realized by applying vertical and in-plane electric fields.

1. Introduction

Recently, liquid crystal (LC) light shutters have been studied extensively for smart window and see-through display applications. By controlling the haze value [1,2], LC light shutter can be switched between the transparent and translucent states. However, they suffer from a serious issue with the power consumption. These devices require continuous supply of power to maintain either the transparent or translucent states. To reduce the power consumption, bistable operation of a light shutter, which consumes power only when it is being switched between the states, is essential.

In this paper, we report bistable switching of a phase grating cell. Polymer walls are formed in an LC cell by phase separation of an LC mixture, induced by the spatial difference of the elastic energy and electric field intensity. We believe that this device could be a potential candidate for power-saving smart window or window display applications.

2. Operating Principle

To switch the state by applying an in-plane or vertical electric field, we formed interdigitated electrodes separated from the common electrode by an insulating layer on the top and bottom substrates. The two interdigitated electrodes are positioned at right angles to each other. When an in-plane electric field is applied to a vertically-aligned LC/reactive mesogen mixture, a large spatial elastic energy is induced along the direction perpendicular to the interdigitated electrodes on each substrate [3]. We formed polymer walls in the LC cell through ultraviolet irradiation while applying an in-plane electric field. When a vertical electric field applied to a polymer-walled liquid crystal (PWLC) phase grating cell is removed, LC molecules remain vertically-aligned due to vertical anchoring. On the other hand, when an in-plane electric field is removed, LC molecules remain homogeneously-aligned due to in-plane anchoring between the LC and polymer structure.

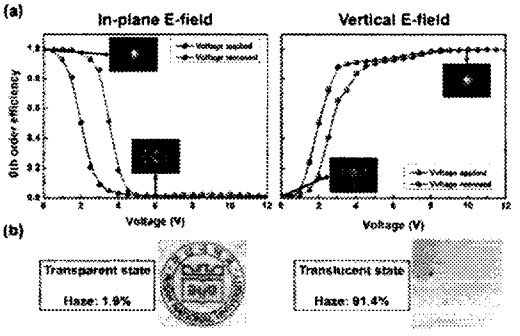

Figure 1: Zeroth-order diffraction efficiency(a) and images of the fabricated PWLC phase grating cell (b)

3. Experimental Results

The diffracted light intensity can be controlled by applying in-plane and vertical electric fields. Owing to the vertical alignment layer and polymer walls, the cell can maintain its state after the applied field is removed, as shown in Fig. 1(a). We have shown that 98.4% of the incident light can be transferred from the zeroth to higher orders. Owing to the high diffraction efficiency, the fabricated LC cell can provide a high-haze (~91.4 %) translucent state under a low in-plane voltage of 6 V and a low-haze (~1.9%) transparent state under a vertical voltage of 10 V, as shown in Fig. 1(b).

4. Acknowledgments

This work was supported by National Research Foundation of Korea (NRF) grant funded by the Korean government (MSIP). (No. 2017R1A2A1A05001067).

5. References

[1] T.-H. Choi, J.-H Woo, J.-M. Baek, Y. Choi, and T.-H. Yoon, "Fast control of haze value using electrically switchable diffraction in a fringe-field switching liquid crystal device," IEEE Trans. Electron Dev. **64**, p. 3213, 2017.

[2] J.-W. Huh, J.-H. Kim, S.-W. Oh, S.-M. Ji, and T.-H. Yoon, "Ion-doped liquid-crystal cell with low opaque-state specular transmittance based on electro-hydrodynamic effect," Dyes Pigments **150**, p. 16, 2018.

[3] D. Voloschenko, O. P. Pishnyak, S. V. Shiyanovskii, and O. D. Lavrentovich, "Effect of director distortions on morphologies of phase separation in liquid crystals," Phys. Rev. E **65**, p. 060701, 2002.

O-2

Synthesis of bent-core azobenzene oligosiloxane end-groups induces to polar order in liquid crystalline phases by achiral molecules

M.L.Rahman[1], S.E.Arsad[1], S.Sarjadi[1], S.Kumar[2], C,Tschierske[3]
[1]Universiti Malaysia Sabah, Kota Kinabalu, Sabah, Malaysia
[2]Raman Research Institute, Bangalore, India
[3]Martin-Luther-University Halle, Germany

1. Introduction

Anisotropic materials having potential applications in display and other devices, liquid crystals (LC) research has made significant progress during the last few decades [1]. Owing to the attractive electro-optic switching characteristics, banana-shaped LCs has been attracted to the scientific attention enormously [2]. The relationship between their molecular structure and their mesomorphic properties is one of the highly investigated research topics for bent core LCs. The polar order of these molecules, owing to their bent shape, displays interesting properties such as ferroelectric or anti-ferroelectric switching [3]. The occurrence of superstructural chirality in the mesophase of bent-core compounds without having any chiral moiety in the molecules is not only of fundamental scientific interest but also of industrial application as this chirality can be switched in external electric fields. In this study, a new series of bent-core liquid crystals with oligosiloxane end-groups were synthesized and characterized.

2. Results and discussion

A bent-core liquid crystalline monomers incorporating resorcinol is the central unit linked to the azobenzene as the side arms with terminal double bonds as polymerizable functional groups, were synthesized and characterized by POM, DSC, XRD and UV-vis spectroscopy. Bent-core compounds, 4a consist of even of carbons and 4b conatins odd number of carbons in each terminal group exhibited intercalated smectic (B6) phases while compounds 4c-f of the same series showed rectangular columnar (B1) phases (top of Fig. 1). A series of bent- core, oligosiloxane units and alkyl segments were derived from these monomers molecules, and the self-organization of these molecules was investigated (bottom of Fig. 1). In this case lower alkyl homologues showed B6 phase and higher alkyl homologues are organized into polar smectic liquid crystalline phases. With increasing length of the alkyl chains, segregation is lost and a transition from smectic to a columnar phase is found. In the columnar phase, the switching process is antiferroelectric and takes place by rotation of the molecules around the long axes, which is switched into a homogeneous chiral structure upon application of an electric field. Hence, it was observed that the some combination of microsegregation with the special packing properties of the bent cores enables the design of new complex soft matter systems with switchable polar order.

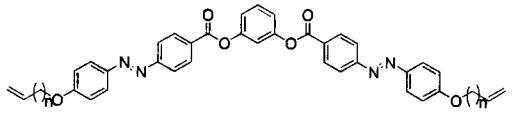

4a: n=2; **4b**: n=3; **4c**: n=4; **4d**: n=5; **4e**: n=6; **4f**: n=8

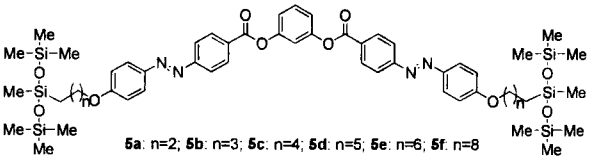

5a: n=2; **5b**: n=3; **5c**: n=4; **5d**: n=5; **5e**: n=6; **5f**: n=8

Figure 1: A series of bent-core azobenzene containing oligosiloxane end-groups

3. Acknowledgements

This research work was supported by the Universiti Malaysia Sabah (SGI0061-2018).

4. References

[1] M. R. Lutfor, G. Hegde, M. Y. Mashitah, M. A. Fazli, H. T. Srinivasa, K. Sandeep, "New pyrimidine-based photo-switchable bent-core liquid crystals", N. J. Chem., Vol. **37**, pp. 2460-2467, 2013.

[2] G. Shanker, P. Mark, C. Tschierske, "Laterally connected bent-core dimers and bent-core-rod couples with nematic liquid crystalline phases", J. Mater, Chem., Vol. **22**, pp. 168-174, 2012.

[3] M. Mathews, S. Z. Rafael, D. K. Yang, Q. Li, "Thermally, photochemically and electrically switchable reflection colors from self-organized chiral bent-core liquid crystals", J. Mater. Chem., Vol. **21**, pp. 2098-2103, 2011.

Peculiarities of mechanical and dielectric properties of a photoswitchable cybotatic-type nematic

M.Kurachkina[1], A.Eremin[1], M.Alaasar[2], C.Tschierske[2], P.Salamon[3]

[1]Department of Nonlinear Phenomena, Institute for Experimental Physics, Otto von Guericke University Magdeburg, Germany

[2]Martin Luther University Halle-Wittenberg, Germany

[3]Institute for Solid State Physics and Optics, Wigner Research Centre for Physics, Hungarian Academy of Sciences, Hungary

1. Introduction

Recently the liquid crystal displays (LCDs) technology, the main consumer of liquid crystalline materials, is constantly looking for new compounds with special physical properties. The discovery of novel types of mesogenic material, the so-called banana-shaped liquid crystals or bent-core liquid crystals (BCLCs), opened new possibilities in the field of liquid crystals. These newly discovered BCLCs materials exhibit polar order and chiral superstructures in their mesophases, although the molecules themselves are not chiral. Since then, a vast number of BCLCs exhibiting a great variety of interesting liquid crystalline phases have been synthesised and investigated. The presence of azo groups in bent-core mesogens structures allow to use reversible trans–cis isomerisation upon photoirradiation [1, 2]. Initially, these materials were considered to be of no use in LCDs industry because of their photosensitive nature. But today, the same phenomenon is the basis of their new applications. The combination of photosensitivity and liquid crystalline properties in the same molecule allows the material to be exploited for different applications in photonics such as optical data storage, photochemical molecular switches, polarisation holography, sensors and nonlinear optics.

2. Results and discussion

In this work, we demonstrate reversible photomanipulation of the elastic constants in azobenzene-containing bent-core liquid crystal incorporating 4-cyanoresorcinol as the central core unit. In addition to the columnar phase, the liquid crystal exhibits the nematic phase with unusually large splay elastic constant and low bent elastic constant. The nematic and columnar phases were studied by dielectric spectroscopy in the frequency range 10 Hz–10 MHz in cells with planar and homeotropic alignment. Using electro-optic and dielectric studies, we show the presence of the sign inversion of dielectric anisotropy. The SHG activity both in cybotactic nematic and in isotopic phases near clearing point was detected. We show reversible photomanipulation of the mechanical properties where the splay elastic constant decreases five-fold under the action of UV. The effect of UV is readily seen on the rheological properties of the liquid crystal. This behaviour cannot be explained by steric considerations only, and presumably results from the clustering.

3. Conclusion

The results of the investigation of the asymmetric bent-core liquid crystalline materials containing 4-cyanoresorcinol as the central core unit and azobenzene-based wings showed the linear changes of relaxation processes in nematic phase and columnar phase, demonstrating the high-frequency and low-frequency process with an activation energy of about 0.44 eV and 0.49 eV respectively. In cybotactic nematic an activation energy was almost twice smaller. It is related to changes and reorganization in the LC structure after N_{CybC}/Col_{rec} transition. We also observed the sign inversion of dielectric anisotropy in nematic phase explained by the formation of cybotactic nanoclusters and the presence of conformers that are allowed by flexible core of bent-core. The elastic anomaly $K_{33}<<K_{11}$, characteristic to bent-core mesogens, could be used in applications where low elastic constants are required. The presence of azobenzene wings in the mesogens under study makes it possible to manipulate the elastic properties by UV light. Besides fundamental studies of the phase structures reported herein, the trans-cis photoisomerization of the azobenzene wings provides additional possibilities and leads to interesting perspectives for the modification of the phase structure, polar order and chirality with these new bent-core mesogens by interaction with circular polarized light.

4. Acknowledgements

The authors acknowledge the support by the Deutsche Forschungsgemeinschaft (Projects ER 467/8-2 and TS 39/24-2).

5. References

[1] Rahman L., Kumar S., Tschierske C., Israel G. Synthesis and photoswitching properties of bent-shaped liquid crystals containing azobenzene monomers. Liquid Crystals, 36(4), 397-407, 2009

[2] M. Alaasar. Azobenzene-containing bent-core liquid crystals: an overview. Liquid Crystals, 43, 2208-2243, 2016

Polarization characteristics of light passed through a cholesteric layer with tangential-conical boundary conditions

V.S. Sutormin[1,2], M.N. Krakhalev[1,2], I.V. Timofeev[1,2], R.G. Bikbaev[1,2], O.O. Prishchepa[1,2], V.Ya. Zyryanov[1]
[1]Kirensky Institute of Physics, Federal Research Center KSC SB RAS, Krasnoyarsk, Russia,
[2]Siberian Federal University, Krasnoyarsk, Russia

1. Introduction

Liquid crystals (LCs) are the unique functional materials owing to their high sensitivity to the external factors. In practical applications, the LC is in contact with the confining surface, which interaction with LC molecules specifies the director orientation at the interface and, consequently, the director orientation in the bulk. Nowadays, the rigid surface anchoring is widely used. In this case, the director orientation is not changed at the interface during the reorientation process of LC in the bulk induced by the external factors. We consider the LC cells with one of the substrates specifying the conical surface anchoring. The conical surface anchoring is characterized by the tilted orientation of director to the substrate and azimuthal degeneration [1], i.e., the azimuthal anchoring strength of LC with the substrate is near to zero. The present work is devoted to the investigation of the polarization characteristics of light passed through the cholesteric layer with tangential-conical boundary conditions.

2. Materials and Methods

The experiment was carried out with sandwich-like cells consisting of two glass substrates coated with polymer films and the cholesteric layer between them. Bottom substrate was covered by the polyvinyl alcohol (PVA) and the top one was covered by the poly(isobutyl methacrylate) (PiBMA). The PVA film was unidirectionally rubbed while the PiBMA film was not treated after the deposition process. The nematic mixture LN-396 (Belarusian State Technological University) doped with the left-handed chiral additive cholesterylacetate was used as a cholesteric liquid crystal (CLC). For the nematic mixture LN-396 the PiBMA film specifies the conical boundary conditions with the tilt angle 50° and PVA film specifies the tangential surface anchoring. The polarization of light passed through the CLC cell was studied by measuring the azimuth of polarization ψ and ellipticity angle χ. The azimuth of polarization is an angle between the major semiaxis of the polarization ellipse and the *x*-axis. The *x*-axis coincided with rubbing direction of PVA film. The ellipticity angle is an arctangent of the ratio between minor and major semiaxes of the polarization ellipse. The measurement of ellipsometric parameters was conducted using the electrooptic setup in which the He-Ne laser beam passed in sequence through the polarizer, CLC cell, quarter-wave plate, analyzer and was detected by a photodetector.

3. Results and Discussion

The orientation structure with simultaneous tilt and twist of the director was formed in the CLC cells with tangential-conical boundary conditions [2]. The dependences of ellipsometric parameters ψ and χ on the voltage applied to the CLC cell was investigated for the samples with different ratios between CLC layer thickness *d* and cholesteric pitch *p*. Figure 1 shows the parameters ψ and χ of light passed through the CLC cell with ratio $d/p = 0.28$. The incident light was linearly polarized with ellipsometric parameters $\psi_0 = 90°$ и $\chi_0 = 0°$. In the absence of an electric field, the linearly polarized light passed through CLC cell became elliptically polarized with $\psi = 16.5°$ and $\chi = -17°$. The ellipsometric parameters remained almost invariable until U = 0.3 V. In the range of control voltages from 0.3 to 3 V the nonmonotonic changes of ψ and χ were observed.

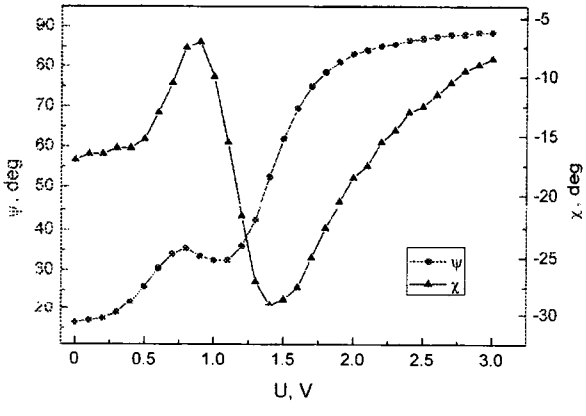

Figure 1: The dependences of ellipsometric parameters y and c on the control voltage *U*. LC layer thickness is *d* = 5.9 mm. The ratio *d/p* is 0.28

4. Acknowledgements

This work was supported by the Russian Science Foundation (No. 18-72-10036).

5. References

[1] B. Jerome "Surface effects and anchoring in liquid crystals" Rep. Prog. Phys., Vol. **54**. pp. 391-451, 1991.

[2] M.N. Krakhalev, R.G. Bikbaev, V.S. Sutormin, I.V. Timofeev, V.Ya. Zyryanov "Nematic and cholesteric liquid crystal structures in cells with tangential-conical boundary conditions", Crystals, Vol. **9**. pp. 249, 2019.

Photo-induced hole dipoles' mechanism of liquid crystal photoalignment

A.Muravsky, A.Murauski, I.Kukhta
Institute of Chemistry of New Materials NAS Belarus, Belarus

Abstract
We explain the observations and show the existence of the new photoalignment mechanism based on photo-induced dipole moments in azo-dye layer. Strong azimuthal anchoring energy >2x10^{-4} J/m^2 is obtained within <0.5 J/cm^2 exposure dose.

1. Introduction

Polarized light absorption in photoalignment material layer induces anisotropic long-range interactions that orient liquid crystals [1]. The main known physical mechanisms standing behind anisotropic interaction nature are photo cross-linking and photo destruction of polymers; photo cis-trans isomerization of azo-dyes. The photo isomerization is reduced to photo rotation, when cis-form cannot be registered due to short life-time. Recent study of AtA-2 azo-dye azimuthal anchoring as the function of exposure dose [3] has revealed the presence of unusual strong anchoring energy peak at low exposure doses (Fig.1), which is outside understanding of the known mechanisms.

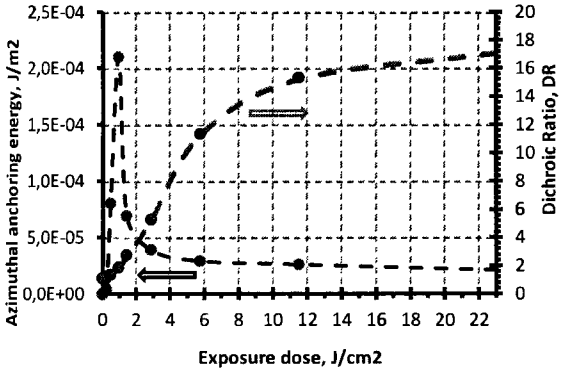

Figure 1: Azimuthal anchoring energy & dichroic ratio of 70 nm ATA-2 dye layer vs. exposure dose

2. Intermolecular bonding

We investigated the AtA-2 azo-dye (Fig.2) in the solid film; and the role of reversible intermolecular bonding between the dye molecules with strong perpendicular dipole moment of ~16D.

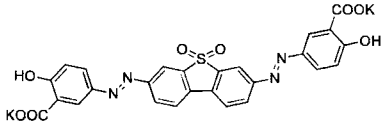

Figure 2: AtA-2 azo-dye structure

The intermolecular bonding of AtA-2 dye is a number of O...K-O coordination bonds that prevent neighbouring molecules from thermal rotation movement in solid film. The bonds energy is the next: $E_{KT} < E_{bonds} < E_{h\nu}$. Thus absorbed photon brings enough energy to break the bonding and change orientation of the absorbed molecule.

3 Self-consistency and the mean field

Upon wet deposition of the dye film all dye molecules are consistent to the mean field having the dipole moments of the dyes compensated by the field. Once the solvent is removed, intermolecular bonds lock translation and rotation movement of the dye molecules. Thus the change of orientation of the single molecule having absorbed the photon keeps the local dipole moment of the mean field unchanged – the hole dipole μ_{AL}, while the magnitude of the hole dipole moment equals to the dipole moment of the AtA-2 dye molecule.

4 Alignment layer anchoring energy

In case of the flat surface the anchoring energy W between the alignment layer and the liquid crystal is proportional to the square of dipole moment $(\mu_{LC})^2$ and the order parameter P_{2LC} of liquid crystal, as well as the square of dipole moment $(\mu_{AL})^2$ and the order parameter P_{2AL} of alignment layer [3]: $W \sim (\mu_{LC}\mu_{AL})^2 P_{2LC} P_{2AL}$.

5 Photo-induced hole dipoles

Exposure of AtA-2 layer with linear polarized light induces selective photon absorption by dye molecules primary oriented along the polarization of light. Thus the order parameter of the hole dipoles formed by the mean field at the location of the absorbed molecule of the alignment layer is close to one, P_{2AL}~1. At the same time dye molecule is not restricted to change its orientation to any direction, thus the order parameter of dye molecules that underwent single photon absorption is close to zero.

The photo-induction of hole dipoles is the new photoalignment mechanism observed for azo-dye molecules with reversible intermolecular bonding.

6. Acknowledgements

Research grant BRFFI-NFENK F18KI-025 is acknowledged for financial support.

7. References

[1] V.G. Chigrinov. V.M. Kozenkov and H.S. Kwok, *Photoalignment of Liquid Crystalline Materials: Physics and Applications,* Wiley, Chichester, 2008.

[2] A.A. Muravsky, V.S. Mikulich, A.A. Murauski, V.S. Bezruchenko, SID Int. Symp. Dig. Tech. Pap. **45**,p.1602, 2015

[3] A. Murauski, *Surface and liquid crystal interlayer interactions: characterizations and applications,* VDM Verlag, 2009.

O-6

In-plane switching deformed helix ferroelectric liquid crystal display cell

I.N. Kompanets, E.P. Pozhidaev, T.P. Tkachenko, A.V. Kuznetsov
P.N. Lebedev Physical Institute (LPI), Moscow, RAS, Russia

As it is well known the principal advantages of in-plane switching (IPS) liquid crystal display cells is the color accuracy due to the small gamma and color shifts, and since the director lies in the substrates plane, the viewing angle is large and symmetric. Together with this, the production of IPS-displays based on nematic liquid crystals is associated with the solution of rather complex technological problems caused by the need to form a grid of interdigitated electrodes.

In this message, we draw attention for the first time to the fact that the IPS electro-optical switching is a natural and inherent feature of a conventional planar-oriented display cell based on the deformed helix ferroelectric liquid crystal effect [1] (DHFLC-effect). In such a cell with continuous (and not interdigital) electrodes, the main optical axis is deflected in the plane of the substrates under the electric field E action [2]. Measured dependence of light transmittance T(E) and calculations results can be argued that in DHFLC cell there is the IPS electro-optical mode. IPS switching operates in kilohertz frequency range providing contrast ratio more than 200:1 in monochromatic light.

The paper will consider possible applications of the effect under consideration in display and photonic devices.

This work is supported by the Russia Ministry of Science & Higher Education, the unique project identifier RFMEFI60417X0191.

References

[1] L. A. Beresnev at all, *Liquid Crystals*, **5**, °N4, 1171-1177, (1989).

[2] E. P. Pozhidaev at all, *Liquid Crystals*, **37**, °N8, 1067 – 1081, (2010).

Design of a dye-doped liquid crystal cell with a constant transmittance-difference contour map

Seung-Min Nam[1], Seung-Won Oh[1], Sang-Hyeok Kim[1], Jae-Won Huh[1], Eunjung Lim[2], Jinhong Kim[2], Tae-Hoon Yoon[1]

[1]Department of Electronics Engineering, Pusan National University, Busan 46241, Korea
[2]LG Chem., R&D Campus Daejeon, Daejeon, 34122, Korea

Abstract
Thus far, the trial-and-error method has been used to find the condition for a dye-doped liquid crystal cell with desired performances. In this paper, we report a systematic design process to find the condition for the desired performances without trial-and-error process.

1. Introduction

Transmittance-control devices can be switched between the transparent and opaque states by controlling the light absorption. These devices are used as smart windows in architectural glazing, switchable sunglasses, and automotive applications [1,2]. Dye-doped liquid crystal (DDLC) devices can be used for fast transmittance control because they have a fast response time of several tens of milliseconds. DDLC devices require a high transmittance difference between its transparent and opaque states while satisfying the desired performance, such as the transmittance in the transparent state, driving voltage, and response time

In this study, we introduce a systematic approach to find the condition for the desired performance in a DDLC device. By excluding the conditions that cannot satisfy the desired performance within constant transmittance-difference contour map, we can easily obtain the condition for the desired performance in a DDLC cell without any trial-and-error process.

2. Design and fabrication process

We calculated the transmittance difference as we varied the cell gap and dye concentration [3]. To find the condition for the maximum transmittance-difference while satisfying the desired performance, we plotted the constant transmittance-difference contour map on the parameter space of the cell gap and dye concentration. By using the calculated constant transmittance-difference contour map, we can easily design a DDLC cell with the desired performance. As shown in Fig. 1, the design process is as follows: i) choose an appropriate liquid crystal (LC) mode for a specific application ii) exclude the condition that cannot satisfy the minimum transmittance in the transparent state. iii) determine the maximum cell gap considering the response time or driving voltage and the maximum dye concentration, considering the saturation concentration of the dye to be mixed with the used LC. iv) select the condition for the maximum transmittance difference [4].

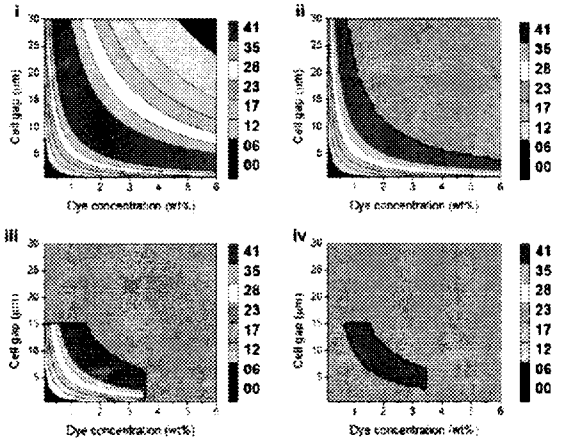

Figure 1: The design process of a dye-doped cholesteric LC cell on a constant transmittance-difference contour map on the parameter space of the cell gap and dye concentration

3. Conclusion

We confirmed experimentally that the design of a GHLC cell with the desired performance could be achieved through the proposed design process. We expect that the proposed design process will offer an effective method for the fabrication of a DDLC cell.

4. Acknowledgements

This work was supported by the National Research Foundation of Korea (NRF) grant funded by the Korea government (MSIP) (No. 2017R1A2A1A05001067).

5. References

[1] C. G. Granqvist, "Oxide electrochromics: an introduction to devices and materials," Sol. Energy Mater. Sol. Cells **99**, pp. 1-13, 2012.

[2] S.-W. Oh, J.-M. Baek, J. Heo, and T.-H. Yoon, "Dye-doped cholesteric liquid crystal light shutter with a polymer-dispersed liquid crystal film," Dyes Pig. **134**, pp.36-40, 2016.

[3] D. F. Swinehart, "The beer-lambert law," J. Chem. Educ. **39**, pp. 333-335, 1962.

[4] S.-M. Nam, S.-W. Oh, S.-H. Kim, J.-W. Huh, E. Lim, J. Kim, and T.-H. Yoon, "Parameter space design of a guest-host liquid crystal device for transmittance control," Crystals **9**, pp. 63-71, 2019.

Liquid crystal displays and anisotropic materials development in Belarus: present and future

V.Bezborodov[1], S.Mikhalyonok[1], N.Kuz'menok[1], A.Smirnov[2], A. Stsiapanau[2] V.Lapanik[3]
[1]Belarusian State Technological University, Minsk, Belarus
[2]Belarusian State University of Informatics and Radioelectronics, Minsk, Belarus
[3]Institute of Applied Physics Problems, Minsk, Belarus

1. Introduction

Research, development and production of liquid crystal displays and materials in Belarus are presented. The original methodology of the creation of advanced devices and anisotropic materials is considered. The proposed approach of design of new devices, anisotropic materials and ordered nanostructured surfaces and layers is based on numerous data obtained in the last decades in the study of liquid crystals and ordered fluids; on the regularities of the evolutionary development of natural organic compounds; on the use of the anisotropy of the molecules of polyfunctional compounds for the design of new molecular structures (molecular engineering), films, liquid crystals, micelles, membranes, etc. and for the creation of anisotropic ensembles of molecules and biological systems.. [1,2]

2. Anisotropic-based approach for design of structured surfaces, sensors, photonic devices and displays

The results of our investigations have shown that the electrochemical anodization technique of metal or inorganic films on a glass substrate, which provide simultaneously a high optical transparency, good alignment properties and ordering of anisotropic molecules, is one of the promising solutions for the design and production of next generation of displays [2]. Based on these results we propose to combine the design of the nanostructured surfaces and anisotropic materials for the creation of high efficient displays, including chemiluminescent; electroluminescent {EL) porous silicon microdisplays; inorganic EL microdisplays based on Al/porous silicon light emitting Schottky junctions; solar cells, photonic devices and etc.

3. Anisotropic materials

Taking into account that polyfunctional 3,6-disubstituted cyclohex-2-enones, *trans*-2,5-disubstituted cyclohexanones, 3,5-disubstitiuted 2-isoxazolines, 5-substituted cyclohexan-1,3-diones, 1,2-disubstitiuted cyclopropanols and substituted unsaturated epoxyketones can be easily converted to the corresponding liquid crystalline and anisotropic compounds, we proposed to use them as the key intermediates for the preparation of different types of anisotropic substances and materials. Different reaction possibilities for the functional groups and the cyclic fragments allow transformations to be achieved selectively and give a chance of preparing anisotropic compounds and materials with novel combinations of the structural fragments of molecules, which are in their turn useful components for new sensors, photonic devices, displays and other practical applications. Our results demonstrate that the combination of anisotropic and corresponding host LC materials, nanostructured surfaces, the UV curable anisotropic substituted vinylketones and the anisotropic photoalignment materials can provide desirable variations of the properties and parameters of the TN- and VA-LCDs; "shock-free" FLCD's with the bistable memory capability, fast-switching chiral-nematic and smectic displays The cells, which have been prepared using the LC materials and the nanostructured inorganic layers on glass substrate (alignment conditions) have several advantages in comparison with the cells containing commercial LCs and alignment materials and possess switching time less than 1 ms and the viewing angle 170-180°.

4. Conclusion

The presented results demonstrate that the combination of anisotropic materials, nanostructured films and surfaces, which are characterized by the ordered relief structure, opens the new approach of the creation of next generation of high quality displays with improved parameters. It is obvious that the proposed methodology is original and creative, and has a number of distinctive advantages in comparison with the well-known technologies, and can be successfully used for the development of new sensors, photonic devices, displays with a wide range of practical application.

5. Acknowledgements

This work was supported by the Belarusian Foundations for Basic Research (Grants № X16P-110 and ГБ 16-132, 137)

6. References

[1] Vladimir S. Bezborodov, Sergei G. Mikhalyonok, Nina M. Kuz'menok, Valery I. Lapanik, Genadz M. Sasnouski, "Polyfunctional intermediates for the preparation of liquidcrystalline and anisotropic materials" Liquid Crystals, Vol. **42**, pp. 1124-1138, 2015.

[2] V. Zhylinski, V. Bagamazava, A. Chernik, V. Bezborodov, I. Zharski, "Design and Application of Anisotropic Nanostructured Conductive and Alignment Coatings" Mol. Cryst. Liq. Cryst. Vol. **612**, pp. 129-134, 2015

O-9

Spectral dependences of transmittance and polarizing ability of stretched PDLC films with homogeneous and inhomogeneous interface anchoring

V.A. Loiko[1], V.Ya. Zyryanov[2], A.V. Konkolovich[1], A.A. Miskevich[1], O.O. Prishchepa[2,3], A.V. Shabanov[2], M.N. Krakhalev[2,3]

[1]Institute of Physics of the National Academy of Sciences of Belarus, Belarus
[2]Kirensky Institute of Physics, Federal Research Center "Krasnoyarsk Scientific Center", Siberian Branch, Russian Academy of Sciences, Russia
[3]Institute of Engineering Physics and Radio Electronics, Siberian Federal University, Russia

Polymer dispersed liquid crystal (PDLC) films, consisting of non-absorbing uniaxially-elongated liquid crystal (LC) droplets within polymer matrix effectively polarize light in the entire transparency region (visible and near IR) of the components used, while the dichroic polarizers can do that only in the dichroic band of own or impurity absorption. Besides, PDLC films allow modulating the intensity, polarization and phase of light by applying the electric or magnetic field. They are particularly promising in the collimated laser devices and projection systems.

Recently, a new approach has been realized to control the optical response of polymer dispersed liquid crystal (PDLC) film in the light-scattering mode [1]. It is based on the surface anchoring transitions caused by ionic surfactant and gives an opportunity to achieve simultaneously the limit polarization characteristics for unpolarized incident light.

In this presentation an optical-mechanical model has been developed to describe the transmittance, polarization and small-angle distribution of light scattered by an uniaxially-stretched polymer films containing the elongated ellipsoidal droplets of nematic liquid crystal doped with ionic surfactant [2]. The model is based on the Foldy-Twersky, anomalous diffraction, and single scattering approximations. We have studied the spectral dependences of the coefficients of coherent (directed) transmission and the polarization degree of forward-transmitted light, the angular distribution and polarization of light scattered in small angles by the stretched PDLC films with homogeneous (without surfactants) and inhomogeneous (with surfactants) surface anchoring. It has been considered the films consisting of ellipsoidal LC droplets with: the bipolar intrinsic structure formed under homogeneous tangential anchoring, the radial structure formed under homogeneous homeotropic (normal) anchoring, and the monodomain structure raised due to inhomogeneous surface anchoring.

The spectral dependence of transmittance and polarizing ability of the polymer dispersed liquid crystal films have been analyzed as well as the small-angle intensity distribution and the polarization degree of scattered light depending on the film thicknesses, refractive indices of LC and polymer, sizes of droplets, their anisometry parameters, concentration, polydispersity, and optical axes small-angle intensity distribution and the polarization degree of scattered light depending on the film thicknesses, refractive indices of LC and polymer, sizes of droplets, their anisometry parameters, concentration, polydispersity, and optical axes orientation and the field of view angle of the optical system. The optical characteristics of films with homogeneous and inhomogeneous interfacial anchoring at the surface of liquid crystal droplets are considered.

A high polarization degree (more than 0.97) can be achieved for the forward-transmitted light in the wide wavelength range (from 0.45 to 0.7 μm) both for PDLC films with monodomain and bipolar LC droplet structures and for films with inhomogeneous surface anchoring of "tangential-normal" type. A coherent transmittance of the films with bipolar droplet configuration and inhomogeneous "tangential-normal" anchoring is smaller than that of the films with monodomain internal structure. The films with homogeneous surface anchoring and radial LC droplet structure do not allow polarizing effectively the forward-transmitted light.

Acknowledgments

The work was performed in the framework of an inter-academic cooperation between the NAS of Belarus and the SB of the Russian Academy of Sciences.

References

[1] Krakhalev MN, Loiko VA, Zyryanov VYa. Electro-optical characteristics of PDLC film controlled by ionic-surfactant method. Techn. Phys. Lett.,Vol. 37, pp.34-36, 2011.

[2] Loiko VA, Konkolovich AV, Zyryanov VYa, Miskevich AA. Polarization of Light by a Polymer Film Containing Elongated Drops of Liquid Crystal with Inhomogeneous Interfacial Anchoring. Opt. and Spectr., Vol.122, pp.984-994, 2017.

Session 2. MicroLED and VR/ARs

Chairman: Philippe Coni

Invited I-3

OLED microdisplays for augmented reality applications

G.Haas
MICROOLED S.A.S, France

1. Introduction

Microdisplays are widely used in head mounted displays (HMDs), electronic viewfinders (EVF) and other near-to-the-eye visualization systems. An overview about the different technologies and applications can be found in [1]. Due to their superior image quality, power efficiency and compactness, emissive type microdisplays based on OLEDs have been strongly increasing their market share for these applications. With the potential and recent advances of wearable Augmented Reality (AR), OLED microdisplays start to enter this application. We will limit here to applications we qualify as wearable AR as defined in Figure 1.

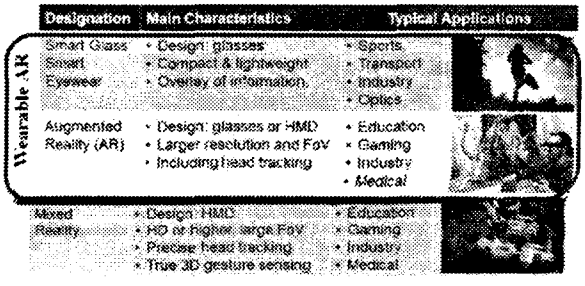

Figure 1: Definition of wearable Augmented Reality

2. Objective

Objectives are to review requirements for microdisplays and related optical systems used in wearable AR, to benchmark them against the performance of different microdisplay technologies, and to present solutions based on our OLED microdisplay technology.

3. Requirements

The general requirement for wearable AR are shown in Figure 2 below:

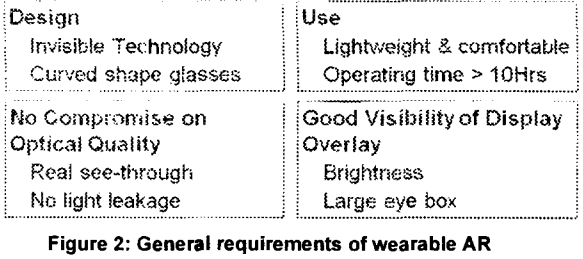

Figure 2: General requirements of wearable AR

From this, we can derive requirements for both the optical see-through system and the microdisplay.

One key element in the consideration here is power efficiency, as only a power efficient system can achieve low weight, compactness, and reasonable operating times. Another one is the emphasis on the optical quality, which means that no obstructive elements or parasitic light leakage is allowed that could impact the view of the user.

4. Main outcomes

A comparison between different technologies for the optical system and the microdisplay will be outlined in the presentation. As an example, Figure 3 shows a comparison between OLED and micro-LED based microdisplays.

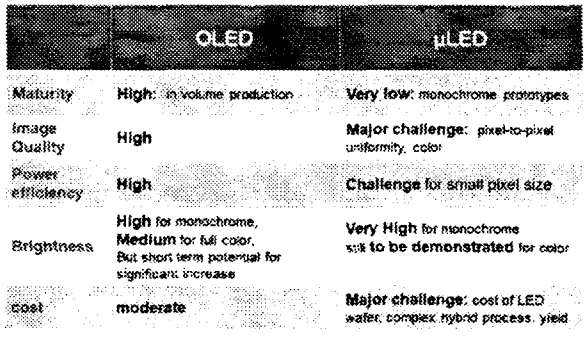

Figure 3: comparison of OLED vs micro-LED based microdisplays

Considering both technical performance and technology maturity it comes out that only systems based on OLED microdisplays combined with optical systems of the free-space optics type can fulfil the above requirements. In future, also some type of waveguide type optics might be used. Figure 4 shows some examples of high brightness OLED microdisplays for AR applications.

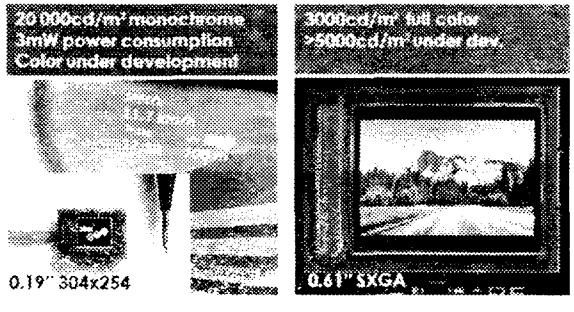

Figure 4: Two examples of high brightness microdisplays for wearable AR

5. Acknowledgements

Part of the work has received funding from the European Union's ENIAC Joint Technology Initiative on nanoelectronics under grant agreement No 621200.

6. References

[1] G. Haas, "Microdisplays for Augmented and Virtual Reality," SID 2018 Symposium Digest of Technical Papers, p. 506, 2018

Invited I-5

Gallium nitride micro-LEDs: a novel, multi-mode, high-brightness and fast response display technology

Martin D. Dawson
Institute of Photonics, Department of Physics, University of Strathclyde, Glasgow G1 1RD, UK

Abstract
Gallium nitride micro-LED technology interfaces very effectively to silicon CMOS to facilitate highly sophisticated data modulation and structured lighting functions. This rapidly emerging capability is poised to play a key role in the prospective convergence of displays with communications, lighting, sensing and imaging systems, including multiple scenarios where the display can be interactive with its environment. We will provide an overview of these new capabilities which are challenging conventional conceptions of display technology and set these in the broader context of the evolution of micro-LEDs.

1. Introduction

Micro-LED technology, based principally on the capabilities of gallium nitride inorganic semiconductor epi-structures, is emerging very rapidly to commercial maturity to provide a new generation of robust and high-performance displays [1]. These devices, which comprise high-density formats of individual LED pixels with dimensions of a few microns to tens of microns, are of the self-illumination type with high-brightness, broad viewing angle, and very rapid (ns) response time. Demonstrator capabilities spanning wearables, to augmented (AR) and mixed reality (MR) systems, through to large screen TVs and displays, are currently being trialed by innovative new businesses and multi-national corporations.

In parallel with these developments, the lighting industry - in its move to solid state lighting - is beginning to embrace new operating models (such as Lighting-as-a-Service) which will embed additional functionality such as optical wireless communications via LiFi. The developments underway posit a move from first-generation, so-called 'smart lighting' towards what might be called digital lighting. Micro-LED technology is also setting performance benchmarks in LiFi, and the exciting prospect is emerging of combining micro-LED based capabilities for displays with lighting and communications, potentially also involving sensing, ranging and imaging functions.

2. Micro-LEDs in Displays, Lighting and Communications

Micro-LED technology fits naturally into high-pixel density 1-D and 2-D emitter array formats to provide electronic visual display capability. Furthermore, the detailed physics of micro-sized pixels offers enhanced modulation bandwidths into the GHz range per pixel [2], more than two orders of magnitude higher than that typical of conventional broad area LEDs. These factors can be combined in new forms of spatially multiplexed or spatially modulated LiFi communications, such as space-shift keying (SSK) or multiple input multiple output (MIMO), to enhance data communications channel capacity [2]. In this format, the display function embodies the spatial registration/distribution of information in a communications link, rather than necessarily embodying direct view physically meaningful images. However, the frame rate or image refresh rate is so fast for micro-LEDs that the displays could operate multi-modally, to implement display and spatially modulated communications functions in parallel.

Furthermore, high refresh rate binary mask patterns can be generated with CMOS-interfaced micro-LED displays, at frame rates which may exceed MHz. These systems can project such checkerboard-like high-frame rate patterns to provide unique digital signatures to each location in the imaged frame, which can be used to implement location, tracking and navigation functions [3]. Thus the projected output of such a display can be used e.g. to track moving objects in the space around it, potentially including viewers of the display.

An additional variant of these digital lighting systems uses LED projections from multiple spatial directions (usually four) in conjunction with a camera to implement photometric stereo imaging. Given the current size scaling of micro-LED displays and the prospective ability to incorporate light sensing functions through front plane integration, it is possible in future that the projected output from a micro-LED display can also image the environment around it.
We will review these exciting emerging capabilities and speculate on how they will develop.

3. Acknowledgements

We acknowledge support from EPSRC under grants EP/K00042X/1 and EP/M01326X/1.

4. References

[1] M.D. Dawson and M.A.A. Neil (Eds). "Special Cluster Issue: Micro-pixellated LEDs for Science and Instrumentation" J. Phys D: Applied Physics, Vol. **41** (9), 2008.

[2] S. Rajbhandari et al., "A Review of Gallium Nitride LEDs for Multi-Gb/s Visible Light Data Communications", Semiconductor Science and Technology, Vol. **32**, 023001, 2017.

[3] J. Herrnsdorf et al., "Positioning and data broadcasting using illumination pattern sequences displayed by LED arrays", IEEE Trans. Comm., **66**, 5582 , 2018.

OLED-on-silicon for near-to-eye microdisplays and sensing

K.Fehse, U.Vogel, P.Wartenberg, B.Richter, S.Brenner, M.Rolle, G.Bunk, S.Ulbricht, J.Baumgarten, C.Schmidt, M.Schober, P.König

Div. Microdisplays & Sensors, Fraunhofer Institute for Organic Electronics, Electron Beam and Plasma Technology FEP, Germany

1. Introduction

Smart eyewear featuring near-to-eye (NTE) displays have evolved as major devices for wearable displays, which hold potential to become adopted by consumers soon. Tiny OLED-on-silicon microdisplays (<1" screen diagonal) are a key component of eyewear displays, creating images from active-matrix organic light emitting diodes (AM-OLED), similar to those that have become popular in mobile phone displays.

2. OLED-on-Silicon technology

All microdisplay technologies on the market comprise an image-creating pixel modulation, but only the emissive ones (for example, OLED and LED) feature the image and light source in a single device, and therefore do not require an external light source. This minimizes system size and power consumption, while providing exceptional contrast and color space. These advantages make OLED microdisplays a perfect fit for near-eye applications. Low-power active-matrix circuitry CMOS backplane architecture, embedded sensors, emission spectra outside the visible and high-resolution sub-pixel micro-patterning address some of the application challenges (e.g., long battery life, sun-iight readability, user-interaction modes) and enable advanced features for OLED microdisplays in near-to-eye displays, e.g., in upcoming augmented-reality (AR) smart glasses as well as significantly improved virtual-reality (VR) headsets.

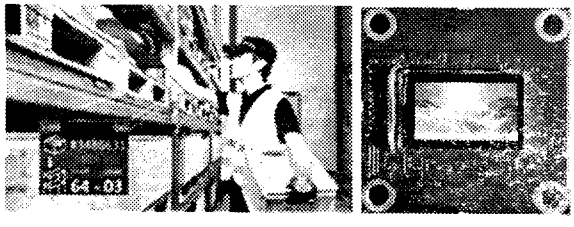

Figure 1: Near-to-eye information display use case (left), new 0.64" 720p OLED microdisplay (right)

3. New 0.64" 720p OLED microdisplay

A new 0.64" 720p OLED microdisplay for application in industrial AR see-through head-mounted displays (ST-HMD) has been developed. It features 1280x720 resolution at a pixel pitch of 11um with four sub-pixels, 8bit/color and parallel interface. For low-latency AR an adequate high frame rate has been targeted. To reduce effects of motion blur a "rolling emit" feature has been implemented next to "global emit".

4. Embedded sensing

Beyond microdisplays for near-to-eye, OLED-on-silicon can be favourably used in optical sensing, e.g., as miniaturized phosphorescence sensor. In this sensor, a chemical marker is excited by modulated blue OLED light. The phosphorescent response of the marker is then detected directly inside the sensor chip. The marker determines the substance to be measured; a typical application is measurement of an oxygen concentration.

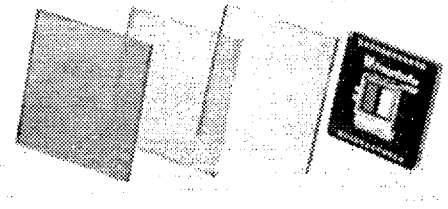

Figure 2: 0.4" OLED-on-Silicon Sensor

5. Acknowledgements

The work leading to these results has received funding from the Federal Ministry for Economic Affairs and Energy of the German government (BMWi) 01MD16008C "Glass@Service", the European Union's ECSEL Joint Undertaking under grant agreement No 661796 ("ADMONT"), the European Union's Horizon 2020 research and innovation program under grant agreement No 644101 (1" WUXGA OLED microdisplay), and was partly funded by grant from Fraunhofer internal programs 162-600717 (ultra-low power OLED microdisplays).

6. References

[1] P. Wartenberg, B. Richter, S. Brenner, M. Rolle, G. Bunk, S. Ulbricht, J. Baumgarten, C. Schmidt, M. Schober, and U. Vogel, " A New 0.64" 720p OLED Microdisplay for Application in Industrial See-Through AR HMD" SID Symposium Digest, Vol. 50. pp. 717-720, 2019.

[2] U. Vogel, B. Beyer, M. Schober, P. Wartenberg, S. Brenner, G. Bunk, S. Ulbricht, P. König and B. Richter, " Ultra-low Power OLED Microdisplay for Extended Battery Life in NTE Displays ", SID Symposium Digest, Vol. 48. pp. 1125-1128, 2017

A microLed imager for AR headset for use in high luminance environment

E. Quesnel[1], A. Lagrange[1], M. Vigier[1], M. Consonni[1], M. Tournaire[1], A. Suhm[1], E. Feltin[2], M. D'amico[3], E. Cao[3], R. Faideau[3], G. Haas [4], L. Charrier[4], P. Coni[5]

[1]Université Grenoble-Alpes, CEA, LETI, MINATEC Campus, 17 rue des Martyrs, 38054 Grenoble, France
[2] NOVAGAN, chemin de Mornex 5 A, 1003, Lausanne, Switzerland
[3] NEXDOT, 102 avenue Gaston Roussel Biotech-bâtiment Pasteur, 93230, Romainvilie, France
[4] MICROOLED, 7 Parvis Louis Néel, BP 50, BHT bâtiment, 38040 Grenoble cedex 09, France
[5] THALES Avionics, 75 avenue Marcel Dassault, 33700 Merignac, France

1. Introduction

Today, popular Augmented Reality headsets suffer from a lack of brightness to allow the diffusion of readable information against a very bright landscape, in particular for avionics use, and more generally, outdoor applications.

We present in this paper, the project "HiLICo", aiming to develop an emissive GaN micro-displays with 1640 x 1032 pixel resolution (WUXGA), 9.5-µm pixel pitch, very high brightness (over 1Mcd/ cm²) and good form factor capabilities that will enable the design of ground breaking compact see-through system for next generation Avionics applications.

2. Objective

To achieve an acceptable user experience and help the pilot with an improved situational awareness, the display shall be readable under the most severe daylight environment. SAE ARP 4102 [1] requires a contrast greater than 1.2 under 34,000 cd/m² of background luminance, corresponding to 100,000 Lux of illuminance on white clouds. According to regulation rules [1], 6800 cd/m² are needed, but for a better user experience, a contrast of 1.5 corresponding to 17,000 cd/m² is targeted.

3. Background

Several display technologies are available today for AR headset such as LCOS, DMD, LCD and OLEDs.

The three first technologies are non-emissive, and require a powerful and bulky backlight system. They suffer from a low efficiency, and product like Hololens or Magic Leap deliver only 320 cd/m² [2]. Oled microdisplays are emissive and so, don't need backlight. But the organic electroluminescent material suffers from ageing issues when delivering fixed images at maximum brightness. MicroLed displays made from Gallium Nitride (GaN) are able to deliver 100 times more luminance than other existing technologies, so, they represent the best choice for outdoor AR device.

4 Microdisplay Requirements

Luminance on the display combiner depends on optical components transmission and combiner reflectance. In the best case the optical system efficiency is around 30%, so, the minimum luminance for the microdisplay shall be 56,000 cd/m². But if we want to keep this contrast for at least 16 levels of grey, we need a minimum of 1 Mcd/m²

5 Advanced Technologies and Challenges

To achieve this goal, the HiLICo project addresses several challenges. Among them (i) the synthesis of high-quality GaN based LED epilayers designed for blue or green native emission, (ii) the design and fabrication of an active matrix in advanced Complementary Metal Oxide Semi-conductor (CMOS) technology to drive each individual pixel and (iii) the coupling of both LED and CMOS structure to eventually come up with a monolithic structure ready for LED array micro-engineering, paving the way to high resolution and very small pixel pitch GaN micro-displays. On this basis monochrome and full-colour emissive micro-displays will be manufactured. For this last display, blue-to-green or blue-to-red colour conversion will be necessary using either quantum dots or 2D multi-quantum wells layers. This task is on itself very challenging considering the expected light conversion efficiency (over 50%) and lifetime (over 10,000H) necessary for the application. A dedicated electronics will be designed and manufactured for a full evaluation of the various micro-display devices. As an ultimate goal, the integration by the end-user (THALES Avionics) of a micro-display in an avionic system should help validating the HILICO technology and concept.

6 Discussion

After a general introduction on the project, the purpose of this talk is to review the various technological routes selected by the HILICO consortium and some of the technological challenges to overcome.

8. Acknowledgements

The authors acknowledge funding from the CleanSky-H2020 HILICO European project (under H2020-EU.3.4.5.6. - ITD Systems, Project ID: 755497).

9. References

[1] Flight Deck Head-Up Displays ARP4102/8, SAE Aerospace Recommended Practice.

[2] https://www.kguttag.com/

Active matrix mini-LEDs backlights drived by circuits of 2T1C and 1T1MOS based on a-Si

B.Liu[1,2], Q.S.Liu[2], J.Li[2], Y.Y.Qiu[2], J.L.Liu[2], Y.Yang[2], H.Y.Xu[2], F.Zhu[2], H.Zhou[1]

[1]Peking University Shenzhen Graduate School, China
[2]Shenzhen China Star Optoelectronics Technology Co., LTD, China

1. Introduction

Mini-LEDs and micro-LEDs have surfaced as a candidate for future displays [1,2]. As for LEDs, there are many advantages such as low investment in production equipments, mature technology of display backplanes, and high reliability. While there are some obstacles towards mass transfer, cost of LEDs and appropriate applications. So far, mini-LEDs backlights with the function of local dimming would be a good choice to introduce this technology into the market [3]. For now, most of mini-LEDs backlights are presented through passive matrix (PM) driving on FPC or PCB substrates. The complexity of layout and patterning process limit the resolution, in addition, FPC or PCB substrates also increase the costs. Hence, active matrix (AM) backplanes on cheap substrates such as glass for mini-LEDs is necessary.

In this work, an AM mini-LEDs backlight with the size of 21.2-inch based on a-Si, function like 432-zones local dimming and switchable BLU modes on a glass substrate, is realized. The two kinds of driving schematics (2T1C and 1T1MOS) are discussed in detail.

2. Results and discussion

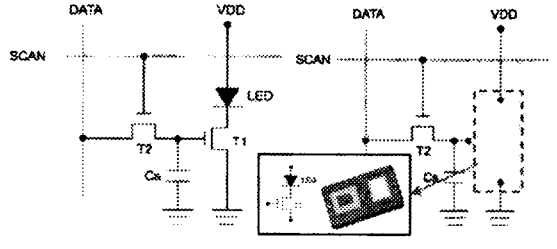

Figure 1: The active driving mechanism of AM mini-LEDs backplane:(a) 2T1C (b) 1T1MOS

16×27 pixels (432-zone) are designed and each pixel owes four LEDs with one set of driving circuits. We employ two kinds of circuit designs (2T1C and 1T1MOS) to output current through voltage of driving switch. The driving schematics of mini-LEDs plane design are shown in Fig. 1. The 1T1MOS-based circuit design is mianly in order to improve the reliability of backlights. Through our researches, the brightness decay of 1T1MOS-based backplane is improved obviously compared with that of 2T1C-based backplane.

Figure 2: The photograph of AM mini-LEDs

Figure 2 shows the photo of AM mini-LED backplane. Each pixel (zone) can be controlled through active-matrix operation. The blue light emitting by LEDs would be converted to white with stacked films, and then achieved better uniformity through a diffuser film. In the next moment, we will test the reliability of the backplane and more improvements are on-going.

3. Conclusion

An AM mini-LED backlight with the size of 21.2-inch, based on a-Si, is demonstrated. The two kinds of driving circuit designs are discussed in detail. The above results provides a universal and practical avenue for mass production of AM mini-LEDs backlights.

4. Acknowledgements

Authors acknowledge CSOT for its supporting grants and Postdoctoral Science Foundation of China (No. 2019M650332).

5. References

[1] A. K. Tripathi, E. C. P. Smits, J. L. Steen, M. Cauwe, R. Verplancke, K. Myny, J. Maas, R. Kuster, S. Sabik, M. Murata, Y. Tomita, H. Ohmae, J. Brand, G. Gelinck, "A conformable Active Matrix LED Display", international Meeting on Information Display (IMID). 2015

[2] H. M. Kim, J. G. Um, S. Lee, D. Y. Jeong, Y. Jung, S. H. Lee, T. Jeong, J. Joo, J. Hur, J. H. Choi, J. S. Kwak, and J. Jang, "High Brightness Active Matrix Micro-LEDs with LTPS TFT Backplane", SID Symposium Digest of Technical, 66-4, 2018.

[3] A. Daami, "Electro-optical size-dependence investigation in GaN micro-LED devices", SID Symposium Digest of Technical, 59-4, 2018

Augmented reality head-up displays: from requirements to solutions

K. Blankenbach
Pforzheim University, Germany

Abstract
The benefits of head-up displays (HUD) are proven for various applications. Today's automotive HUDs show mostly operational data. This paper discusses requirements of augmented reality (AR) HUDs.

1. Introduction

Many modern cars are equipped with HUDs visualizing mostly speed and directions (Fig. 1 left). Those HUDs have typically a field of view (FOV) of about 8° by 3° (h x v). They base on a projection system using small displays, curved mirrors and a combiner in the windshield [1]. AR-HUDs (Fig. 1 right) will provide more benefits for manual (wayfinding) and autonomous driving (building trust). They require new techniques due to large FOV.

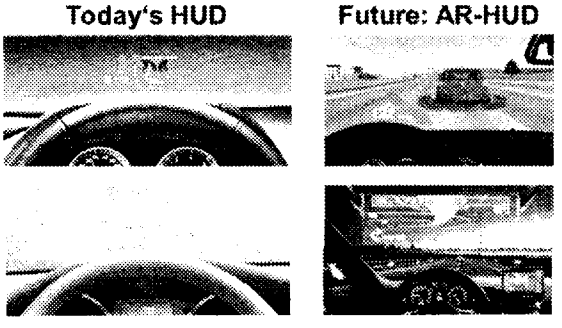

Figure 1: From today's HUD with small field of view (FOV, left) towards AR-HUDs (right) with large FOV. Sources: BMW, MERCEDES, PIONEER

2. Considerations on AR-HUD Field of View

The useful AR distance and FOV depends on the "amount" of augmentation and the traffic scenario. The basic parameters for the vertical FOV_V and the distance d are visualized in Fig. 2 top:

- Calculation of angles by $\tan(\alpha) = h/d$, where h is the height of the eye, distance d as object to eye
- Minimum distance for urban traffic: $d_{min} \sim 5$ m
- Maximum distance for highways: $d_{max} \sim 80$ m

With these assumptions, we can calculate the vertical FOV_V values from α_V according to Fig. 2 top:

- FOV_V for look-down from $\alpha_{Vmin} - \alpha_{Vmax} \approx 15°$
- 1° to 2° have to be added system performance.
- Framing cars and annotated information require a look-up angle α_{Vlu} of at least 5°. This results in a total FOV_V of about 20° for highway use cases.
- AR augmentation of close objects like shops and traffic signs require at first approach 20° for look-up angle α_{Vlu}. This results in 40° for vertical FOV.

Corresponding considerations are made for the horizontal FOV_H for different scenarios, Fig. 2 bottom:

- Passing a car on highway: $\alpha_H \approx 20°$, Fig. 1 right
- Urban wayfinding: $\alpha_H \approx 40°$
- Annotated information in cities: $\alpha_H \approx 60°$

This raises the FOV (h x v) by more than one order of magnitude compared to present HUDs in series production. So new technologies are required.

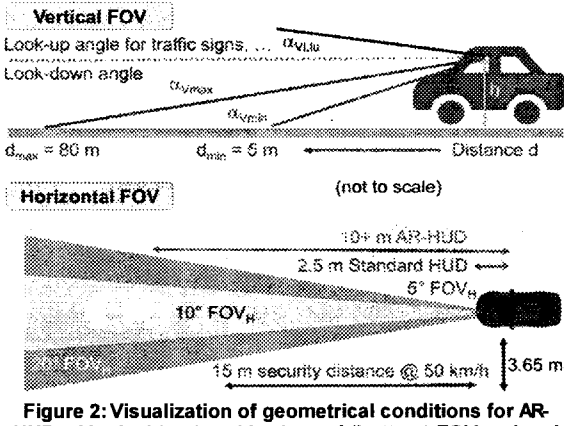

Figure 2: Visualization of geometrical conditions for AR-HUDs: Vertical (top) and horizontal (bottom) FOV and real object distance d

3. Requirements and Solutions

The optical power output rises with the FOV in approximately linear relation. Expanding from 8° to 60° (h) and 3° to 40° (v) results in 100x. The luminance of the HUD's is calculated by

$$L_{Lightsource} = \frac{L_{HUD}}{T_X \cdot R_X} \quad (1)$$

T_X represents transmission in the optical path and R_X for reflectance. The reflectance of holographic combiners is significantly higher (about 85%) thus enabling AR-HUDs, holographic waveguides [2] reduce their volume. The contrast ratio must exceed on bright roads:

$$CR = \frac{L_{HUD}}{L_{Road}} + 1 \;\; 3{:}1 \quad (2)$$

4. Summary

AR-HUDs with a FOV larger than 40° by 10° require holographic methods and highest light output for readability for augmented data on bright background.

5. References

[1] Sako, Ketal, "Development of New Head-Up Display System Utilizing RGBW LCD and Local Dimming Backlight," SID Symposium Digest of Technical Papers, Vol. 47, p. 680-683 (2016).

[2] Richter, Petal, "Volume Optimized and Mirror-less Holographic Waveguide Augmented Reality Head-up Display, " SID Symposium Digest of Technical Papers, Vol. 49, p. 725-728 (2018).

O-14

An intrinsically eye safe approach to high apparent brightness augmented reality displays using digital holography

A.Kaczorowski, A.Newman, A.O.Spiess, D.F.Milne
VividQ Ltd., Research Division, CB3 0AX Cambridge, United Kingdom

Abstract
Achieving the luminance of real-world scenes is a challenge for many display technologies when seeking to deliver an experience that approaches the dynamic range of the human eye. Digital holography offers a number of significant advantages in this respect, due both to the high optical efficiency, and the ability to redistribute available luminous flux to individual points as required. This property is especially important when the aim is to present sparse digital elements that need to be clearly perceived against a bright real-world background in an AR or MR application. In this work we show that a configuration capable of delivering apparent display brightness equivalent to that of the daytime sky is achievable with components viable for a consumer head mounted display, and identify the constraints necessary to ensure that such a device would be intrinsically eye safe.

1. Context and motivation

To create a convincing reproduction of real-world scenes, the brightness of the image produced may be required to reach of the order 10'000 cd/m^2 to display content over a daytime sky. Reproducing this level of brightness is a challenge for traditional display technologies, as the correspondence between a display pixel and a point in the replay field limits the peak brightness, and is a particular limitation where sparse areas of high brightness are required. Although displays with individually light-generating pixels, such as OLED, offer an improvement over backlit displays, they still present the challenge that in order to achieve extremely high brightness, each pixel must still be capable of generating significant radiant flux, and hence have current handling requirements that are challenging for a high-resolution display.

2. Achieving high brightness and efficiency using diffractive, holographic display

Holographic displays, utilizing a phase-only liquid crystal spatial light modulator (LC SLM) as an image-forming device, present a range of advantages over competing technologies. Because phase modulation is performed in the Fourier plane (as opposed to amplitude modulation in the image plane), a relatively large fraction of the initial luminous flux can be arbitrarily re-directed into a selected number of image points [1]. This plays a crucial role for Augmented and Mixed Reality devices, which have an inherently small image coverage. Because the laser illumination of the holographic display is separate from the modulator itself, high optical efficiency can be achieved without dissipating significant amounts of heat at the display (as it is the case in traditional LCD displays).

3. Methodology and Results

We analyzed the efficiency of the optical components in the holographic setup as well as the power requirements. As an example, Figure 1 shows a sample Augmented Reality scene as shot through VividQ's benchtop holographic projector [3].

The display presented achieved object brightness in excess of 10'000 cd/m^2 from 1mW of optical power. This figure can be significantly surpassed for sparse replay fields. We discuss the optical requirements and demonstrate, how such a display is made intrinsically eye-safe.

Figure 1: Holographic display demonstrating exceptional optical efficiency [3]

4. About VividQ

VividQ is a Cambridge based start-up developing unique holographic technologies that enable realistic, true-to-life viewer experiences. We are building software solutions for the next generation of holographic 3D display, aimed at Augmented and Mixed Reality applications.

5. References

[1] D.W.F. van Krevelen, R. Poelman, "A Survey of Augmented Reality Technologies, Applications and Limitations" The International Journal of Virtual Reality, Vol. **9**, no. 2, pp. 1-20., 2010.

[2] C. Slinger, C. Cameron and M. Stanley, "Computer-generated holography as a generic display technology," in Computer, vol. **38**, no. 8, pp. 46-53, 2005.

[3] VividQ Ltd., "Real-time Holographic Mixed Reality Demo", https://youtu.be/4n12cSshzNs, 2019.

[4] VividQ Ltd., Official Webpage, www.vivid-q.com

O-15

Controlled integrated vacuum elements on niobium field cathodes for microdisplays

G.Gorokh[1], I.Taratyn[2], A.Pligovka[1], A.Lozovenko[1], A.Zakhlebayeva[1]
[1]Belarus State University of Informatics and Radioelectronics, Brovka St., 6, Minsk, Belarus
[2]Minsk Research Institute of Radiomaterials, Kizhevatova St., 86Minsk, Belarus

1. Introduction

The paper presents the methods of creation and research results of matrices of electronic elements on field cold cathodes with given geometric and electrophysical parameters. The developed controlled matrices are small-sized, highly efficient sources of electron beams with low energy consumption for microelectronic devices, such as microdisplays. Field emission elements with nanostructured cathodes in the triode and diode configurations are implemented based on original structural and technological methods for the electrochemical formation of vertically oriented arrays of metal oxide niobium nanostructures, compatible with the latest nanotechnologies used in the manufacture of promising optoelectronic and nanoelectronic products.

2. Results

Arrays of vertically oriented metal oxide nanostructures were formed by electrochemical anodization of the two-layer Al/Nb system [1]. The array of nanostructures had the following parameters: column diameter - 50–150 nm; location period - from 500 nm to 70 nm; scatter in height - not more than 5%; array height - 0.5–1 μm. Figure1 shows micrographs of the surface and the cross section of the resulting array of niobium nanostructures.

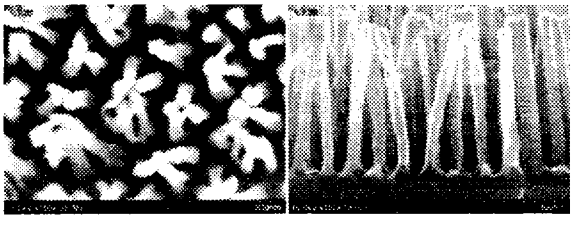

Figure 1: SEM of the surface and the cross section of niobium nanostructures array

Geometric models of matrices of vacuum elements have been developed and investigated. The distribution of electric field lines was simulated when a voltage of 10 to 150 V was applied between the anode and cathode. The design and manufacturing technology of a crystal with a matrix of field emission elements consisting of 100 field elements interconnected by a common control bus is developed. The cathode control bus is located directly on the plate, the vacuum part of the elements is placed in cavities formed using specially developed processes of local plasma-chemical and liquid etching of dielectric and conductive layers, providing insulation functions and acting as a control grid and anode. In each cavity, there is one field emission nanostructured cathode from an array of niobium metal oxide columns. A schematic representation of the matrice of field cathodes is presented in Figure 2.

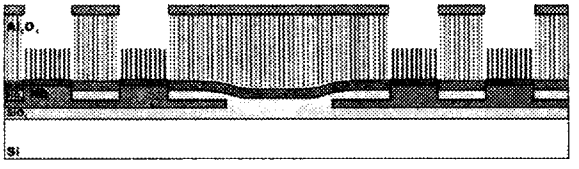

Figure 2: Schematic representation of the matrice of field cathodes

The matrices of elements based on field cathodes were fabricated. Figure 3 shows electron microscopic images of the formed matrices at different stages of their manufacture.

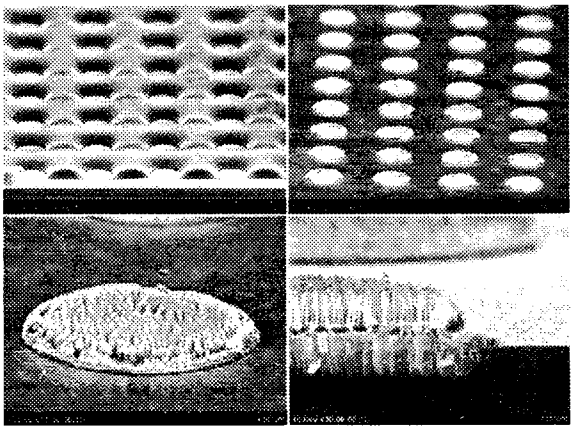

Figure 3: SEM images matrices of cold cathodes and individual cathodes based on niobium nanostructures

The fabricated matrices of emission elements had the following characteristics: control voltages 20–32 V/μm; threshold voltage 2 - 4.5 V/μm; emission current of at least 30 mA/cm^2 at a voltage of 16 V.

3. Acknowledgements

The scientific and technical program "Technology-SG", grant 2.3.2.1, supported the work.

4. References

[1] A. Pligovka, A. Lazavenka, G. Gorokh, "Anodic Niobia Column-like 3-D Nanostructures for Semiconductor Devices" IEEE Transactions on Nanotechnology, Vol. **18**. pp. 790-797, 2019.

Session 3. Liquid crystal displays

Chairman: Prof. Kristiaan Neyts

Invited I-7

Liquid crystal display and photonics devices based on photoalignment

V.Chigrinov

Foshan University, Foshan, China
HKUST, HK

Display and photonics liquid crystal devices are growing rapidly and there is no chance of any ot technology to be more advanced in these applications. A strong competition in the market will make further developments of new LC technologies extremely important and is a good chance to show superiority.

Photoalgnment and photopatterning materials can be effectively used in LC alignment and patterning for n generations of liquid crystal display and photonics devices that provide extremely high resolution a optical quality of alignment both in glass and plastic substrates, photonics holes etc. New LC display a photonics devices include ORW E-paper, field sequential color ferroelectric LC projectors (FLC-LCO photo-patterned quantum rods and 100% polarizers, q-plates, sensors, switchable lenses, windo with voltage controllable transparency, security films, switchable antennas.

Invited I-8

Photoinduced optical anisotropy (PIA) in condensed media – nature, properties, applications. 100 anniversary of weigert effect

V.V. Belyaev[2,3], V.M. Kozenkov[1], D.N. Chausov[2], L.I. Smirnov[1]
[1]Kripten, Dubna, Russia
[2]Moscow Region State University, Moscow, Russia
[3]RUDN University, Moscow, Russia

In 1919 F. Weigert published a paper [1] on an effect detected by him. In solid solutions of complex molecules of organic dyes induced anisotropy of optical properties appeared under ecitation by polarized light. This paper stimulated investigation of anisotropy of different materials by optical methods. Significant results have been obtained for data on anisotropy of primary processes of light radiation and absorption that relate to specific features of intermolecular interaction in condensed matter. The effect is used in holography, integrated, fiber and polarization optics, in systems for information recording, storage, processing and displaying.
In review to-date PIA investigations and its applications will be presented. The review will include parts as follows:
1. General classification of the effect and mechanism of optical anisotropy formation under impact of irradiation onto condensed matter.
2. Active molecular photoorientation in transparent media: Buckingham effect, non-linear magneto-optical effects (optical analogs of Cotton-Mouton and Faraday effects), non-linear (cooperative) optical effects in partially ordered (LC) media (optical analogs of Freedericks effect)
3. PIA in absorbing media.

Acknowledgements
The work is supported by Russian Foundation for Basic Researches (grant No.18-07- 00727_a).

References
[1] F. Weigert, Über einen Effekt der Strahlung in lichtempfind lichen Schichten. Verhandl. der Deutschen Phys. Ges., Bd 21, 479 (1919)

Q-16

The role of reactive monomer in PI-free technology for the alignment ability and image sticking performance

Wei Cui[1,2], Min Zhang[1], Te-Jen Tseng[2], Chung-Ching Hsieh[2], Chung-Yi Chiu[2]
[1]Peking University Shenzhen Graduate School, Shenzhen 518055, China
[2]Shenzhen China Star Optoelectronics Technology Co., Ltd, Guangdong, China

Abstract
Polyimide-free technology is a technology in which an additive can replace polyimide film to align LC molecules. In this technology, the additive added in liquid crystal (LC) host can not only affect the alignment behavior, but also affect the reliability of the panel, such as image sticking. Because the polymer is polymerized from the additive in LC, the system of the additive is very important. In this paper, we studied the alignment and image sticking performance fabricated by two different additive systems:1. the mixed system of additive and reactive monomer; 2. the single additive system. From the results of cell and 28" panel, we can conclude that the mixed system has similar alignment ability and voltage holding ratio to the single additive system, however, has better image sticking performance than the single additive system.

1. Introduction

Liquid crystal displays (LCDs) are the most popular type of flat-panel displays and are used in television sets, notebook computers, smartphones, tablets and so forth because they have features such as high resolution, low power consumption. So far, the LCDs have usually used a twisted nematic (TN) mode [1], in-plane switching mode [2], fringe-field switching mode [3], multidomain vertical alignment (MVA) mode [4] and patterned vertical alignment (PVA) mode [5]. Among these modes, vertical alignment (VA) mode has a significantly high contrast ratio because vertically aligned liquid crystal (LC) molecules induce little retardation. Among the VA modes, polymer-stabilized VA mode has get considerable interest for their fast response time, low power consumption, and wide viewing angle. To achieve VA, VA layers, which are mainly made from polyimides having side chains, are usually prepared on a pair of substrate [6]. The preparation of the VA layers usually requires large amount of solvent, high–temperature operation for post-baking and cleaning process. Recently, conventional alignment layer-free technologies have been proposed [7,8] and some of them have been for VA.

The key factor of the PI-free technology is the additive system in LC host, which not only plays the role of alighnment, but also affects the electro-optical property and reliability of the panel.

In our previous work, we have demonstrated a polymer-sustained vertical alignment (PSVA) panel without conventional alignment layer. However, the effect of different additive systems on the alignment ability and reliability of panel is not studied clearly. In this paper, we compared the mixed system of additive and reactive monomer (RM) with the single additive system.
From the results, we can find that the mixed system showed similar alignment ability and voltage holding ratio (VHR) with the single additive system. However, the mixed system had better image sticking performance than the single additive system. From the pretilt angle shift, it can be concluded that the mixed system of additive and RM had better pretilt stability than that of the single additive system.

2. Experiment

The PI-free liquid crystal was purchased from JNC, DIC or Merck Corp. The concentrations of additive is about 0.1~2.0% and the concentrations of the reactive monomer is about 0.1~2%. To evaluate alignment performance, the 10*10 VA cells and 28" panel were fabricated by sandwiching the nonpatterned ITO glass (downward one) and the multidomain electrode substrate (upper one). The cell gap of the fabricated cell and panel were maintained to be 3.2μm. The intensity of the UV light in the wavelength range from 300 to 365 nm was 1.32 mW/cm^2. The exposure energy was adjusted in the range from 80 to 800 mJ/cm^2.

3. Results and discussion

The additive and RM molecule structures, the different additive systems used for the PI-free LCD and the diagram of the polymerization process were shown in scheme 1. The additive structure containd 4 groups: 1. The alignment group;
2. The core group; 3. The polymerization group; **4**. The polarity group. The RM structure is the normal structure used in polyimide-aligned PSVA. The polymerization process of two different additive system were same to study the effect of materials to alignment and reliability performance.

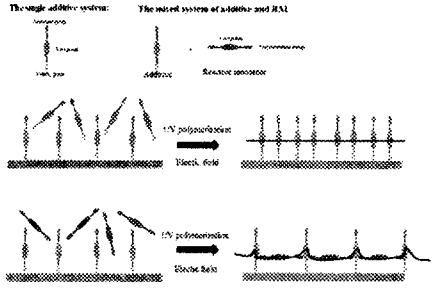

Scheme 1: Two additive system used for the self alignment LCD and the diagram of the polymerization process

First, the cells without the conventional alignment layer were proposed (Fig. 1). From the potographs of the PI-free cells under crossed polarisers, it was found that both the cells fabricated by the mixed system (additive + RM) and by the single additive system showed dark states without applying any electric fields. This indicated that the LC molecules were vertically aligned in initial states. When the electric field (7 V) was applied across the PI-free cell after polymer stabilization, disclination line were not appeared in the cells with different additive systems. This results clearly indicate that the cells with different additive systems showed the similar alignment ability.

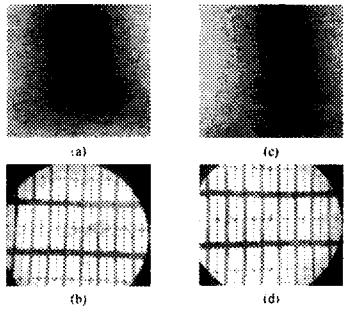

Figure 1: The dark state and the alignment status of the cells fabricated by the single additive system (a-b) and the mixed system (c-d)

Then the voltage holding ratio (VHR) was meatured. Figure 2 showed that the cells with different additive systems had similar VHR value of above 97% at 60°C , which reached the same level compared with the cell with polyimide alignment layer.

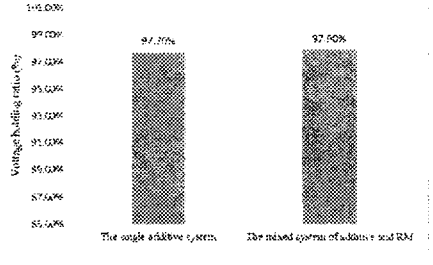

Figure 2: The value of different additive systems

Then PI-free TV panels of 28 inch were developed, and the alignment (Fig. 3) and image sticking perfomance (Fig. 4) stressed at 40°C for 72 h were meatured. Fig. 3 exhibited that both two kinds of 28" panels fabricated by different additive systems showed good alignment ability similar to 10*10 cells.

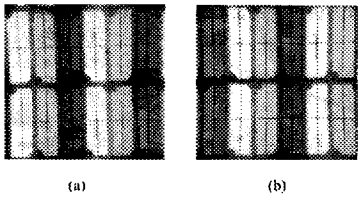

Figure 3: The alignment image of 28" panel fabricated by mixed system (a) and single additive system (b)

Figure 4 showed the IS photograph of panel stressed at 40°C for 72 h. It could be clearly found that the panel with single additive system had obvious IS image and no IS image was found in the panel with mixed additive system. The value of Just Noticeable Difference (JND) showed more explicit information of the IS performance: the JND value of 28" panel with mixed system was 0 and the the JND value of 28" panel with single additive system was biggere than 4. This shows that the mixed system has better IS performance than that with only additive system.

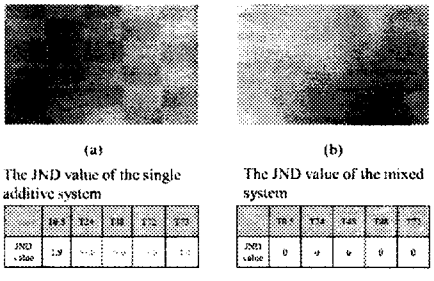

Figure 4: The photograph of the 28" panel stressed at 40°C for 72 h fabricated by the single additive system (a) and the mixed system of additive and RM (b) at 0 gray

Many cause affects the IS phonomenon. To analyze the factor of materials, we meatured the pretilt angle shift of black area and white area. Fig. 5 showed that the better IS performance of the mixed system was derived from the better pretilt angle stability. We also use test cell to measure the pre-tilt angle of LC at alignment. Test cell is designed to measure electrical and optical characteristics easier, because it has no TFT. From the pretilt angle shift of test cell, we could find that the measurement result of pre-tilt angle shift by test-cell match with that of real panel.

Then we concluded that the mixed system (additive + RM) had better pretilt angle stability due to better polymer density than the single additive system.

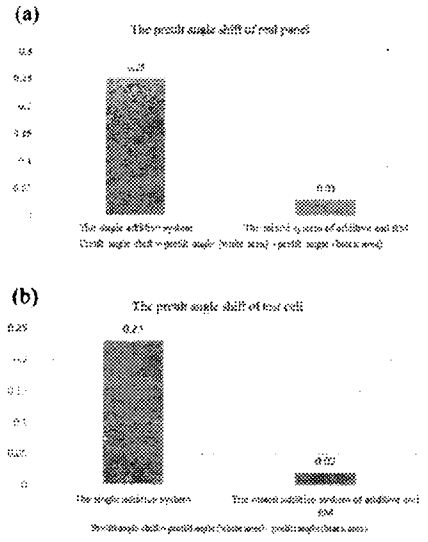

Figure 5. The pretilt shift of the panel (a) and test cell (b) stressed for 72 h.

4. Conclusions

In conclusion, we studied the role of RM in the alignment and image sticking performance. From the study, we can find that the RM has no obvious effect on the alignment ability, and the cell with single additive system showed similar alignment status with that of mixed systems. However, the 28" panel with mixed system of additive and RM showed better image sticking performance than the panel with single additive system. And the data of pretilt angle shift demonstrated that the polymer formed by the mixed system of additive and RM had better pretilt angle stability. Our work advance the development of PI-free technology and provides insights into the development of the material of PI-free LC.

5. Acknowledgment

This work is supported by Guangdong (China) Innovative Research Team Program NO.2011D079.

References

[1] Schadt M. Nematic liquid crystals and twisted-nematic LCDs. Liquid Crystals, 2015, 42(5-6): 646-652.

[2] Oh-e M, Kondo K. Quantitative analysis of cell gap margin for uniform optical properties using in-plane switching of liquid crystals. Japanese journal of applied physics, 1997, 36(11R): 6798.

[3] Lee S H, Lee S L, Kim H Y. Electro-optic characteristics and switching principle of a nematic liquid crystal cell controlled by fringe-field switching. Applied physics letters, 1998, 73(20): 2881-2883.

[4] Takeda A, Kataoka S, Sasaki T, et al. 41.1: A Super- High Image Quality Multi - Domain Vertical Alignment LCD by New Rubbing - Less Technology//SID Symposium Digest of Technical Papers. Oxford, UK: Blackwell Publishing Ltd, 1998, 29(1): 1077-1080.

[5] Lee G D, Son J H, Choi Y H, et al. Control of the defect in the liquid crystal director field on the slit of the patterned vertical alignment cell. Applied physics letters, 2007, 90(3): 033509.

[6] Fang Y Q, Wang J, Zhang Q, et al. Synthesis of soluble polyimides for vertical alignment of liquid crystal via one-step method. European Polymer Journal, 2010, 46(5): 1163-1167.

[7] Haba O, Hiratsuka D, Shiraiwa T, et al. Homeotropic orientation of nematic liquid crystals induced by dissolving polypropyleneimine dendrimer having peripheral mesogens. Optical Materials Express, 2014, 4(5): 934-943.

[8] Jeng S C, Kuo C W, Wang H L, et al. Nanoparticles-induced vertical alignment in liquid crystal cell. Applied physics letters, 2007, 91(6): 061112.

[9] Song Lan, Xingwu Chen, Hongquan Wei, et al. Self-Alignment of Liquid Crystal for Multi-Domain Liquid-Crystal Display. SID ,36-2, 2018.

A novel bistable LCD with function of monostable operation

T.Takahashi, R.Takahashi, Y.Kudoh
Kogakuin Univ., Japan

1. Introduction

We propose a novel LCD mode named Bistable of Twisted Direction Switching (BTDS) LCD enables to work not only a memory LCD with the bistability but also as a conventional LCD with the monostability. The fundamental schematic model is shown in Fig. 1. When this LCD is performed as a memory LCD using the bistability, the twisted direction of the director orientation in the cell is switched between the right twist (Φ) and the left twist ($\pi-\Phi$). The twisted angle Φ can be designed to any value within the bistable condition.

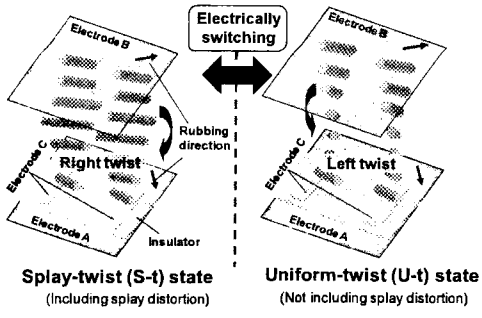

Figure 1: Schematic model of BTDS cell in each memory state

2. Condition of Cell Parameters for Bistability

The Gibbs energies caused by the distortion of director orientation inside the cell due to the twisted alignment state of both right twist [Φ] and left twist [$\pi-\Phi$] were designed to be equal by the numerical calculation. For example, the cell parameters used for calculations were as follows; a pretilt angle, amount of chiral dopant, an angle formed by rubbing directions between upper and lower substrates. Moreover, since the azimuthal anchoring works on each substrate surface, then two orientation states can exist independently due to an appropriate magnitude of energy barrier between each state. If those states can be switched electrically, a bistable LCD can be realized. Since we can design any twisted angle Φ in our BTDS LCD mode, we believe that there is also a high flexibility in the optical design.

3. Electrical Operation of BTDS Cells

3.1 Switching for Bistable Mode

In the S-t state, if the electric field is applied along with the cell thickness direction, the orientation state can be transitioned into the U-t state. On the other hand, in the U-t state, when the electric field is applied to in-plane direction such as an IPS[1] or an FFS[2] modes, the orientation sate is transitioned again into the S-t state.

The example of the LC cell in the bistable mode applied to a reflection type is shown in Fig. 2, using a $\lambda/4$ plate and one polarizer. The cell parameters were follow; pretilt angle $\theta_0=35°\Phi$, = 70°, a ratio of cell thickness and chiral pitch d/p_0 was approximately 0.03, and retardation Δnd = 0.32 μm. Then, 24.1 of the optical contrast ratio was obtained.

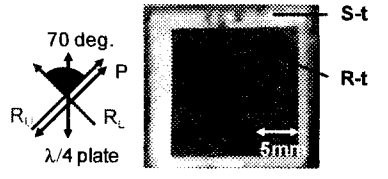

Figure 2: Reflective type of BTDS cell operating in bistable mode

3.2 Normal Video Display with Monostable Mode

Under the S-t state, even if the horizontal electric field with any value of the voltage is applied, the orientation state remains in the S-t state and does not transition to the U-t state. That is, by applying the horizontal electric field in the s-t state, a normal type of LCD which is displayed the voltage controlled grayscale image can be realized. Alternatively, even in the U-t state, the monostable operation is possible in the same way by using the applied electric field in the cell thickness direction. A moving image can be displayed as a normal LCD, and still image can be displayed using the bistable memory function as needed, although, the still image is a binary display without grayscale.

4. Conclusion

We proposed BTDS-LCD using nematic LCs and described the fundamental principle of it. While this BTDS-LCD is a novel LCD mode that exhibits bistable memory function applicable as an electronic paper, it is also capable of moving picture display with grayscale images as a monostable mode like ordinary LCDs, and those modes can be switched arbitrarily.

5. Acknowledgements

We would like to offer our special thanks to Dr. Toko of Stanley electric Co., Ltd. who provided helpful comments and suggestions. We would like to express our sincere gratitude to Merck for providing LC materials and Nissan chemical for providing alignment materials as an experimental material for this research.

6. References

[1] R. A. Soref: J. Appl. Phys., 45(12), 5466(1974).
[2] S. H. Lee, S. L. Lee and H. Y. Kim: Appl. Phys. lett., 73, 2881(1998).

O-18

New way to create high-speed LCDs based on the use of modified nanomaterials

V.Lapanik, A.Lugovsky, S.Timofeev
Institute of Applied Physics Problems, Belarus

Abstract
Modified "detonation nanodiamond" (MDND), graphene oxide (MGO) and nanoclay (MNC) were doped to nematic (NLCs) and ferroelectric liquid crystals (FLCs). The effect of modified nanomaterials on the physical and electro-optical properties of liquid crystals was investigated.

Diamond is one of the most popular materials which can exist in the form of nanoscale particles. Special class of nanodiamond material with characteristic sizes of 4 to 5 nm, often called in the literature "ultradispersed diamond" (UDD) or "detonation nanodiamond" (DND), were produced by detonation of carbon-containing explosives.
For the functionalization of detonation nanodiamonds, we attached carboxylate groups by grafting. Activation of COOH-surface functionalized groups allowed attachment of various organic tails [1]. It is established that the effect of MDND on the dielectric properties of LCs depends on the size of nanoparticles and the type of rod-like elongated organic molecules attached to the MDND. It was found that nanoparticles of small size (4-5 nm) do not significantly affect the LCs parameters. At the same time, MDND-based conglomerates with a diameter of about 50 nm or about 100 nm can increase or decrease the dielectric anisotropy and LCs response time by 1.5-2.5 times, depending on the polarity of the tails.

Liquid crystals with ferroelectric properties are characterized by a very fast switching speed due to the linearity of the electro-optical effect (in the microsecond range). However, the lack of a stable orientation due to its destruction, even with a small mechanical action, is the main obstacle preventing the commercialization of such devices. To solve the above problems, we investigated the influence of graphene on the dielectric properties of LCs, since the dielectric characteristics of LCs have the greatest influence on the threshold and dynamic parameters of various devices based on liquid crystals [2].

From the experiment, we found that the dielectric spectra of pure nematic composition and composition doped with graphene are almost identical, except for one effect. The addition of graphene reduced the dielectric anisotropy sign inversion frequency by 100 kHz. Study in this area is promising, since many research centers are actively involved in the development of dual-frequency LC materials, through the synthesis of new classes of compounds. It is an expensive and lengthy process. In our case, this problem can be solved more easily.

It was found that the addition of graphene significantly affects the dielectric properties of ferroelectric LCs, and also leads to an increase in spontaneous polarization and a decrease in viscosity. The addition of graphene increases spontaneous polarization by 20 - 25% and increases the tilt angle by 15 - 20%. In turn, these parameters have the greatest impact on the response time of the ferroelectric LCDs (reduces the response time by 70 - 90%). It should also be noted that the addition of MGO to FLCs leads to the effect of bistability, improves orientation and resistance to mechanical deformations. Thus, we can conclude that MGO is promising as an additive to LCs for the development of high-speed and bistable displays.
MNC is a very promising candidate for the creation of LCs composites because of the high cation exchange capacity, the very small size of the plates and the large surface area. In addition, the chemical nature and porous structure of the surface of the MNC can be easily modified. Samples of FLCs doped with MNC are characterized by large values of the spontaneous polarization compared with "pure" FLCs. The significant decrease in the switching times observed in the experiments is obviously also due to a significant decrease in the rotational viscosity of the FLCs when MNC is added to it.

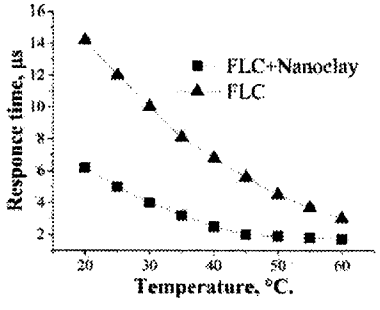

Figure 1: The response time of FLCs and FLCs doped with MNC

References

[1] V. Lapanik, A. Lugovsky, S. Timofeev, W. Haase, " Influence of the size and the attached organic tail of modified nanodimond on the physical properties of liquid crystal " Liquid Crystals, Vol. **41**. N 9. pp. 1391-1397, 2014.

[2] V. Lapanik, S. Timofeev, W. Haase, " Electro-optic properties of nematic and ferroelectric liquid crystalline nanocolloids doped with partially reduced graphene oxide " Phase transitions, Vol. **89**. N 2. pp. 133-143, 2016.

Study on promoting transmittance on dielectric multi-layers for IGZO LCD displays

Ningbo Yi[1,2], Lixia Li[2], Sibang Long[2], Sen Yan[2], Feng Zhao[2], Shimin Ge[2], Shan Li[2], Lei Luo[2]
[1]Peking University Shenzhen Graduate School, Shenzhen 518055, China
[2]Shenzhen China Star Optoelectronics Technology Co., LTD, Guangdong, China

1. Introduction

In recent years, IGZO is widely used in TFT-LCD owing to its good electric properties comparing to a-Si[1-3]. The first prototype of 85-inch 8K4K 120Hz LCD with BCE-IGZO structure from CSOT in the world attracted many peers' eyes in 2016[4]. With the increase of TV size and refresh rate from customer's demand, IGZO is good choice to satisfy the technical index instead of a-Si. To overcome this shortcomings, complex layers of SiOx and SiNx is a welcome solution for GI and top passivation insulator (PV) layers with the high permittivity and process. From our previous study in numerical simulation, the complex layer could result in color shift and low transmittance for R, G and B. In this paper, the optimization experiments was carried out to demonstrate the theoretical prediction and adopted in a demo of IGZO TFT LCD displays.

2. Results and Discussions

From the experiment in this study, the multiple layers of SiOx and SiNx in bottom gate and top passivation insulator of aperture area might introduce different efficiencies for R/G/B components in backlight. Due to the phase mismatch between different dielectric materials (n_{SiOx} ~ 1.5, n_{SiNx} ~ 1.9) and guided-wave absorbent mode existence in optically denser medium, the layered structure of SiOx and SiNx plays a critical role for optical propagation to improve the transmittance. Therefore, it is useful to promote the performance of display with a-IGZO channel to optimize the insulator layers structure to realize high transmittance for backlight through single glass.

3. Transmittance in Aperture Area

In TFT-LCD, transmittance is one of most important factors for open cells in relation to the contrast ratio and luminance. Notably, transmittance is also calculated from the single glass transmittance for backlight. The cost and energy consumption of backlight is a critical problem if an open cell with low transmittance. Transmittance is related to not only materials and process, but also the arrangement of different materials due to the theory of optics physics. As shown in Figure 2, there are several peaks of strong optical absorption corresponding to the central wavelength of R, G and B, which could lead to low efficiency of optical transmission in dielectric multi-layers for total backlight. It demonstrated that the dielectric multi-layers with different structures and ratios could results in various transmission band gaps in the experiment. Therefore, it could be an important method to promote the transmittance for LCD displays via optimizing the layers structures.

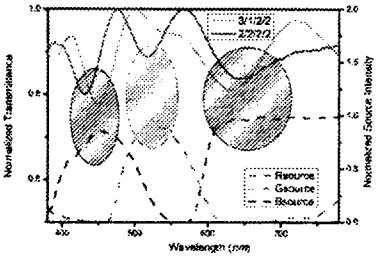

Figure 2: The transmittance spectra of multilayered structure and color filter in simulation and experiment. Inset: the distribution

4. Acknowledgements

The authors gratefully acknowledge the members in CSOT's programs on IGZO TFT-LCD displays. Thank for the support from team in Peking University Peking University Shenzhen Graduate School. This work was supported by China Postdoctoral Science Foundation (2019M650004).

5. References

[1] Meng Wang*, Yang Zhao*, Qi-Ming Gan*, Feng Zhao*, CK Zhang*, Long-Qiang Shi*, Li-Mei Zeng*, Chao Dai*, Ted Lee*, Hou-Liang Hu*, Jerry Wu*,Chung-Yi Chiu*, Chia-Yu, "Development of 32-in. 8k4k LCD with Oxide Semiconductor and GOA Technology", IDW 2015 digest, PP 195-198, 2015.

[2] Shi-Min Ge*, Shan Li*, Shu-Jhih Chen*, Xiang-Yong Kong*, Yan-Hong Meng*, Wen Shi*,Long-Qiang Shi*, Wei Wu*, X Liu*, Qi-Ming Gan*, Yang Zhao*, CK Zhang*, Chung-Yi Chiu*,Chia-Yu Lee* "Development of Cu BCE-Structure IGZO TFT for a High-ppi 31-in. 8K x 4K GOA LCD", SID 2017 digest, PP 592-595, 2017.

[3] Long-Qiang Shi*, Shu-Jhih Chen*, Yi-Fang Chou*, Li-Mei Zeng*, Mian Zeng*, Tian-Hong Wang*, Ren-Lu Chen*, Cong-Wei Liao*, Xiao-Wen Lv*, Wen-Ying Li*, X Liu*, Chia-Yu Lee*, "Design of Highly Reliable Depletion-Mode a-IGZO TFT Gate Driving Circuit for 31-in. 8K4K 287-ppi TFT-LCD", SID 2017 digest, PP 68-71, 2017.

[4] Lee*, Alan Lien** Ryutaro Oke, Takashi Nakai, Junichi Maruyama, Daisuke Kajita, Kaori Miyazaki, Masahiro Ishii,Hideki Matsukawa, Masahiro Ishii, Hideki Matsukawa, "World's First 55-in. 120Hz-Driven 8k4k IPS-LCDs with Wide Color Gamut", SID 2015 digest, PP 1055-1058, 2015.

The controllable of alignment state of polyimide-free liquid crystal displays by adjusting parameter of process technology

Yu Zhang[1,2], Song Lan[2], Qian Li[2], Xingwu Chen[2], Te-Jen Tseng[2], Chung-Ching Hsieh[2]
[1]Peking University Shenzhen Graduate School, China
[2]Shenzhen China Star Optoelectronics Technology Co., Ltd, Guangdong, China

1. Introduction

Nowadays, liquid crystal displays (LCDs) have attracted considerable attention due to their special properties, including high contrast[1], high transmittance[2], rapid response[3], *etc.* LCDs are widely used in information-oriented society, such as television sets , notebook computers, digital signal, etc. To date, various LC modes are used to fabricate LC device, such as twisted nematic (TN) mode[4], in-plane switching (IPS) mode[5], fringe-field switching (FFS) mode[6], polymer-stabilized vertical alignment (PSVA) mode[7]. Among these various modes, PSVA mode have a significantly high contrast ratio due to LC molecules are vertically aligned with the help from vertical alignment (VA) layers. Polyimide layers (PI) are widely used as VA layers in conventional LCD modes for LC initial alignment.. However, the preparation of VA layers usually requires large amount of chemical solvent, high temperature during post-bake, cleaning possess. Otherwise, some technology margin is limited by PI layer. Therefore, it is necessary to develop polyimide- free technology in LCD fabrication process to avoid risk, cost reduction and enhance performance.

In this report, we systematically investigated the influence of the concentration of additive, the routes and temperature of possess, liquid crystal drop filling pattern and diffusion distance on the polyimide-free liquid crystal display. We explores a series of LC cells containing SVA additive with different concentration, including mass ratio of 1 %, 2 %, 3 %. Adjusting process temperature and routes, we raised temperature at 120 °C before UV light irradiation, then compared alignment force variation at different concentration of additive. We also investigate the effect of additive diffusion distance on polyimide-free liquid crystal display by changed LC drop filling pattern. The obtained LC cells were characterized and tested using microscope, liquid crystal reliability measuring instrument. In this report, we will describe the alignment state, voltage holding property(VHR), and electro-optical property of SVA-LC cells. We presume the inner relationship among alignment force, additive concentration and diffusion distance. The self alignment force will decrease with diffusion distance increasing, increase with concentration increasing.

2. Results and discussions

To improve alignment state, innovation process was applied in this study, added heating process before UV light irradiation. As shown as figure 1, it can be clearly observe edge light-leaking and light spot before heating. After heating at 120 °C for 1 h, LC cells' light spots were significantly reduced and present well alignment state. Adjusting additive concentration from 1 % to 3 %, light spots and alignment state can be improve before heating. After heating, light spots and alignment state can all further improve, LC cells present well vertical alignment state.

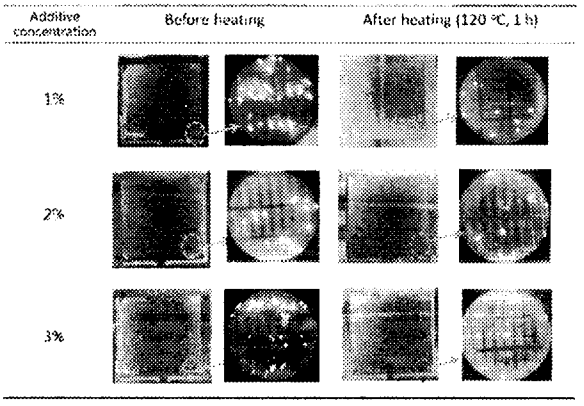

Figure 1: The comparison images of vertical alignment state before and after heating with different concentration additive

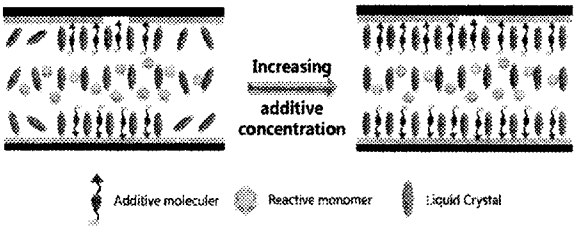

Scheme 1. Schematic illustrations of synthetic procedure of vertical alignment LC cell

The presume mechanism which significantly improved alignment state is the arrangement of additive is the key influence factor to maintain LC molecule vertical alignment state, shown as scheme 1. With increasing additive concentration, more LC molecule will maintain vertical alignment with the additives' help. The alignment force become stronger with additive concentration increasing. Then, molecule and additive will rearranged during heating process. The high concentration additive will be equally distributed in LC cells, each LC molecular will esthetic vertical alignment force and maintain

vertical alignment state. In a word, additive concentration increasing and heating process prompt LC molecule esthetic balance and strong vertical alignment force, thus LC cells represent well alignment state.

At the same concentration additive condition, additive diffusion distance is another important factor in this study. Therefore, different LC one drop filling (ODF) patterns were employed, as shown as figure 2 a, b. The same LC drop counts in pattern A and pattern B , the difference of two patterns is distance between first LC drop filling location with seal side location, pattern A is 20 mm, pattern B is 10 mm. Figure 2 c shows LC cells with different ODF pattern present different dark state and light state. LC cell using pattern A can clearly observe edge light-leaking at dark state. At bright state, edges of cell cannot maintain well alignment. The images taken by microscope clearly indicate LC molecule disorderly arrangement at edge area. In contrast, LC cell using pattern B shows well alignment edge and middle at dark and bright state. Before and after UV light irradiation, voltage holding property (VHR) of LC cells were tested, shown in figure 3. After UV light irradiation, LC cells with pattern A or pattern B will keep high VHR, high VHR will benefit of device reliability.

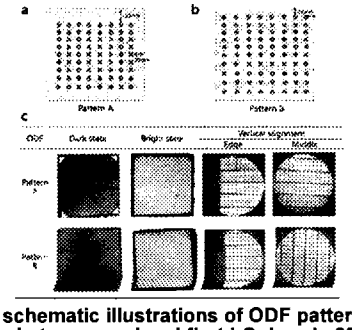

Figure 2a: schematic illustrations of ODF pattern A, the distance between seal and first LC drop is 20 mm
Figure 2b: schematic illustrations of ODF pattern B, the distance between seal and first LC drop is 10 mm
Figure 2c: observation images by different ODF pattern at dark and bright state, and vertical alignment images at edge and middle area

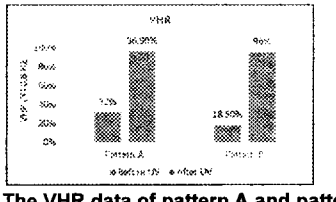

Figure 3: The VHR data of pattern A and pattern B before and after UV irradiation

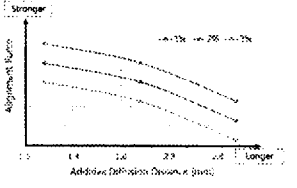

Figure 4: The trend line of alignment force changed with adjusting additive diffusion distance and additive concentration

According to the above data, the inner relation among alignment force (AF), additive concentration (C) and additive diffusion distance (D) is shown as figure 4. The self-alignment force will decrease with diffusion distance increasing, increase with concentration increasing. Again assuming that relation follows inclusion theory, it follows that equation (1).

$$AF \propto C/D \qquad (1)$$

3. Conclusion

In this report, we systematically investigated the influence of the concentration of additive, the routes and temperature of possess, liquid crystal drop filling pattern and diffusion distance on the polyimide-free liquid crystal display. The inner relationship among alignment force, additive concentration and diffusion distance was presumed. The self-alignment force will decrease with diffusion distance increasing, increase with concentration increasing.

4. Acknowledgements

The authors gratefully thank the supports of Shenzhen China Star Optoelectronics Technology Co., LTD, Shenzhen, China. This work was supported by China Postdoctoral Science Found (2019M650309).

5. References

[1] Hanaoka K. et al. A New MVA-LCD by Polymer Sustained Alignment Technology. SID,p.1200 .

[2] Zhang X. H. et al. Critical Effect of Polymer Bumps in PS-VA LCD.SID, 44,p.611(2013).

[3] Chen T. S. et al. Advanced MVA III Technology for High-Quality LCD TVs.SID, 52,p.776(2009).

[4] Shadt M. Nematic liquid crystals and twisted-*nematic LCDs. Liq Cryst. 2015;42:646-652.*

[5] Oh-e M.,Kondo K. Electro-optical Characteristics and Switching Behavior of the In-plane Switching Mode.Appl.Phys.Lett., 67, p.3895

[6] Lee S. H. et al. Electro-Optical Characteristics and Swithching Principle of a Nematic Liquid Crystal Cell Controlled by Fringe-Field Swithcing. Appl. Phys. Lett. 73, p.2881(1998).

[7] Pai C.H. et al. Fast-Response Study of Polymer -Stabilized VA-LCD. SID,18, p.960(2010).

[8] Jeng S-C, Kuo C-W, Wang H-I, et al. Nanoparticles induced vertical alignemnet in liquid crystal cell. Appl. Phys. Lett.2007.

[9] Inoue Y., Kimura M., et al. A Novel Reactive Monomer for Self Vertical Alignment Liquid Crystal Displays, SID, 474, 34-1(2019).

Controlling pre-tilt angles using rubbed PEDOT / PSS and DMOAP films for ITO-free LC devices

Y.Kudoh, H.Yoshioka, T.Takahashi
Kogakuin University, Japan

1. Introduction

Currently, poly(3,4-ethylenedioxythiophene) polystyrene sulfonate or PEDOT / PSS is expected as a new transparent electrode material to replace the rare metal, indium tin oxide (ITO). The PEDOT / PSS film has a possibility to use not only transparent electrodes but also alignment films of liquid crystals (LCs) [1, 2]. PEDOT / PSS shows a good compatible with a plastic flexible substrate due to a low-temperature process since it is an organic material. If two functions such an electrode and an alignment film can be realized by using the PEDOT / PSS film, a low-cost LCD with plastic substrates may be realized due to a simple process. In our previous report, the electro-optical characteristics of the LC cell injected 5CB were reported,[3] and under 1° of small pretilt angle for the rubbed PEDOT / PSS film was observed. However, for application to various display modes, the vertical orientation and the high pretilt angle are required to apply PEDOT / PSS. And it is very important to realize them by a low-temperature process of amperometry 100°C in order to prevent deterioration of the organic conductive material and the flexible substrate. The dimethyloctadecyl [3- (trimethoxysilyl) propyl] ammonium chloride (DMOAP) is known as a vertical alignment material and can be easily deposited by spin coating. Also, unlike polyimide alignment materials, the effect can be obtained just by volatilizing the solvent. In this report, we propose a method to induce a high pretilt angle by laminating DMOAP film on PEDOT / PSS layer.

2. Method

A PEDOT / PSS solution TC-09 (Iwatsu Manufacturing) was spin-coated at 3000 rpm × 20 s onto the cleaned glass substrates coated with ITO and dried at 120 °C for 30 min. Here, the ITO electrode was supplementary used to maintain the stability of the measurement of pre-tilt angles. Thereafter, the rubbing treatment was carried out for the substrates and the hydrophilic treatment was applied. Then, the DMOAP (Sigma-Aldrich) solution diluted with methanol (FUJIFILM Wako Pure Chemical) was spin-coated at 3000 rpm × 20 s onto the PEDOT / PSS layer and dried at 120 °C for 30 min. Homogeneous orientation cells with 20μm thickness were assembled using the substrates. ZLI-2293 (Merck) of cyano-based nematic LC was injected into the cells with isotropic phase and cooled down to the room temperature.

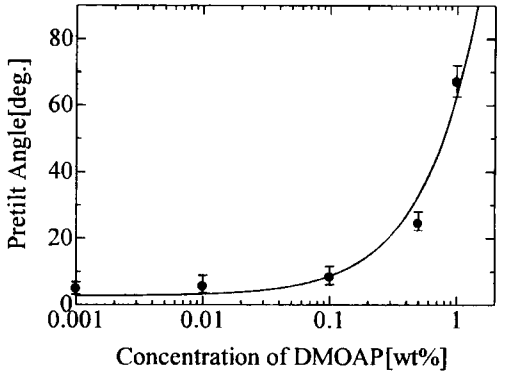

Figure 1: Measurement result of pre-tilt angles

3. Result and Discussion

Figure 1 shows the measurement result of pre-tilt angles by magnetic null method. The higher the concentration of DMOAP solution, the higher pre-tilt angle was obtained. This was because by using a high concentration DMOAP solution, the film thickness became thick and the influence of the rubbed PEDOT of the base was diminished. Furthermore, it was confirmed that the influence of the anisotropy generated by the rubbing treatment strongly gave the orientation control force even if the DMOAP film existed.

3. Acknowledgements

We would like to thank Iwatsu Manufacturing for supplying the PEDOT / PSS solution, we also thank Merck for supplying the LC material.

References

[1] T. R. Chou, S. H. Chen, Y. T. Chiang, Y. T. Lin, and C. Y. Chao, "Highly conductive PEDOT:PSS films by post-treatment with dimethyl sulfoxide for ITO-free liquid crystal display," J. Mater. Chem. C, vol. 3, no. 15, pp. 3760–3766, Apr. 2015.

[2] J. De Smet, A. Avci, P. Joshi, D. Cuypers, and H. De Smet, "P-159L: Late-News Poster : A Liquid Crystal Based Contact Lens Display Using PEDOT: PSS and Obliquely Evaporated SiO2," SID Symp. Dig. Tech. Pap., vol. 43, no. 1, pp. 1375–1378, Jun. 2012.

[3] Y. Kudoh, H. Yoshioka, and T. Takahashi, "Liquid Crystal Alignment on Rubbed PEDOT/PSS Films ," Japanese Liquid Crystal Society Ekisho-Tronkai-Yokoshu, PA 35, Sept. 2016. (In Japanese)

Collimated backlight for liquid crystal displays

Brecht Berteloot[1,2], Jeroen Beeckman[1], Gert Stuyven[2], Koenraad Vermeirsch[2], Kristiaan Neyts[1]
[1]Ghent University: Liquid Crystal and Photonics group, Belgium
[2]ScioTeq, Belgium

1. Introduction

In this work, a collimated backlight design is presented. Traditionally backlights are either direct-lit in which an array of LEDs are directly behind the LC- panel, or edge-lit, in which case there is a light guide behind the LC-panel and LEDs are placed at the side of this light guide. These designs have their advantages and disadvantages but in both cases they emit light under a wide angle.

Using a collimated backlight can however provide several advantages compared to a normal backlight with regards to contrast ratio, transmission, color, 3D-applications and energy consumption. [1,2]

In literature, directional backlights can be found which achieve a degree of collimation in the range of 15° down to 4.9° (full width half maximum values). This collimation is however only achieved in the horizontal direction, while the collimation in the vertical direction is still close to 20° or more. [1,2,3]

2. Design of the collimated backlight

The design of the backlight uses a grid of LEDs, as in a direct-lit backlight. The light of these LEDs are collimated by using 2 consecutive lenses. The first lens is placed close to the LED. Its goal is to collect all the light of the LED and emit it under a narrower angle. The second lens is bigger and is used to collimate the light further. The design was simulated and optimized by means of the Optic Studio software package.

2.1 Used components

The chosen LED is sold by OSRAM (model: LUW GVCP) and ray-files for this LED are available online, which have been used in the simulation.
To keep the design "prototype-friendly", it has been decided to use a standard aspheric lens as the first lens. The second lens is a freeform lens which has been optimized for use in combination with this LED and the aspheric lens. In order for the backlight to have a complete illumination plane, these second freeform lenses have been cut into a hexagon and are stacked next to each other in a hexagonal array as shown in fig. 1.

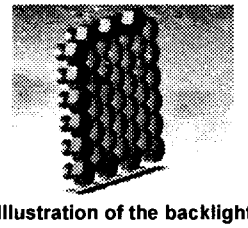

Figure 1: Illustration of the backlight design

2.2. Simulated Performance

The designed backlight shows a uniformity of 73% (at 11mm from the backlight). The hexagonal pattern is visible with a higher brightness in the center and at the edges of each hexagonal lens. The collimation is 4.7° for both vertical and horizontal directions. This angle is defined by the positions where the intensity is reduced to 10% of its maximum.

3. Prototype Fabrication and Results

The LEDs and the aspheric lenses were ordered and the designed freeform lenses were fabricated (printed) by Luximprint. Three frames were built (for the PCB, first- and second lenses) of which the position was tunable in both translation, rotation and tilt with respect to each other (6 degrees of freedom).

As can be seen in fig. 2, the backlight is not uniform and dark gaps are visible between two lenses. When a light diffuser is applied after the second lens, a uniform area is achieved at 8 cm from the backlight. By measuring the size of the beam in function of the distance from the backlight, the collimation is measured to be 8.6° and increases to 10.4° when the light diffuser is used (where intensity is reduced to 10% of its maximum).

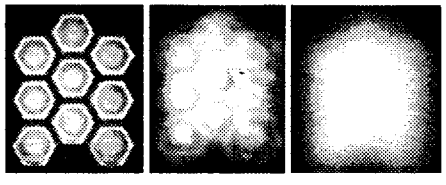

Figure 2: Image of the prototyped backlight at 1cm (left) and 8 cm (middle) from the backlight. The right figure shows the uniformity at 8cm when a light diffuser is used.

4. Acknowledgements

This work is supported by ScioTeq and a Baekeland Mandate funded by the Flemish Institute for Innovation and Entrepreneurship VLAIO.

5. References

[1] Tun-Chien Teng, Wen-Shing Sun, et al., "A slim apparatus of transferring discrete LEDs' light into an ultra-collimated planar light source," Opt. Express 21, 26972-26982 (2013).

[2] Y. Gao, Z. Luo, et al.,"A high performance LCD with wide luminance distribution,"J. Disp. Tech. 11(4),315- 324 (2015).

[3] Jui-Wen Pan, Chen-Wei Fan, "High luminance hybrid light guide plate for backlight module application," Opt. Express 19, 20079-20087 (2011)

Session 4. OLED materials

Chairman: Prof. Victor Belyaev

Invited I-10

Theoretical analysis of charge carrier injection and transport in QLED layers

Yong-Seog Kim, Sun-Kyo Kim
Hongik University, Seoul, Korea

1. Introduction

A theoretical analysis on carrier injection and transport through layers of QLED device was attempted assuming dynamic equilibrium of trapping and detrapping charge carriers. Assuming traps in exponential or Gaussian energy distribution, the effect of parameters on the current-voltage relationship for the device was investigated. The energy level and distribution of charge traps, Schottky barrier, and the ratio of de-trapping rate constant to the trapping rate constant were found to affect the current-voltage relationship significantly in the charge transport layer. The results suggest that the parameters must be modulated simultaneously in order to achieve a charge balance in the QD layer of the QLED device.

2. Theory of Charge Injection and Transport through QLED layers

When carriers are injected into a charge transporting layer from an electrode, the carrier distribution could be described by the Poisson's equation as in eqn. 1)

$$\frac{dF(x)}{dx} = \frac{q[p(x)+p_t(x)]}{\varepsilon} \qquad (1)$$

where F(x) is an electric field, q is a carrier of the current carrier, p(x) is the density of free carrier carriers, $p_t(x)$ is the density of trapped carrier carriers, and ε is a dielectric constant of the layer.

By combining equations of continuity, Poisson's equation and trap energy distribution, and integrate over the whole thickness, a self-consistent electric field that satisfies the Poisson's equation is obtained as follows[1]:

$$\int_0^d dx = \frac{\varepsilon\varepsilon 0}{q}\int_{F(0)}^{F(d)} \frac{1}{\frac{J}{q\mu F(x)}+\int_{-\infty}^{0}\frac{H_b}{kT_c}\exp\left(\frac{E}{kT_c}\right)\frac{1}{1+\frac{\gamma q\mu F\exp\left(\frac{E}{kT}\right)}{J}}} dF(x) \qquad (2)$$

With the boundary condition,

$$V = \int_0^d F(x)dx \qquad (3)$$

J-V curves can be obtained using the numerical integration process, following a similar procedure described in a previous study[2].

A. Effects of Trap Density on J-V relationship

The effects of trap density on the J-V curves are calculated and shown in Fig. 1. When the trap density is higher than $1x10^{17}$ cm^{-3}, a distinctive TFL region with a stiff slope was calculated to appear. Further increase in trap density lengthens the TFL current range and the TFL voltage, V_{TFL}. V_{TFL} was increased ~ 2 orders of magnitude as the trap density was increased 3 orders of magnitude from 1016 cm-3 to 1019cm-3.

This result implies that the control of trap density is very critical in achieving the charge carrier balance in the QLED device and in lowering the turn-on voltage (or threshold voltage) of the device.

B. Effects of Field Effect Mobility on J-V relationship

The effects of field effect mobility of the charge transport layer on the J-V curve are shown in Fig. 2. When the mobility was varied from 10^{-6} cm^2/Vs to 10^{-3} cm^2/Vs for the calculation, the current density was increased proportionally without changing the shape of the J-V curve, shifting the curves in the vertical direction as noted from the figure. The change in mobility does not influence the slope and regions of the J-V curves, instead, the current density was calculated to increase propositional to the increase in the mobility as expected from Mott-Gurney's law where current density increases linearly with the mobility. These results suggest that the change in carrier mobility would not improve the charge balance over the whole operation range since the change in the mobility would shift the J-V curve in the vertical direction, without affecting the shape of the curves.

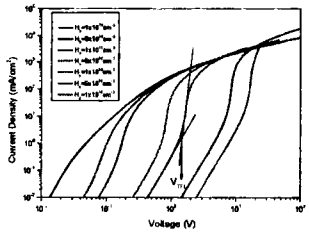

Figure 1: Effect of trap density on J-V relationship

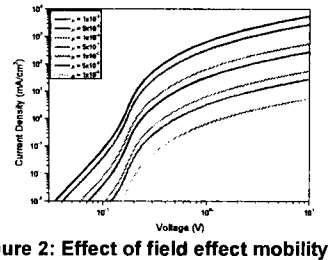

Figure 2: Effect of field effect mobility on J-V relationship

3. References

[1] M. A. Lampert, Physical Review **103,** 1648 (1956).

[2] P. Kumar, S. Jain, V. Kumar, S. Chand, and R. Tandon, Journal of Physics D: Applied Physics **41,** 155108 (2008).

TADF emitters for deep-blue OLEDs

H.Sharifidehsari, T.Baumann
Cynora GmbH, Bruchsal, Germany

In the OLED device, the power consumption is mainly determined by the emitter technology. Today's OLED displays typically utilize phosphorescent technology for the red and the green pixel. This technology is very efficient with an internal quantum efficiency (IQE) of ~100%. However, despite years of research, phosphorescence is not applied for the blue pixel due to its very short lifetime [1]. Therefore, panel makers still have to use rather inefficient fluorescent blue emitters with an IQE of ~25% or slightly more. However, a new technology has emerged that is capable to solve this issue: the TADF (thermally activated delayed fluorescence) technology [2].

This technology was introduced in 2010/2011 [3, 4]. Like phosphorescence, it can deliver 100% IQE, but TADF is actually based on fluorescent emission that is fed through a very efficient reverse intersystem crossing (RISC) mechanism (see Fig. 1).

The TADF technology can be used in two different approaches: either as emitter in the self-emitting (or classical TADF) approach, or together with a co-emitter (also called the hyper-approach, see Fig. 1). The classical approach has the advantage to be simple since it includes only a host and the emitter material in the emissive layer. Even though the TADF emission is usually slightly broader than the fluorescent emission, a full-width at half maximum (FWHM) of < 60 nm can be achieved, which is sufficient narrow for the blue pixels in mobile devices [5].

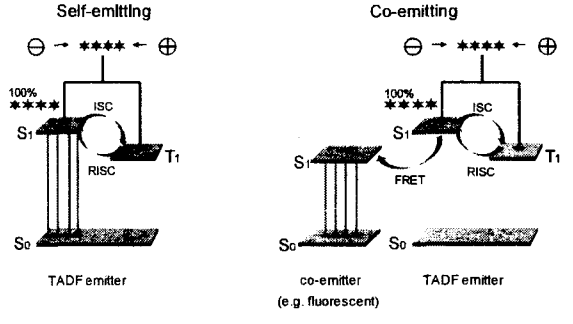

Figure 1: Schematics of the self-emitting (left) and the co-emitting approach (right)

In the case where a very specific emission spectrum is necessary, the co-emitting approach can be used. In this approach, both the charge recombination and the triplet to singlet conversion through RISC occur on the TADF emitter.

Thus, the TADF emitter also guarantees the high efficiency in this approach. But instead of an emission from the TADF material, the singlets are transferred to the co-emitter, which finally emits the light of the OLED device.

At the beginning of 2018, CYNORA was the first company to report deep-blue high-efficiency OLEDs using the classical TADF approach. In the meantime, the company has reached the required color and efficiency for deep-blue OLED pixels in the self-emitting and in the co-emitting approach (see Table 1).

Table 1. Performance of deep-blue TADF OLEDs at CYNORA using the self-emitting and the co-emitting approach

	Self-emitting	Co-emitting
CIEy@1000 cd/m² (1931 CIE)	0.15	0.15
EQE@1000 cd/m² (%)	24	18
LT95@1200 cd/m² (h)	5	10

The numbers given in Table 1 are the best performance that has been shown for deep-blue high-efficiency OLEDs so far. For the blue pixel in OLED display products the peak of the emitter always needs to be around 460 nm and the CIEy coordinate always has to be ≤ 0.15. OLEDs that do not satisfy these two color requirements are not considered deep-blue enough for display applications. Furthermore, the performance of blue pixels can only be compared when their color is also comparable since the three main performance factors (color, efficiency and lifetime) are all connected.

References

[1] H S. R. Forrest, Philos. Trans. A, 373 (2015).

[2] D. Volz, J. Photonics Energy, 6, 020901 (2016).

[3] H. Yersin, DE102010025547 (2010).

[4] A.Endo, K.Sato, K.Yoshimura, T.Kai, A.Kawada, H. Miyazaki and C. Adachi, Appl. Phys. Lett., 98, 083302 (2011).

[5] T. Baumann, D. Volz, SID Symposium Digest of Technical Papers, 45-3 (2017).

O-24

Highly efficient blue OLED

Lixin Xiao, Mengying Bian, Xuan Guo, Fan Li, Jiannan Gu, Zhijian Chen
State Key Laboratory for Mesoscopic Physics and Department of Physics, Peking University, Beijing 100871, China

Based on our work on deep blue OLED [1-3], very recently, we have synthesized a deep blue emitter TPEA that combines the advantages of TTF-HLCT to enhance the $\eta_{exciton}$ for high EL efficiencies and the merits of AIE to ensure low roll-off of device efficiency. The anthracene groups are twisted from the central TPE moiety, which effectively prevents bathochromic shift of emission as shown in its crystallographic structure. In addition, a D-A structure was built by using methoxy and cyano to improve the charge balance in the devices. In addition, the material possesses high thermal stability with a T_g of 155 °C. The non-doped device achieved the high performance with a V_{on} of 2.6 V at a luminance of 1 cd m^{-2}, a $\eta_{PE, max}$ of 11.1 lm W^{-1}, a $\eta_{CE, max}$ of 9.9 cd A^{-1}, and a low η_{CE} roll-off. The doped device based on TPEA was fabricated to acquire deep blue emission with CIE coordinates of (0.15, 0.09), showing a $\eta_{ext, max}$ up to 8.0% and the highest $\eta_{PE, max}$ of 7.3 lm W^{-1} among all the TTF and HLCT deep-blue emitters. Inspired by these preliminary results, we believe that the combination of the merits of TTF-HLCT and AIE would be a promising molecular design principle for exploring highly efficient deep blue emitters [4].

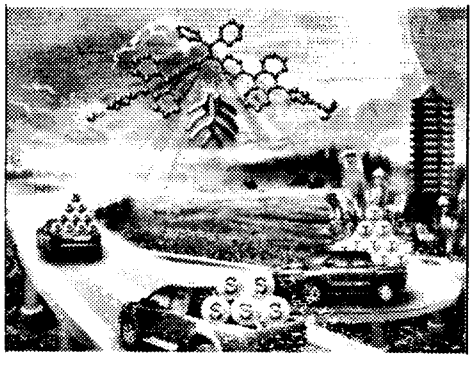

Figure 1: A combinational molecular design to achieve highly efficient deep blue electrofluorescence

References

1. Lixin Xiao et al. "A Pure Blue Emitter (CIEy≈0.08) of Chrysene Derivative with High Thermal Stability for OLED" J. Mater. Chem. C, 2015, **3(8)**, 1794-1798
2. Lixin Xiao et al. "A Deep-Blue Emitter with Electron Transporting Property to Improve Charge Balance for Organic Light-Emitting Device", ACS Appl. Mater. & Interfaces, 2012, 4(6), 2877-2880
3. Lixin Xiao et al. "Spirobifluorene derivative: a pure blue emitter (CIEy approximate to 0.08) with high efficiency and thermal stability", J. Mater. Chem., 2012, 22(30), 15136-15140
4. Lixin Xiao et al. "A Combinational Molecular Design to Achieve Highly Efficient Deep Blue Electrofluorescence", J. Mater. Chem., 2018, **6**, 745 – 753

Highly efficient and bright blue organic light-emitting devices based on solvent engineered, solution-processed thermally activated delayed fluorescent emission layer

Zheng Xu[1,2], Bo Qiao[1,2], Suling Zhao[1,2]
[1]Key Laboratory of Luminescence and Optical Information, Beijing Jiaotong University, Ministry of Education, Beijing, 100044, People's Republic of China
[2]Institute of Optoelectronics Technology, Beijing Jiaotong University, Beijing,100044, People's Republic of China,

Organic light-emitting diodes (OLEDs) have been successfully developed and have now entered the commercial marketplace, such as smart phones, flat panel displays and solid-light emitting applications. OLED displays give high contrast, large viewing angle and low energy consumption, together with high brightness and vivid colors. Thermally activated delayed fluorescent (TADF) materials are ideal candidates for high efficient OLEDs. Inefficient blue emission is one of the key bottlenecks limiting the development of solution processable displays and white light sources, which is essentially governed by the film quality of the solution-processed emission layer (EML).

In this work, we use an efficient blue TADF emitter, bis [4-(9,9-dimethyl-9,10-dihydroacridine) phenyl]solfone (DMAC-DPS), as EML and propose a solvent engineering strategy to achieve high efficiency and brightness. The strategy employs synergetic solvents to improve the film morphology of the solution-processed DMAC-DPS EML. The improved film quality enhances the carrier injectionwhile reduces the surface trap charges, as revealed by the hole-/ electron-only device performance and the transient electroluminescence measurements.

As expected, the blue OLEDs employing synergetic solvent strategy presents an increment of 22.8% in efficiency and 19.4% in luminescence, which reaches the highest efficiency of 15.76 cd/A and an efficiency of 9.63 cd/A at a luminance of 1000 cd/m2. These values are generally higher than the reported values from the blue OLEDs based on solution-processed DMAC-DPS EML.

References

[1] Yang, J.; Song, D. D.; Zhao, S. L.; Qiao, B.; Xu, Z.; Wang, P.; Wei, P., Highly efficient and bright blue organic light-emitting devices based on solvent engineered, solution-processed thermally activated delayed fluorescent emission layer. Org. Electron. 2019, 71, 1-6.

[2] Wang, P.; Huang, Q. Y.; Zhao, S. L.; Qin, Z. L.; Xu, Z.; Song, D. D.; Qiao, B., Investigating the evolution of excitons in polymer light-emitting diodes by transient measurement. Org. Electron. 2019, 68, 45-49.

Real-time threshold voltage and mobility compensation for large-size AMOLED displays

Dongwei Li[1,2], Yufeng Jin[2], Hailong Jiao[1], Gary Chaw[2]
[1] Peking University Shenzhen Graduate School, Shenzhen 518055, China
[2]Shenzhen China Star Optoelectronics Technology Co., LTD, Shenzhen, China

Abstract
A new real-time compensation method of Vth and μ for large size AMOLED display named linear charging sensing (LCS) has been developed. This compensation method can accomplish the Vth and u sensing within tens or hundreds microseconds which can realize the sensing for all the pixels of FHD (1920× 1080) AMOLED display within one frame time in theory. By simulation analysis, LCS compensation method has very high accuracy for Vth sensing with a tiny error of 0.07V for ΔVth=0.5V and no error for ΔVth=-0.5V. Further verified in FHD AMOLED panel, the method can make a great improvement for image sticking and luminance uniformity.

2. Introduction

The Active Matrix Organic Light Emitting Diode (AMOLED) display technology have developed rapidly in the past decades. However, the image sticking and luminance unifromity resulted from the TFT V_{th} and μ shift are still problems. The main approach to solve the problems is V_{th} and μ compensation at present [1][2]. In this work, we studied a real-time compensation method for large size AMOLED display, named linear charging sensing. The theory of this method is that charge the stray capacitance of the sensing line by the current I_{DS} of driving TFT and ensure the voltage change of sensing line is linear. And then quickly sense the V_{th} and μ. The sensing time of LCS compensation method is 10^3 magnitudes shorter than source follow method. It can sense the V_{th} for all the pixels of FHD display within the blank time of one frame in theory, which meets the needs for real time compensation.

3. Experiment And Discussion

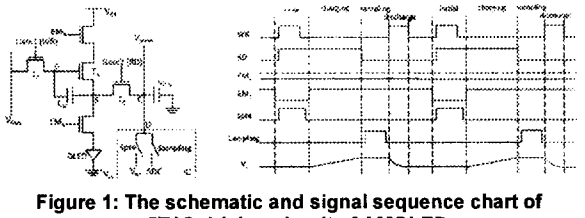

Figure 1: The schematic and signal sequence chart of a 5T1C driving circuit of AMOLED

The sensing process can be divided into three stages. In the first stage (called initial stage), the V_{data} and V_{cm} are written into the G and S spot of driving TFT, respectively and which sets the $V_{GS}=V_{data}-V_{cm}$. In the second stage (charging stage), the stray capacitance of sensing line stars to charge. In this stage, the V_{GS} remains stable because of the C_{st} so that the I_{DS} unchanged. Therefore, the boosting of the V_S and V_C is proportional to time only. In the third stage (sampling stage), the Sam switch opens and the driving system senses the voltage. After the voltages are sensed twice by the same method, we can calculate the V_{th} of driving TFT. The method of sensing μ is similar to that of V_{th}. After sensing V_{th} and μ, we can compensate ΔV_{th} and μ by external driving IC in a very short time.

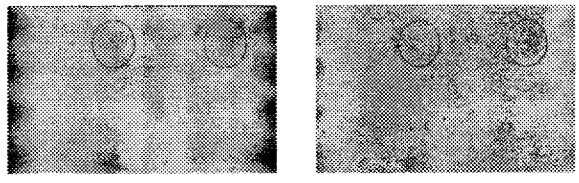

Figure 2: The performance of LCS compensation method in FHD AMOLED panel

We further analyzed the slight error of the accuracy for V_{th} sensing by simulation. The simulation result illustrates that the error of LCS method is mainly caused by the change of μ and the RC loading of gate signal. The optimum proposal is proposed to realize more accurate compensation. We also verified the performance of LCS compensation method on a FHD AMOLED display which shows good luminance umiformity and without image sticking.

4. Conclusion

The LCS compensation method shows a very good performance for the improvement of image sticking and display uniformity.

5. Acknowledgements

Authors acknowledge CSOT and Peking University Shenzhen Graduate School for the supporting grants.

6. References

[1] S. Takasuqi et al., Advanced Compensation Technologies for Large-Size UHD OLED TVs, Journal of SID, 24(7), 235-238 July 2016
[2] J. H. Fu et al., A Fast TFT Threshold Voltage Sensing Method Based on Iterative Feedback, SID 2017 DIGEST, 16(3), 204-206, 2017

Session 5. Display materials

Chairman: Prof. Xiao Wei Sun

Invited I-11

Nanocomposites based on porous silicon: from idea to implementation

V. Bondarenko
Belarusian State University of Informatics and Radioelectronics, Belarus

1. Introduction

Silicon technology has become so powerful that it pervades all spheres of our life. That is why namely silicon is the most desirable semiconductor to be a host for integration of radically new solid-state microsystems including but not limited to electronic, magnetic and optical devices. At the same time, it is common knowledge that the monocrystalline silicon (*c*-Si) demonstrates a negligibly weak photoluminescence (PL) and is non-ferromagnetic at all. For the last 50 years, many different approaches have been studied to impart ferromagnetic properties to the *c*-Si or improve its PL. However, state-of-the-art silicon technology is still not able to meet the industrial requirement of successful integration of magnetic, electronic devices and light emitting diodes (LED) in one silicon chip.

Silicon nanostructuring followed by an incorporation of other ("guest") materials is a promising alternative to modification of the *c*-Si itself. This way opens an opportunity to push the boundaries of traditional silicon technology, because the resulting nanocomposites will show the properties that are not typical for the *c*-Si and can be easily tuned by the nature of the incorporating materials.

This paper presents a review of a long-term activity of our research group aimed at finding a simple and efficient approach to synthesize nanocomposites in silicon with outstanding optical and magnetic properties. To achieve this challenging objective we used a general idea of the formation of ordered arrays of pores in silicon (*por*-Si) and their further filling with different materials to provide target properties [1]. Fabrication procedures, versatile characterization of the obtained nanocomposites and their ongoing and possible applications are discussed in this review.

2. Experimental

The *por*-Si samples of principally different morphologies were formed by electrochemical and metal-assisted chemical etching of the *c*-Si. Electrochemical and electroless methods were used to deposit rare-earth elements (REEs), magnetic and coinage metals and ZnO in the *por*-Si. Morphology of the samples was studied by scanning electron microscopy, energy-dispersive spectroscopy and X-ray diffractometry. Magnetic characterization was performed by measuring the magnetization at the temperatures from 77 to 700 K by static ponderomotive method. PL spectra were recorded at the room temperature using a complex of a monochromator-spectrograph with CCD camera. Plasmonic properties were studied by simulation of electric field, recording reflectance spectra and surface enhanced Raman spectroscopy of analytes adsorbed on the surface of nanocomposites.

3. Results and Discussion

Different combinations of the pores' geometries and deposition regimes of the "guest" materials allowed managing the nanocomposite type. We fabricated arrays of "guest" nanoparticles (NPs) laying on the *por*-Si external surface and pore-shaped nanowires (NWs) incorporated in the pores.

The nanocomposites based on magnetic metals' NPs and NWs in the *por*-Si layer of a 10-μm thickness were shown to demonstrate magnetic anisotropy, giant magnetoresistance and coherent spin waves. These properties are important magnetic recording, magneto-optics and sensing.

Deposition of the REEs (Er, Tb, Eu and Gd) in the *por*-Si resulted in fabrication of hydroxides of these elements in the pore channels. An oxidation step followed by annealing at a high temperature in inert atmosphere led to creation of the nanocomposites demonstrating an intensive PL with sharp emission peaks of the REEs.

In case of ZnO the *por*-Si thickness significantly affected the oxide deposition. If it is about 1 μm, the ZnO will grow on the surface of the porous layer, while the 10 μm thickness will result in the ZnO crystallization in the pore channels. Remarkably, the last nanocomposite was found to show slight magnetic properties and a strong visible PL that are of a great interest for magneto-optics, micro-LED and sensor applications.

The plasmonic nanocomposites were shown to extremely enhance absorption of visible and IR light and PL efficiency of REEs' NPs adsorbed on their surface.

4. Conclusion

We were able to induce ferromagnetic properties in the *por*-Si by introduction of Ni, Co or Fe into its pores. The PL was enhanced in the same way through the introduction of REEs and ZnO. In addition, we found that deposition of coinage metals on/in the *por*-Si leads to formation of nanocomposites with strong plasmonic properties.

5. Acknowledgements

The author is grateful to the members of the laboratory "Materials and structures of nanoelectronics" whose dedicated work made this complex research possible.

6. References

[1] E. Chubenko, S. Redko, A. Dolgiy, H. Bandarenka, V. Bondarenko, "Porous Silicon as Host and Template Material for Fabricating Composites and Hybrid Materials. In: Porous Silicon. From Formation to Application. Editor: G. Korotchenkov. CRC Press Taylor & Francis Group, pp.141-162, 2016.

Approaches to enhance electroluminescent efficiency of light-emitting diodes based on quasi-two-dimensional perovskite

Yanbing Hou, Wentao Bi, Bo Song, Pengcheng Jia, Junhan Guo, Zixiao Chen, Qiuhong Cui, Yufeng Hu, Zhidong Lou, Feng Teng
Institute of optoelectronic technology, Beijing JiaoTong University, Beijing 100044, China

1. Introduction

Quasi-two-dimensional (quasi-2D) perovskites with $(A_1)_2(A_2)_{n-1}Pb_nX_{3n+1}$ multi-quantum well structures are considered as the potential electroluminescence (EL) materials due to their controllable quantum confine effect which would lead a high EL efficiency. However, the quasi-2D perovskite films fabricated with solution processing technologies consist of different *n* phases and orientated layers, which limits the performance of quasi-2D perovskite light-emitting diodes (PeLEDs). To improve the performance of PeLEDs, it is essential to obtain perovskite thin films with both large exciton binding energy, complete surface coverage and suitable morphology. Here some approaches are developed to improve the performance of quasi-2D PeLEDs.

2. Experiments and results

2.1 Poly(ethylene oxide) passivated quasi-2D perovskite

In this part of work, the enhanced optical and electrical properties of quasi-2D perovskite achieved by poly(ethylene oxide) (PEO) passivation. The introduction of PEO can not only passivate the surface defects of $(PEA)_2MA_{n-1}Pb_nBr_{3n+1}$ films, but also suppress the formation of low luminous efficient *n*=1 single-layered quasi-2D perovskite phase. The photoluminescence quantum yields (PLQY) of the composite film has been approximately increased by 350% compared with pure quasi-2D perovskite film. The EL devices based on emitting layer (EML) of PEO:quasi-2D perovskite composite film have achieved a brightness of up to 41800 cd/m^2 and a maximal current efficiency of 25.1 cd/A. The EL intensity of the device with PEO passivation dropped to 70% of the initial value after around 7 hours under a constant current density of 10 mA/cm^2, which indicates the excellent operation stability. The composite film of quasi-2D perovskite and PEO would serve as promising materials for LED application.

2.2 Improved multi-quantum well structure

The morphology of quasi-2D perovskite film is not controlled easily for solution processing, which leads to low optical and electrical properties. A post-treatment method is used to change the vertical phase distribution of quasi-2D perovskite films. After this phenylethylammonium bromide (PEABr) surface post-treatment, phase purity of quasi-2D perovskite $(PEA)_2FA_2Pb_3Br_{10}$ film is obviously enhanced, which helps to improve multiple quantum wells structures and reduce the electric field induced dissociation of excitons at perovskite EML/electron transporting layer (ETL) interface. The PeLEDs based on $(PEA)_2FA_2Pb_3Br_{10}$ EML with PEABr surface post-treatment method achieve a current efficiency of 45.9 cd/A and T_{50} lifetime as high as 9.2 h, which is enhanced by approximately 150% and 400%, respectively.

2.3 Reduction in electric-field induced deactivation

An important weakness remains unsolved to the efficiency roll-off of PeLEDs with increasing brightness or drive voltage. Comparing the difference in quenching factors calculated from electric-field modulated PL and electric-filed depended lifetime of excited state of quasi-2D perovskite films, we found that the major electric-filed induced deactivation happens in funnel energy transfer process that is one of key factors to result in efficiency roll-off at high drive voltage of quasi-2D PeLEDs. The detrimental effect can be improved by doping cesium (Cs) cation in quasi-2D perovskite, which can improve the surface morphology and suppress the electric field induced dissociation of exciton for the PeLEDs. The prepared quasi-2D perovskite $(PEA)_2FA_2Pb_3Br_{10}$ film with Cs doping exhibits a remarkable PLQY up to 74%. The PeLEDs based on $(PEA)_2FA_{1.8}Cs_{0.2}Pb_3Br_{10}$ EML shows low efficiency roll-off green emission with maximum current efficiency of 55 cd/A.

3. Conclusion

Quasi-2D perovskite is one kind of the most potential EL materials. The suitable approaches and optimization for quasi-2D perovskite can make it serve as distinct and promising materials for efficient and stable LED application.

4. Acknowledgements

This work was supported by Natural Science Foundation of China (Grant Nos.61775011, 61735004, 61674012, and 61675018).

O-28

Production of retardation film with pixel strusture

V.Mikulich, A.Boboreko, P.Moiseenko, V.Shevtsov
HOLOGRAPHY INDUSTRY JSC, Republic of Belarus

1. Introduction

At present the commercial success of LC displays is achieved due to the high characteristics of quality: viewing angles, contrast, price, etc. For example, LC display have been used for creation of 3D images by means of forming images on the display for the left and right eye and using of polarizing glasses for the left and right eye. It allows us to see the resulting 3D image. Such a system can be implemented by means of using of a pattern phase retardation film which is placed on the display screen. The retardation film is a structured phase plate with display pixels order resolution which allows to form lines of images for the left and right eye without loss of image quality [1].

2. Results and discussion

One of the approaches to obtaining of 3D images is a pattern formation by means of photoalignment, namely, the surface is coated with a photocrosslinkable polymer or an azo-dye and is irradiated with polarized light through the pattern, which forms a definite direction of the optical axis. Next, this base material is covered with a polymerizable liquid crystal which is oriented towards the direction of the pixel-formed optical axis and irradiated with UV light for the fixation of LC molecules in the film. As a result, there obtained retardation film with different optical axis directions in pixels. Such an approach is simple to describe, but technologically difficult to implement. This process is characterized with labor-consuming operations, the necessity of using of high-intensity polarized radiation sources, and there arise difficulties with the quality control of individual operations of technological process [2].

In order to obtain such pixel structures we have developed a method of forming of different directions of optical axes in pixels using holographic embossing, which is used in the manufacturing of relief-phase holograms. Thus, the film surface is covered with a specially developed polymer material, which is further embossed by means of a holographic matrix with some predetermined directions of diffraction gratings. It makes possible to form the necessary direction of the optical axes in pixels. Then, this structured base material is covered with a polymerized liquid-crystal material which is polymerized by means of UV irradiation (after being died and oriented). The process is carried out roll to roll with high productivity. At present, the minimal pixel sizes are 100 per 100 microns, with the possible disorientation of the optical axes in the neighboring pixels within an angular degree. The nearest aim is to reduce the size of pixels to 10 per 10 microns, while the transition zones between pixels are not more than one micrometer.

For the production of retardation films with pixel structure we use a polymerized liquid crystal of our own production with the required values of viscosity, refractive index and phase transition temperature. It allows to obtain structured optically transparent retardation films without any loss of light.

3. Conclusions

The technology mentioned above is not limited to the manufacturing of retardation films, but it can also be used to obtain the functional units of various optical devices.

4. References

[1] T. Kawai, " 3D displays and applications" Displays, Vol. **23**, I. 1-2. pp. 49-56, 2002.

[2] E. A. Shteyner, A. K. Srivastava, V. G. Chigrinov, H.S. Kwok, A. D. Afanasyev "Submicron-scale liquid crystal photo-alignment", Soft Matter, Vol. **9**, I. 23, pp. 5160-5165, 2013.

O-29

An optical screen for light guiding in the vertical direction

S.K. Lazarouk[1], A.A. Leshok[1], A.V. Dolbik[1], A.Yu. Kliutski[1], K.T. Kolchenko[1], A.A. Kisel[1], D.V. Zhigulin[1], S. Ya. Prislopski[2]
[1]Belarusian State University of Informatics and Radioelectronics, Belarus
[2]B.I.Stepanov Institute of Physics NASB, Nezavisimosti Ave. 68, 220072 Minsk, Belarus

1. Introduction

Display devices with light guiding in the vertical direction with respect to the screen surface could be used for information security. Also the vertical light guiding could be used for interchip optical interconnects [1]. We have developed the optical screen based on macroporous alumina or macroporous silicon membrane which can provide the light propagation in the vertical direction while the other directions are prohibited.

2. Experimental Setup

Experimental structures were created by the magnetron sputtering deposition of the Al/Si film with 0.1 μm thickness and the subsequent deposition of pure Al film with 1.0 μm thickness on the n-type monocrystalline silicon wafer. The deposited films were subjected to anodic treatment in a 20 % aqueous solution of orthophosphoric acid via preformed photoresist masks at their surfaces that resulted in the formation of the composite film of nanostructured silicon embedded in the alumina matrix. Not anodized areas protected by the photoresist mask have formed metal electrodes between anodized regions. Thus sets of Schottky contacts have been formed that can emit light in avalanche breakdown mode (LED). Along with the mentioned above structures microchannel wafers of 100-150 μm thickness with through-holes (vias) with diameters of 5-6 μm are also produced.

3. Results and Discussion

Microchannel silicon wafer or microchannel alumina membrane has been formed as was described in [1] and used for light guiding in the vertical direction. The light source was either nanostructured silicon LED or laser beam with wavelength in the visible region of the spectrum for example 532 nm. The silicon photodetector has been used for the light registration. Figure 1 shows optical microscopy images of the microchannel silicon wafer providing an optical signal transmission in the vertical direction relative to the surface of the chips.

Figure 2 shows the scattering indicatrice of laser beam propagation through microchannel silicon wafer. The indicatrice of light propagation for the macroporous alumina membrane with the same pore sizes is similar. Thus we have demonstrated light guiding in the vertical direction.

4. Conclusion

We have demonstrated the ability to provide the propagation of radiation only in the vertical direction. The fabricated structure opens up new possibilities for the development of silicon photonics.

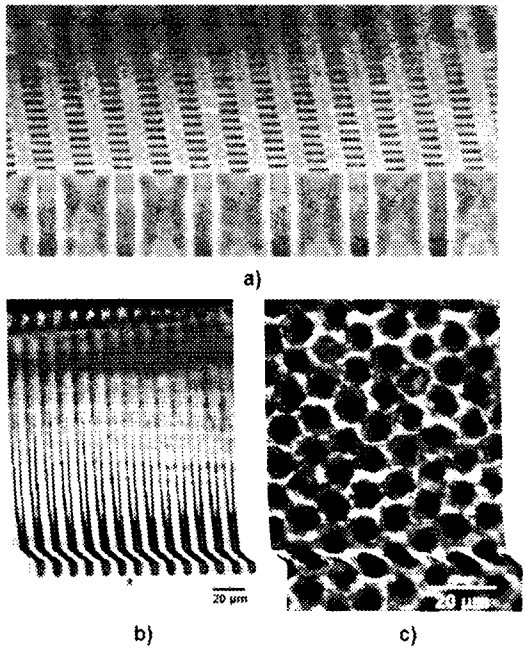

Figure 1: Cross-section (a, b) and bottom (c) images of the silicon microchannel silicon wafer used for vertically oriented display screen

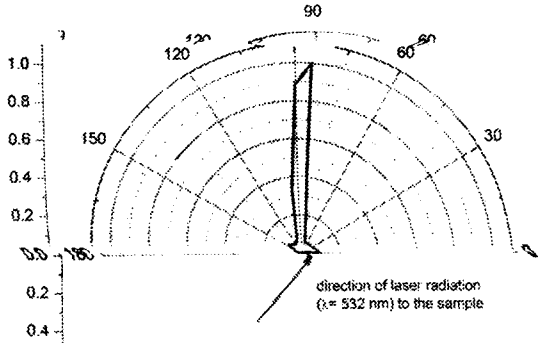

Figure 2: Indicatrice of vertically oriented display screen

5. References

S.K. Lazarouk, A.A. Leshok, T.A. Kozlova, A.V. Dolbik, L.D. Vi, V.K. Ilkov and V.A. Labunov, "3D Silicon Photonic Structures Based on Avalanche LED with Interconnections through Optical Interposer", International Journal of Nanoscience, Vol. **18**, pp. 1940091(1-5), 2019.

Upconversion emission from erbium doped sol-gel derived $BaTiO_3$ powders and coatings

N.V.Gaponenko[1], R.Subasri[2], D.S.Reddy[2], K.R.C.Soma Raju[2], K.S.Rao[2], L.S.Khoroshko[1], Yu.D.Karnilava[1], A.V.Mudryi[3], V.D.Zhivulko[3]

[1]Belarusian State University of Informatics and Radioelectronics, Minsk, Belarus

[2]Centre for Sol-Gel Coatings, International Advanced Research Centre for Powder Metallurgy and New Materials (ARCI), Balapur, Hyderabad - 500 005, Telangana State, India

[3]Scientific-Practical Materials Research Centre of the National Academy of Sciences of Belarus, Minsk, Belarus

1. Introduction

Upconversion is a process where light can be emitted with photon energies higher than those of the light generating the excitation (www.rp-photonics.com/upconversion). Diverse inorganic matrices doped with trivalent lanthanides - erbium and holmium exhibit upconversion, transferring infrared light into visible. Thus the effect attracts attention for detection and visualization of infrared radiation. Recently we reported that sol-gel derived barium titanate possessing refractive index about 1.9 in amorphous state can be used as component of optical interference filter in combination with low refractive index films as silica [1] or magnesium fluoride. At the same time room-temperature luminescence of lanthanides in sol-gel derived barium titanate makes the material and method promising for light conversion [2, 3]. In this work we investigate erbium upconversion emission from sol-gel derived $BaTiO_3$ films and powders.

2. Experimental

Three types of Er-doped $BaTiO_3$ sol-gel derived samples were fabricated and annealed for 1 hour: (i) powder annealed at 1000 °C,(ii) Er-doped $BaTiO_3$ film on glass annealed at 450 °C and (iii) Er-doped $BaTiO_3$ powder annealed at 1000 °C and dispersed in SiO_2 film on silicon or glass substrates.

3. Results and Discussion

Erbium upconversion emission was observed from Er doped $BaTiO_3$ powder annealed at 1000 °C and Er doped $BaTiO_3$ powder annealed at 1000 °C and dispersed in SiO_2 film on silicon or glass. Typical room-temperature spectrum of upconversion PL is given in Figure 1. Intensive bands at 524, 554, 657, 799 and 840 nm, corresponding to $(^4F_{7/2}, {}^2H_{11/2}) \rightarrow {}^4I_{15/2}$, $^4S_{3/2} \rightarrow {}^4I_{15/2}$, $^4F_{9/2} \rightarrow {}^4I_{15/2}$, $^4I_{9/2} \rightarrow {}^4I_{15/2}$ and $^4I_{9/2} \rightarrow {}^4I_{15/2}$ transitions of trivalent erbium respectively are well resolved. The results might be interesting for solar cells on transparent substrates and silicon with convertors of infrared irradiation into visible [4] as well as for design of infrared detectors.

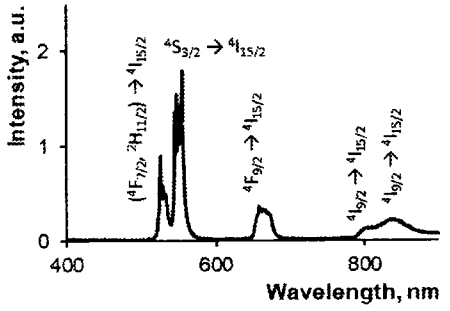

Figure 1: Upconversion emission spectrum of $BaTiO_3$:Er powder dispersed in SiO_2 film on silicon, excitation wavelength 980 nm

4. Acknowledgements

Funding from State Committee on Science and Technology of the Republic of Belarus and Department of Science and Technology, India under the India-Belarus bilateral joint cooperation through grant number 17-001 (Belarus) and INT/BLR/P-18/2016 (India) grant number is gratefully acknowledged.

5. References

[1] N.V. Gaponenko, P.A. Kholov, K.S.Sukalin, T.F. Raichenok, S.A.Tikhomirov, **R**. Subasri, K.R.C. Soma Raju, A.V. Mudryi, "Optical Properties of Multilayer $BaTiO_3/SiO_2$ Film Structures Formed by the Sol–Gel Method" Physics of the Solid State, Vol. **61**. pp. 397-401, 2019.

[2] W. Strek, D. Hreniak, G. Boulon, Y. Guyot, R. Pazik, "Optical Behavior of Eu^{3+}-doped $BaTiO_3$ Nano-crystallites Prepared by Sol–gel Method" Optical Materials, Vol. **24**. pp. 15-22, 2003.

[3] J. Li, M. Kuwabara, "Preparation and Luminescent Properties of Eu-doped BaTiO3 Thin Films by Sol–gel Process" Science and Technology of Advanced Materials, Vol. **4**. pp. 143-148, 2003.

[4] Shalav, A., Richards, B.S., Green, M.A., "Luminescent Layers for Enhanced Silicon Solar Cell Performance: Up-conversion" Solar Energy Materials and Solar Cells, Vol. **91**. pp. 829-842, 2007.

Electro-optical response of PDLC films with conical boundary conditions

M.N. Krakhaev[1,2], O.O. Prishchepa[1,2], K.A. Feyzer[2], V.S. Sutormin[1,2], V.A. Loiko[3], A.V. Konkolovich[3], A.A. Miskevich[3], V.Ya. Zyryanov[1]

[1]Kirensky Institute of Physics, Federal Research Center KSC SB RAS, Krasnoyarsk, Russia
[2]Institute of Engineering Physics and Radio Electronics, Siberian Federal University, Russia
[3]Stepanov Institute of Physics of the NASB, Minsk, Belarus

1. Introduction

Polymer dispersed liquid crystals (PDLC) are the liquid crystal (LC) droplets dispersed in polymer matrix. Optical properties of such composite materials depend on the orientational structure inside droplets which, in turn, depends on the boundary conditions at LC-polymer interface. For instance, the bipolar director configuration with two point defects at the opposite droplet's poles is formed within droplets at tangential surface anchoring. An electric field applied to this PDLC film causes the transformation of orientational structure and reorientation of bipolar droplet axis along the field. In the result, PDLC film can be switched from a light-scattering state to transparent one [1].

At the conical boundary conditions with $\theta = 40°$ angle between the director and the normal to surface, the axial-bipolar structure is formed with two point defects at the opposite poles and the ring surface defect at equator [2]. Under applied electric field, this structure is oriented by a bipolar axis along the field. In this case the control voltage required to reorient the structure are less in several times than for bipolar droplets [3].

2. Results and Discussions

In this paper; the electro-optical response of PDLC films with the axial-bipolar structure has been studied. These droplets manifest essential distinction in scattering properties depending on the orientation of the bipolar axis relative to the light polarization direction. So, the light polarized along the bipolar droplet axis is scattered intensively while the light polarized perpendicular to the bipolar axis passes almost without scattering. In initial state, the bipolar droplet axes within PDLC film are oriented randomly. An electric field applied in the film plane tends reorienting the droplets by the bipolar axes along the field so that a transmittance of PDLC film under voltage will depend on the polarization of incident radiation (Fig. 1). Low control voltages, a high transmittance of light polarized perpendicular to the applied field $T_\perp$ and a large value of $T_\perp/T_\parallel$ ratio are characteristic for these PDLC films.

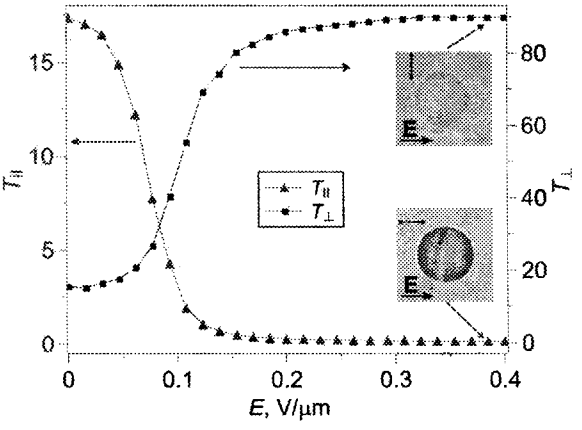

Figure 1: Transmittances $T\|,\perp$ of the polarized components of laser radiation depending on the applied electric field E. The microphotos of axial-bipolar droplet in the polarized light are presented on the insertions. The polarizer direction indicated by the double arrow

3. Acknowledgements

The study was funded by Russian Foundation for Basic Research (No 18-42-243006).

4. References

[1] P.S. Drzaic, "Liquid crystal dispersions" World Scientific. 1995. 430 p.

[2] M.N. Krakhalev, O.O. Prishchepa, V.S. Sutormin and V.Ya. Zyryanov, "Director configurations in nematic droplets with tilted surface anchoring", Liquid Crystals, Vol. **44**, pp. 355-363, 2017.

[3] M.N. Krakhalev, O.O. Prishchepa, V.S. Sutormin, V.Ya. Zyryanov, "Polymer dispersed nematic liquid crystal films with conical boundary conditions for electrically controllable polarizers", Optical Materials, Vol. **89**, pp. 1-4, 2019.

O-32

Gradient pretilt angle alignment materials with different photosensitivity for tunable polarization-independent self-aligned LC lens

V.S. Bezruchenko[1,2], Al.A. Muravsky[1], An.A. Murauski[1], A.I. Stankevich[2], U.V. Mahilny[2]
[1]Institute of Chemistry of New Materials NAS of Belarus, Belarus;
[2]Physical Department of Belarusian State University, Belarus

Abstract

Alignment materials with different photosensitivity thresholds, capable of changing the pretilt angles from 90° to 0° under UV-B exposure have been developed. Inhomogeneous exposure of alignment layers allows formation of refractive index gradient inside the LC cell. The concept of polarization-independent self-aligned LC lens uniform cell gap and low-voltage driving is presented.

1. Introduction

Several methods of tunable LC lens fabrication have been proposed during the last 40 years [1]. One the promising methods is the patterned alignment layer based on photosensitive alignment materials allowing control of the pretilt angle with inhomogeneous non-polarized UV exposure [2-3]. LC lenses fabrication by patterned alignment is simple and technological owing single cell-gap and two electrodes only, which is the key point to obtain reliable LC devices.

2. Gradient Pretilt Angle Alignment Materials with Different Photosensitivity Threshold

The transition threshold control from 90-0° is carried out by vertical alignment group ratio adjustment of the copolymer composition (Fig. 1).

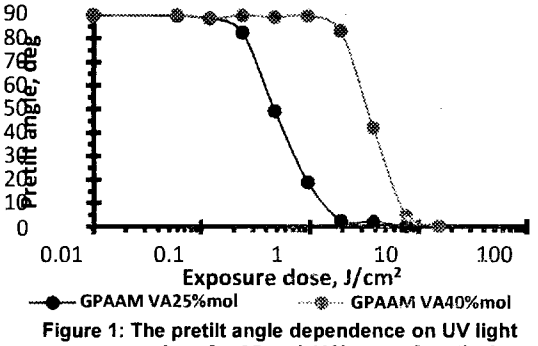

Figure 1: The pretilt angle dependence on UV light exposure dose for 25 and 40%mole of vertical alignment groups

3. Self-alignment of Polarization-independent LC lens based on Adjustment of Alignment Layers Photosensitivity

The polarization-independent LC lens based on gradient pretilt angle alignment materials consists of two polarization-dependent LC lenses with uniform cell gap. Self-alignment is realized through simultaneous exposure of alignment layers with different photosensitivity coated on both sides of the double-sided ITO glass substrate (Fig. 2).

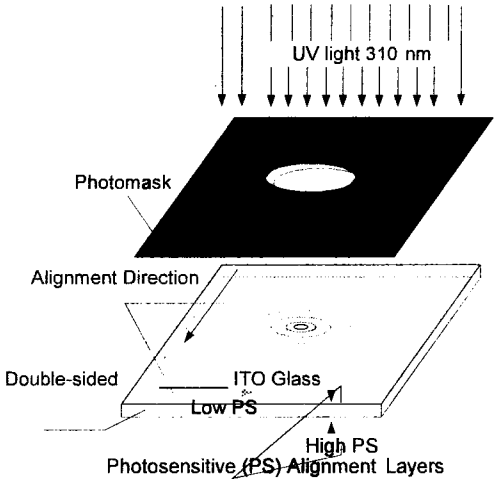

Figure 2: Self-aligning exposure scheme of polarization-independent LC lens

Polarization independence is achieved by perpendicular crossing of the azimuthal alignment direction of the polarization-dependent LC lenses. These LC lenses are controlled in parallel and controlled with low AC voltage levels 0-12V. **Conclusions**

Gradient pretilt angle alignment materials with different photosensitivity threshold are presented. The materials were successfully applied for polarization-independent self-aligned LC lens fabrication.

5. References

[1] J.F. Algorri, D.C. Zografopoulos, V. Urruchi, J.M. Sánchez-Pena, "Recent Advances in Adaptive Liquid Crystal Lenses" Crystals, Vol. 9(5). pp. 272, 2019.

[2] V.V. Sergan, T.A. Sergan, P.J. Bos, "Control of the molecular pretilt angle in liquid crystal devices by using a low-density localized polymer network" Chem. Phys. Lett., Vol. 486(4-6). pp. 123-125, 2010.

[3] V. Biazruchanka et al, "Alignment material for liquid crystal lens and liquid crystal lens system" : Patent US 9513510 B1, 2016

O-33

Materials for tritium solid-state radioluminescent light sources (SRLS). Modified technique of phosphor screens manufacturing

E. Zelenina, E. Pechertseva
Khlopin Radium Institute, Russia
Saint-Petersburg State Institute of Technology, Russia

1. Introduction

Radioluminescent light sources (RLS) are very promising energy-saving types of devices which are highly sought in various fields of industry due to their energy independence, self-reliance and longevity. The key idea of SRLS is bonding the working isotope (tritium) in the solid matrix and combining it with the phosphor. This approach allows to decrease the radiological hazard and create safe and endurable light sources of various forms and sizes [1]. The main factor of raising the SRLS effectivity is providing the closest contact between the tritiated carrier matrix and phosphor screen. Also, achieving the optimal thickness for the phosphor screen is a crucial task for the SRLS creating. The screen being too thin will not be able to provide enough brightness, and the one too dense will absorb all the light. So the development of the working method of making the strong and uniform phosphor screens of adjustable thickness is indeed a very promising challenge.

2. Experimental

For our experiment we used the tritiated titanium carrier matrix on the stainless steel plate, so that we get the tritium ionizing radiation sources with surface area of 1 cm^2 and fixed activity 420 mCi per source. For the experiment we took the inorganic zinc-sulphide radiophosphors: FK-2; FK-3; FK-4; Z-3/11; Z-16/3; G-2/1, and zinc-sulphide cathodophosphor: P31-G1A. We have conducted series of experiments to develop the working technique of phosphor coating, firstly on the glass plates and then on the tritiated carrier matrix.

3. Results

Firstly, the phosphors preselection was done to choose the best ones according to their spectrum and brightness characteristics. For the preselection tests phosphor layer was fixed on the sticky tape and tightly hitched to the tritiated source to provide the closest contact of the phosphor and the source. Then, for the phosphor screens we used the type of method that uses the phosphor grains fully covered with the binder - sol-gel suspended sedimentation, based on the method stated in [2], which includes water, potassium silicate, polymeric surface-active agent and electrolyte. We have modified this technique since in the exercise it has been noted that the existence of surface-active agent in the suspension suppresses the effect of coagulating electrolyte $Sr(NO_3)_2$. The modified sol-gel technique allowed getting the strong, thin and uniform phosphor screens avoiding the usage of the secondary dispersing agents. Using this technique we prepared two sets of samples of phosphor screens with various thicknesses. Then the brightness and luminescence spectra were measured, and the optimal thickness of the phosphor screen was stated.

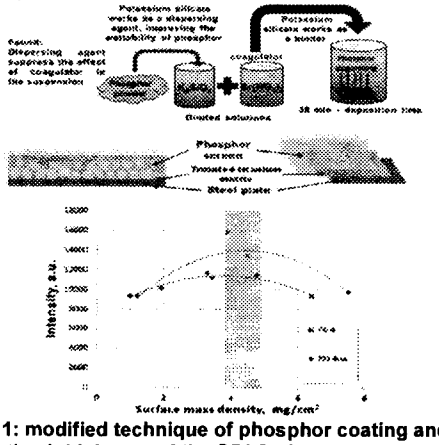

Figure 1: modified technique of phosphor coating and the optimal thickness of the SRLS phosphor screen

4. Conclusions

The technique of coating the phosphor screens of various thickness on the tritium sources was developed. The spectral and brightness characteristics of the phosphor screens were studied at the tritium ionizing radiation source and the optimal screen thickness of 4-5 mg/cm^2 was determined. It was demonstrated that coating the phosphor screen directly on the tritium β-source gives a 15% increase of brightness in comparison with the coating on the glass.

5. Acknowledgements

This work was financially supported by the Department of Innovations of RF State Corporation of Atomic Energy "Rosatom" in Conceptual Projects Awards 2018; project number #460.

6. References

[1] Prospects for the Development of Tritium-Based Solid-State Radioluminescent Light Sources, E. Zelenina, M. Sychov, A. Kostylev, K. Ogurtsov / Rdiochemistry, vol. 61, №1, 2019.
[2] Russian Federation patent №: 2032243; 27.03.1995

O-34

Electromagnetic MEMS motors for display technologies

I.Timoshkov[2], V.Kurmashev[1], D.Grapov[2], A.Vetcher[3], G.Govor[3]
[1]Belarusian State Academy of Communications, Minsk, Belarus
[2]Belarus State University of Informatics and Radioelectronics, Minsk, Belarus
[3]Scientific Practical Materials Research Center of National Academy of Science, Minsk, Belarus

1. Introduction

The fourth revolution of the industry is powered by a wide range breakthrough, new technology, innovative ideas and creative activities. All these things were naturally born, mostly, by the interdisciplinary science and technology. Soft magnetic composites are the bright example of the different technologies integration to get final commercial technologies to get the final products with enhanced properties. Micro displacement and micro positioning became a very important factor for new display technologies such as ink jet, 3D printing, nanoimprint. New generation of technologies allows increasing productivity and improving quality. MEMS micromotors are the core of such instruments for display production.

2. Soft magnetic composite for MEMS micromotors

In the report we systematized the methods, technologies and structures of heterogeneous materials with soft magnetic properties, pros and cons are discussed. The main mechanisms of magnetization reversal of such structures are reviewed, as well as the effect of inhomogeneities on the main magnetic properties: magnetic induction, permeability, coercive force, and loss. The basic requirements to these materials for practical use in electromagnetic systems are analyzed.

We developed the technology of iron powder treatment to create the nanometer coating on the surface of each particle. The final magnetic details are produced by technology of powder metallurgy with macro and micro moulds. Unique specific parameters of a soft magnetic composite material were achieved: magnetic induction of saturation – 2.1 T, working frequency range - up to 1 MHz, permeability – up to 1000, total loss – 8 W/kg, Curie temperature - above 800C. These allow to produce machines with the large number of poles and high frequency of switching, thus improving specific mass and size parameters. UV -LIGA MEMS technology combined with electroplating was developed to produce hybrid stepper micromotor based on soft magnetic composites. The technology part was successfully tested with two types of thick film photoresists: SU-8 liquid photoresist (electroplating forms are reusable up to 10 times), dry film photoresist (provides cheap and scalable production). Photoresist film thickness was 50-1000 μm. Glass high resolution photomask or affordable polymer flexible film photomask are both applicable for this technology.

Electroplating allows deposition of conductive amorphous alloys based on metals like Fe, Ni, Co with additives like B, P. Special process was developed to allow insertion of conductive powder filaments into soft magnetic matrix formed by plating. Special surface chemical treatment is used to reduce adhesion of electrodeposited part to substrate. It provides easy removal of part from photoresist-based microform.

Described technology is suitable for the following applications for display production equipment:

- manufacturing of microforms for micropressing technology;
- mechanical parts manufacturing – gears, racks etc;
- magnetic cores manufacturing;
- stators and rotors for BLDC and stepper motors (including linear). Combination of soft and hard magnetic materials in one process/design.

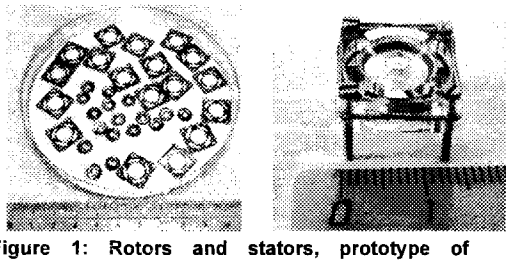

Figure 1: Rotors and stators, prototype of micromotors

3. References

[1] I. Timoshkov, Q. Gao, G. Govor, A. Sakova, V. Timoshkov, and A.Vetcher "Nanomodified composite magnetic materials and their molding technologies" , AIP (American Institute of Physics) Advances (Vol.8, Issue 5, 2018

Session 6. Production technologies

Chairman: Prof. Qun Yan

Invited I-12

Vertically oriented graphene based walls and columns obtained by ICP CVD method on moving substrates as prior stage of the roll-to-roll technology

V.Labunov[1], D.Radziuk[1], D.Grapov[1], P.Rozel[2], E.Khokhlov[2], V.Shiripov[2], A.Basaev[3], N.Kargin[4]

[1]Belarusian State University of Informatics and Radioelectronics (BSUIR), Minsk, Belarus
[2]IZOVAC Technologies Ltd., Minsk, Belarus
[3]SMC (Technological Centre), Zelenograd (Moscow), Russia
[4]National Research Nuclear University "MEPhI", Moscow, Russia

1. Introduction

Superior optoelectronic properties of graphene have made this material as a special applicant in displays, touch and graphene-based screens with smaller and long-lasting batteries including the field of mobile telephony [1]. Recently we have introduced the process for the formation of vertically oriented graphene (VOG) walls with a curved morphology by ICP CVD method [2]. Such VOG walls represent a very promising material for different applications (e.g. miniature batteries and other optoelectronic devices) due to its unique orientation and open carbon network structure. For the first time such VOG walls have been grown directly on a moving substrate that is a prerequisite for its production by the roll-to-roll technology providing higher yield of the production process at lower cost of the product.

2. Experimental part

Here we present recent results in the continuation of [2]. New vertically oriented graphene based walls and columns were formed by the ICP CVD apparatus, manufactured by IZOVAC Technologies Ltd. (Minsk, Belarus) with the moving substrate, simulating the roll-to-roll process. Such technological parameters as propane/argon partial pressure, duration of deposition (min), heating time (min) and temperature (< 500°C) of a moving substrate were examined in the use of this method.

3. Results and Discussion

VOG morphology and thickness depends on the technological parameters of the process. SEM images reveal two distinct VOG coatings obtained on a moving copper or Al_2O_3 substrates (Figure 1A and B). In Figure 1A VOG coating was prepared at 2/5 propane partial pressure, 5 min of deposition time and at 450°C of a moving copper foil substrate. This coating is composed of curved VOG walls with a height of ~40 nm and the thickness below ~17 nm. In contrast, in Figure 1B and D vertically oriented graphene based columns with a height of ~5 μm and ~230 nm diameter were produced on a moving Al_2O_3 substrate (4/5 propane partial pressure, 225 min of deposition time at 400°C). Both materials exhibit characteristic Raman peaks of graphene based materials (Figure 1C).

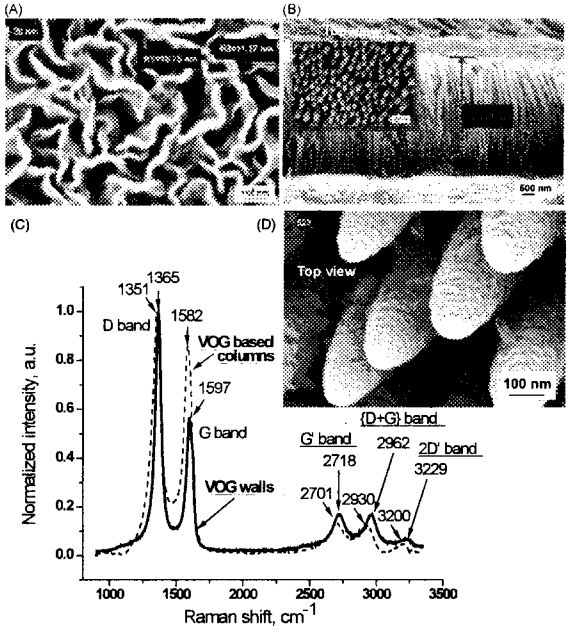

Figure1: Representative SEM images of two types of coatings: (A) thin vertically oriented graphene (VOG) walls produced on a moving copper foil substrate; (B) and (D) thick vertically oriented graphene based columns prepared on a moving Al_2O_3 substrate in the use of ICP CVD apparatus, manufactured by IZOVAC Technologies Ltd. (Minsk, Belarus). (C) Raman spectra of these two types of VOG based materials (λ_{exc} = 473 nm)

4. Conclusions

VOG based wall and columns can be produced by the ICP CVD method on a moving substrate, simulating the roll-to-roll technology.

5. Acknowledgements

This work is supported by the joint Belarussian-Armenian BRFFR grant № T18ARMG-001.

6. References

[1] F. Bonaccorso, Z. Sun, T. Hasan, A. C. Ferrari "Graphene Photonics and Optoelectronics", Nat. Photonics, Vol. 4, pp. 611-622, 2010.

[2] P. Rozel, D. Radziuk, L. Mikhnavets, E. Khokhlov, V.Shiripov, I. Matolínová, V. Matolín, A. Basaev, N. Kargin, V Labunov, "Properties of Nitrogen/Silicon Doped Vertically Oriented Graphene Produced by ICP CVD Roll-to-Roll Technology", Coatings, Vol. 9, pp. 1-14, 2019.

Full roll-to-roll fabrication process of large-area flexible OLED with silver-nanowire transparent electrode

C. Kim, S. Jeong, S.M. Cho
School of Chemical Engineering, Sungkyunkwan University (SKKU), South Korea

1. Introduction

The organic light emitting diodes (OLEDs) have attracted great interest owing to their high efficiency, design flexibility and environmental friendly in the lighting and display industry. However, for the general lighting and signage applications, cost of the OLED panel is still too high compared to another lighting source like a fluorescent lamp or inorganic LED. To lower the fabrication cost of OLED panels, not only the materials but also the fabrication process should be changed. Compare to conventional batch process, the roll-to-roll process has advantages like low fabrication cost, fast process time. In order to accomplish all fabrication process in roll-to-roll type, we adopted silver-nanowire embedded flexible transparent electrode on a PET substrate as an anode for OLED. For encapsulation, a moisture-barrier layer composed of Al_2O_3 and polymer layers were deposited with the roll-to-roll equipment. Finally, phosphorescent blue OLEDs were deposited with the roll-to-roll thermal evaporator.

2. Experiment

First, Silver-nanowires were coated on the polyimide (PI) donor film using a Meyer rod installed in the roll-to-roll coater. Silver-nanowire dispersed solution (0.5 wt% in IPA) was continuously supplied behind the Meyer rod while the PI donor film kept passing through underneath the Meyer rod. Right after coating, the solvent evaporated with dryer and finally, the silver-nanowire network was formed on PI donor film. Second, UV-curable embedding layer was blade coated on top of the silver-nanowire network and thermally annealed to remove the impurities in the UV-curable embedding layer which affect the lifetime of OLED. And moisture barrier layer composed of Al_2O_3 and polymer layers were deposited on top of it. Third, optical epoxy coated PET acceptor film was laminated. After thermal curing, due to the surface energy difference between PI donor film and PET acceptor film, the silver-nanowire embedded layer was transferred to PET acceptor film. Finally, the insulator was printed on top of the fabricated silver-nanowire embedded electrode for patterning [1]. With the fabricated electrode, OLEDs were deposited via the roll-to-roll thermal evaporator. After the OLED deposition SUS foil was laminated with desiccant dispersed adhesive for top-side encapsulation.

3. Results

The specular transmittance of the fabricated electrode was 85% at 550nm with 8 Ω/sq sheet resistance. The surface roughness of the fabricated electrode was very smooth owing to the embedding process (RMS: 3nm). With a screen printer, we printed various pattern of insulator on top of the fabricated electrode. And the efficiency of OLED fabricated by the roll-to-roll process was almost same as the conventional batch process. We also fabricated large-area OLED signage by the fully roll-to-roll process. Due to the size limitation of screen-printer, the maximum size of one pattern was 300mm x 150mm. with a series of screen-printing process, we fabricated 1 m long and 150 mm wide large-area OLED signage

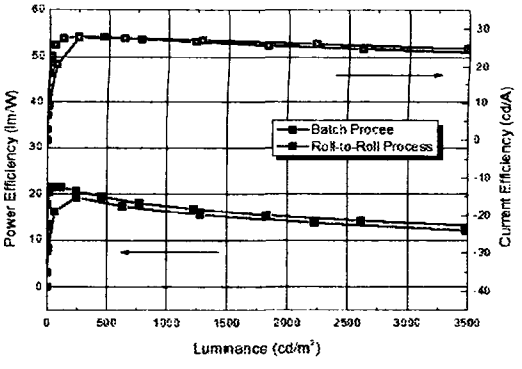

Figure 1: Efficiency of the fabricated OLED

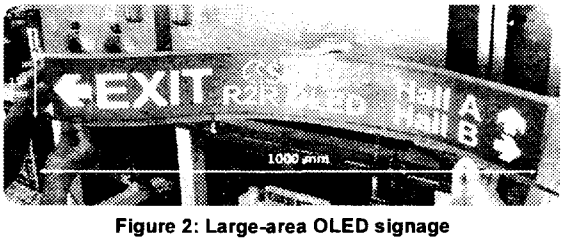

Figure 2: Large-area OLED signage

4. Conclusion

We fabricated large-area OLED panels with the full roll-to-roll process from the silver-nanowire embedded flexible transparent electrode to hybrid moisture barrier film. The performance of the fabricated OLED was comparable to batch processed OLED. With the roll-to-roll process, we expect much short process time and low process cost.

5. References

[1] E. Jung, C. Kim, M. Kim, H. Chae, J. H. Cho, S. M. Cho, "Roll-to-roll preparation of silver-nanowire transparent electrode and its application to large-area organic light-emitting diodes," Org. Electron., Vol. 41, pp.190-197 (2017)

Mass production of patterned polymerizable liquid crystal devices by roll-to-roll technology

A.Muravsky[2], P.Moiseenko[1], A.Boboreko[1], V.Shevtsov[1], A.Murauski[2]
[1]Holography industry JSC, Belarus
[2]PRUE 'MTLCD', Belarus

Abstract
Roll-to-Roll fabrication of patterned liquid crystal films and film-based devices is one of the most promising and anticipated LCD technology of today. The constraint of mass production is the suitable alignment process. The problem of high anchoring patterned liquid crystal alignment on plastic substrates has been challenged for over a decade. We solved it. The possibility of R2R fabrication of retarders with custom azimuthal angle, patterned retarders and vortex retarders is demonstrated.

1. Key Points and Factors

Studying of alignment materials [1] and method [2] revealed that efficient fabrication of 'polymerizable liquid crystal devices on flexible substrates' needs re-thinking of the whole concept with respect to the factors pointed below.

The breakthrough innovation in production of patterned PLC devices by R2R technology is based of revolutionary approach to LC alignment process utilizing both novel low temperature materials and innovative high-speed patterned alignment technology.

Flexible substrate rolls require *low temperature process* materials with operation temperatures below 70°C enabling all kinds of standard plastic films including PET, TAC, PC and others available awing for reduction of substrate cost.

R2R technology means *full compatibility* of the process flow with the present available *roll handling equipment* allowing utilization of standard equipment for reduction of processing costs. However all process operations performing at each single rolling are *synchronized* for *high-speed* process with *high yield*.

The polymerization rate of suitable liquid crystal monomer film provides *degree of polymerization over 90+%* before rolling the substrate.

A wide range of thin film polymerizable liquid crystal devices were developed and currently are available by roll-to-roll technology in Minsk, Belarus.

2. Security Labels

Innovative security labels with hidden polarization images with dynamic effects that appear when your turn the polarizer, vario images (Fig.1) and many others were developed.

a) b)

Figure 1: Vario image observed through polarizer: a) & b) change each other with polarizer rotation

3 Retarder Film

Thin film **retarder** on TAC substrates with custom azimuthal angle with respect to the roll direction are available in rolls and sheets. The λ/4 and λ/2 retarders @ 550 nm with diagonal 45 deg azimuthal alignment are available, while other retardation values are possible as well.

High resolution patterning of azimuthal direction allows **Patterned Retarder** with azimuthal angle step of less than < 2 deg. On optimizing both retardation value and azimuthal angle distribution we were able to fabricate **Vortex Retarder** also known as **q-plate** by R2R technology applicable for generation of orbital angular momentum of laser light beam at specified wavelength.

4. References

[1] U.V. Mahilny, A.I. Stankevich, A.A. Muravsky, A.A. Murauski, Novel Polymer as Liquid Crystal Alignment Material for Plastic Substrates, J. Phys. D: Appl.Phys. **42**, p. 075303, 2009.

[2] A. Muravsky, V. Agabekov, G. Zhavnerko, U. Mahilny, A. Stankevich, Patterned rubbing alignment technology, SID Int. Symp. Dig. Tech. Pap. **41**, p 1727, 2010.

Calculation of the optical scheme of an augmented reality video module

A.M. Artamonov, K.A. Abdusalamau
Izovac AR, Belarus

1. Introduction

At present the optical properties of coatings applied to the waveguide displays of AR glasses are not clearly investigated, and there are also difficulties in designing an optical scheme of a video module of AR glasses [1].

2. Optical module

2.1 Module scheme and its composite elements

Figure 1 illustrates the optical module scheme. Where: 1 – emitting diode; 2 – lenses responsible for transmitting radiation to the beamsplitter; 3 – beamsplitter; 4 – microdisplay; 5 – lens; 6 – waveguide. Figure 2 illustrates the augmented reality display waveguide with areas for coating [2].

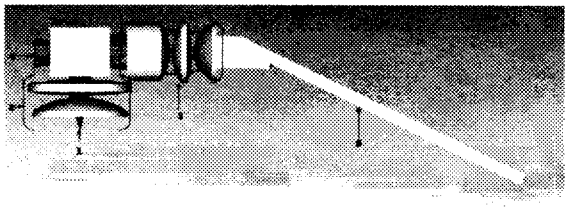

Figure 1: Optical module scheme

Figure 2: The waveguide scheme with areas for coating

3. Optical properties of augmented reality display waveguide

3.1 The required coating parameters

Four versions of coating parameters for semireflective mirrors were studied [3]. Reflection coefficients for each version are:

Version 1: Zone1: 40%, Zone2: 55%, Zone3: 63%, Zone4:80%.

Version 2: Zone1: 30%, Zone2: 45%, Zone3: 53%, Zone4:70%.

Version 3: Zone1: 15%, Zone2: 35%, Zone3 :43%, Zone4:60%.

Version: Zone1: 20%, Zone2: 25%, Zone3: 34%, Zone 4: 50%.

Figure 3 shows the values of the radiation power reflected from each zone for all versions of coating parameters.

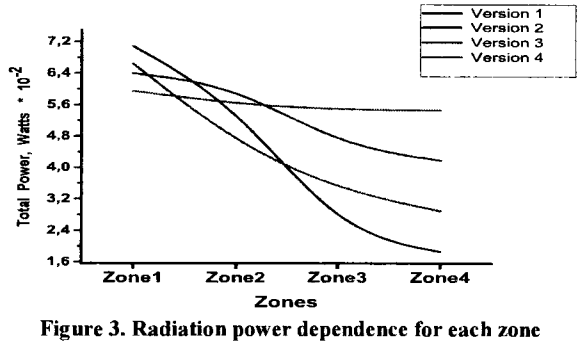

Figure 3. Radiation power dependence for each zone

3.2 Modeling optical properties of coatings of waveguide AR displays

Based on the calculation of optical coating properties of three materials (Ta_2O_5/SiO_2, TiO_2/SiO_2, Nb_2O_5/SiO_2) and at different angles of incidence, optimal thickness and number of layers of applied coatings were calculated, and also optimal materials for each semireflective surface were selected. They are: Zone1: TiO_2/SiO_2, d=2.693 μm, N=30; Zone2: Nb_2O_5/SiO_2, d=2.285 μm, N=27; Zone3: Ta_2O_5/SiO_2, d=2.767 μm, N=29, Zone4: TiO_2/SiO_2, d=2.707 μm, N=27. It is shown that the optimal angle of incidence is the angle $\theta = 30^0$. Figure 4 shows the dependence of reflection coefficients on wavelength of the incident radiation of optimal materials for each zone.

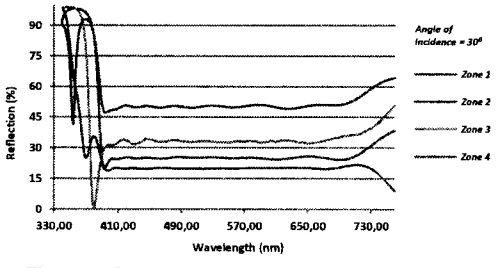

Figure 4. Dependence of reflection coefficients on wavelength for each zone

4. References

[1] L. Tommaso De Paolis, P. Bourdot, "Augmented Reality, Virtual Reality, and Computer Graphics", 5th International Confer ence, AVR 2018 Otranto, Italy, June 24- 27, 2018 Proceedings, Part II, 719 p.

[2] D. Schmalstieg and G. Reitmayr, The world as a user interface: Augmented reality forubiquitous computing, Central European Multimedia and Virtual Reality Conference, 2005.

[3] P.P. Yakovlev, B.B. Meshkov. Design of Interference Coatings – Mashinostroenie, Moscow, 1997, 185 p.

Coating equipment for mass production based on langmuir-blodgett technology

H.K.Zhavnerko, V.Ya.Shiripov, Ya.A.Khakhlou
IZOVAC Group, 155 M. Bogdanovicha Str, Minsk, Belarus

A unique technology and equipment for applying to the surface of films with a thickness of one molecule were developed [1]. Technology features allow making the process of film formation continuous, up to the implementation of the Roll - Roll scheme for flexible products. Meanwhile a defect-free coating is formed from 2 to 100 nm in thickness, depending on the structure of the molecules of the applied material. Depending on the nature of the material, coatings can have various consumer properties, in particular, protective ones with high wear resistance in friction processes (they withstand up to 10,000 cycles of abrasive wear with a hard steel fabric under a load of 10 N / cm2), hydro and oleophobic properties, a very low coefficient of friction, resistance to aggressive environmental influences (acids, alkalies, UV radiation). Accordingly, the range of applications of such coatings is quite wide - from display appliance, photonics to nano and molecular electronics. Examples are easy-to-clean coatings for optics, cover glass for solar cell modules, in ophthalmology, in the construction industry (architectural, low-emission and decorative glass), for ceramics, etc. The low coefficient of friction (0.04) makes such coatings promising in friction units. The developed installation of a conveyor type can easily be integrated into a continuous type technological process, herewith there are no fundamental limitations on the size of the modified area. In particular, equipment for modifying sheet glass of the maximum Jumbo size (6,000 mm x 3210 mm) can be supplied.

Upon the request of the Customer the product line can be additionally equipped with systems for prewash and surface activation of glass, light and heat treatment, loading and unloading devices, etc.

The equipment can be produced to suit the requirements of a specific Customer and will ensure the formation of layers not only on the surface of flat products such as sheet glass, but also on the surfaces of products of complex shape. It is possible to simulate the process using a laboratory version of the installation, see fig. 1.

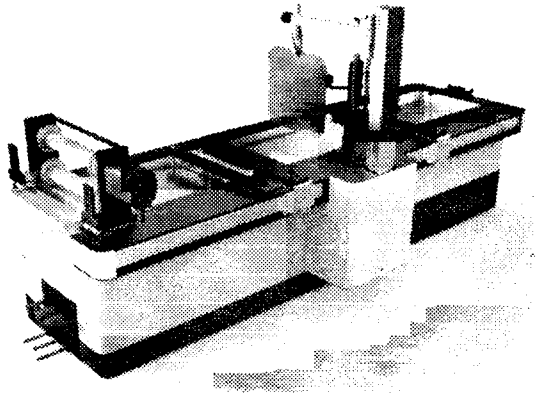

Figure 1. LB equipment GT-160

Low equipment capital costs, as well as the cost of its operation, class the developed technology with the most cost-effective among surface treatment technologies and coating formation.

References

[1] G.K. Zhavnerko, V.Ya. Shiripov. Device for formation of nanostructured coatings on solid surfaces. Taiwanese Patent No.: I542532 (2016)

[2] G.K. Zhavnerko, V.Ya. Shiripov., Hydro and oleophobic coatings for glass. GT technology and promising application areas - World of Glass Journal, May, 2017, 14 p.

Silver nanowires as transparent conductive films in the near-infrared spectral range

M.Marus[1], A.Hubarevich[2], Y.Mukha[2], A.Smirnov[2], Xiao Wei Sun[1]

[1]Guangdong University Key Lab for Advanced Quantum Dot Displays and Lighting, Shenzhen Key Laboratory for Advanced Quantum Dot Displays and Lighting, Department of Electrical & Electronic Engineering, Southern University of Science and Technology, China

[2]Laboratory for Information Displays and Optical Processing Systems, Belarusian State University of Informatics and Radioelectronics (BSUIR), Belarus

1. Introduction

Transparent conductive films (TCFs) comprise a crucial component of optoelectronic devices, such as displays, light-emitting diodes, solar cells and touch screens. Indium tin oxide (ITO) currently dominates among TCFs in the visible spectral range due to the high transmittance at low resistivity [1]. However, the remarkable decrease of the transmittance in the near-infrared range (NIR) restricts from using ITO as highly efficient NIR TCF. Here we show that silver nanowires (AgNWs) possesses up to 95% transmittance for whole 0.75-2.5μm near-infrared spectral range.

2. Discussion

AgNWs possess high transmittance in the visible spectrum range [2], however their transparency in the near-infrared range remained understudied. Figure 1 shows the transmittance of AgNW TCF compared to the ITO TCF and planar 30 nm thick Ag layer in the NIR. ITO remains highly transparent (>80%) up to 1.1 μm wavelength, then its transparency decreases

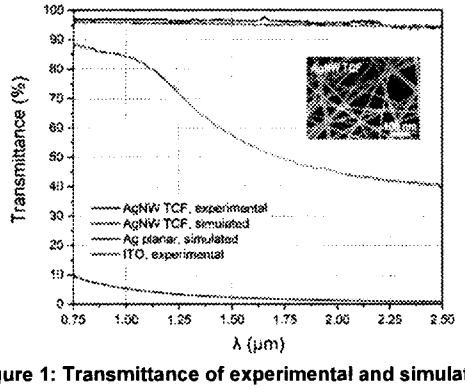

Figure 1: Transmittance of experimental and simulated AgNW TCF compared to simulated planar 30 nm thick Ag layer and experimental 164 nm thick ITO TCF. The diameter and length of AgNWs are ~30 nm and ~30 μm (aspect ratio ~1,000), respectively. Substrates (PET in case of AgNW TCF and glass in case of ITO TCF) were excluded from consideration. The inset shows the SEM image of AgNW TCF (scale bar 100 nm).

down to 60 and 40% at wavelength above 1.5 and 2.5 μm, respectively, due to increase of the reflectance and absorbance [3]. AgNWs reaches 95% for the whole 0.75-2.5μm range and exceeds the ITO TCF by 12.5, 37.8 and 55.2% for 1, 1.5 and 2.5μm, respectively.

Table 1. NIR transmittance of AgNW and ITO TCFs.

λ	AgNWs	ITO	$T_{AgNW} - T_{ITO}$
1μm	96.6%	84.1%	+12.5%
1.5pm	95.3%	57.5%	+37.8%
2.5μm	93.9%	38.7%	+55.2%

3. Summary

AgNWs benefit from strong optical transmittance across the whole 0.75-2.5μm range, which makes them particularly interesting for NIR optoelectronic applications. Compared to ITO TCFs, AgNW TCFs offer 12.5, 37.8 and 55.2% higher transmittance at 1, 1.5 and 2.5 μm, respectively.

4. Acknowledgements

This material is based upon work supported by National Key Research and Development Program of China, which is administrated by the Ministry of Science and Technology of China (No. 2016YFB0401702), National Natural Science Foundation of China (No. 61674074 and 61405089), Development and Reform Commission of Shenzhen Project (No. [2017]1395), Shenzhen Peacock Team Project (No. KQTD2016030111203005), Shenzhen Key Laboratory for Advanced quantum dot Displays and Lighting (No.ZDSYS201707281632549), Guangdong University Key Laboratory for Advanced Quantum Dot Displays and Lighting (No. 2017KSYS007), Distinguished Young Scholar of National Natural Science Foundation of Guangdong (No. 2017B030306010). We thank the start-up fund from Southern University of Science and Technology, Shenzhen, China.

5. References

[1] K. Ghaffarzadeh and R. Das, "Transparent Conductive Films and Materials 2019-2029: Forecasts, Technologies, Players," IDTechEx, 2019.

[2] M. Marus, A. Hubarevich, H. Wang, A. Stsiapanau, A. Smirnov, X. W. Sun, W. Fan, "Comparative analysis of opto-electronic performance of aluminium and silver nano-porous and nano-wired layers," Opt. Express 23 (20), 2015.

[3] I. Hamberg and C. G. Granqvist, "Transparent and infrared-reflecting indium-tin-oxide films: quantitative modeling of the optical properties," Appl. Opt. 24 (12), 1985.

Session 7. Metrology and standards

Chairman: Prof. A.Gurskii

Requirements and evaluation of displays in autonomous cars

K. Blankenbach
Pforzheim University, Germany

Abstract
Autonomous driving has a huge impact of on displays: number, larger and more time to watch. This requires new approaches for optical evaluations.

1. Introduction

Future cars expand autonomous driving capabilities thus enabling an extensive use of in-vehicle displays. Cars will evolve toward the third living space. This raises the expectations from functional to emotional displays [1] and HMIs on more and larger displays. Additional displays for leisure and work will be integrated. Fig. 1 shows selected examples:

- Design for extensive manual driving (top left)
- Pillar-to-pillar singe large display and retraceable steering wheel with displays (top right)
- Displays for work and fun (bottom left)
- Curved displays is doors for leisure (bottom right)

Those displays are watched for longer time (hours) as today (seconds) which raise the bar on image quality, readability in bright light (no hoods etc.) and lifetime. Displays in autonomous cars dominate the interior design and therefore a high quality, seamless integration in mandatory for premium products.

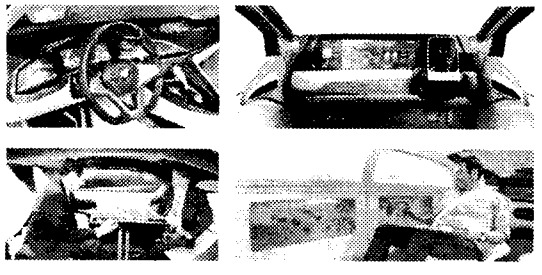

Figure 1: Interior design with various displays for autonomous cars: driving, leisure & work. Sources: BMW, NISSAN, PANASONIC, MERCEDES

2. Fundamentals of Optical Evaluation

Automotive displays are challenging in evaluation as the intended lifetime is about 15 years. Fig. 2 provides an overview of the fundamental challenges.

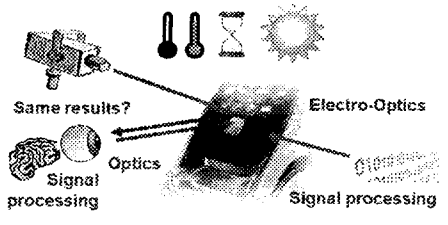

Figure 2: Visualization of optical evaluation for automotive displays like environment and display performance and image enhancement & perception (signal processing). Source: VOLVO (display)

3. Selected Examples for Automotive

Beside traditional methods for evaluating the optical performance of automotive displays, additional tasks for displays in autonomous cars are required, an overview is provided in [2]. The following list provides selected examples for basic measurements:

- Luminance: Define measurement for OLEDs (full screen or white box with black background).
- Contrast ratio: Lowest luminance for black to avoid postcard effect for LCDs during night drive. Verify dimming algorithms and effects on image quality for matrix backlights.
- Grey scale reproduction: Image enhancement algorithms for optimized perception in bright ambient light conditions.
- Color: All displays should be calibrated to same color despite potential metamerism.

Beyond that, displays in autonomous cars have to fulfil automotive application requirements such as:

- Lifetime: Define limits for OLED burn-in for given temperature profile and content (opera-tional data and entertainment). All large displays are expensive and difficult to replace in case of failure and have therefore to be tested extensively.
- Ambient light: Fig. 1 shows that most displays are stronger exposed to ambient light as today. High effective and durable (touch) reflection reduction coatings are required and tested.
- Power consumption and heat: All possible power saving methods have to be applied which can have influence on image quality.
- Viewing angle: Large interior LCDs are observed form a larger viewing cone than today (compare Fig. 1 top left to bottom right).
- Response time is typically long for low temperature operation. The effect on e.g. video perception has to be evaluated.

This effort is required for high quality reproduction of advanced HMIs and entertainment.

4. Summary

Future autonomous cars will be equipped with many and large displays. This sets new challenges for optical evaluation as significantly longer time is spent on watching displays like video and infotainment.

5. References

[1] Knoll, P. "The use of displays in automotive applications," J. Soc Info Display, p. 165-172 (1997)
[2] Blankenbach, K. "Advanced automotive display measurements: Selected challenges and solutions," J. Soc Info Display, p. 517-525 (2018)

O-41

Fourier optics technology for viewing angle measurements: past, present and future

V.Collomb-Patton, P.Boher, T.Leroux

ELDIM, France

Abstract

The proposed paper will explain the technical bases of the Fourier Optics Technology (OFT) for viewing angle measurement of displays and the evolution of the ELDIM systems over the years. There multiple capacities to obtain luminance, color, spectral, polarization or reflection data will be explained and illustrated by various application examples. New OFT systems dedicated to the characterization of NIR light sources will be also presented.

1. Introduction

Viewing angle properties are certainly among the most common characteristics measured on LCDs since the beginning of this technology in the eighties. Historically, the goniometer was the first equipment used to perform angular measurements [1]. In this case, various mechanical movements allow the scanning of the complete display-viewing field with a directional detector. Main drawback of those systems is the "one after each other" nature of the measurements which results in very long acquisition times if more than a few directions are required.

ELDIM was founded in 1991 to promote an innovative display measurement method based on Fourier optics. A specific optic was designed in order to convert angular field map into a planar one allowing very rapid measurements of the full viewing cone with high angular resolution. This fast viewing angle measurement system was first publicly introduced at Eurodisplay'1993 in Strasbourg [2].

The first generation of systems measured luminance in a cone of ±60° with an angular resolution around 1° and a maximum spot size of 1mm. Our systems have been improved throughout years to reach extremely high performances at every level and also new measurement capacities.

2. Paper content

In the proposed paper the principle of the Fourier optics will be presented. We will explain how a practical instrument can be designed with special focus on different aspects of the system. First, the collection efficiency and the accuracy which are related to the optical setup will be examined. The challenge to make large spot sizes for large TVs will be explained [3]. Technical details with some examples of application will be given concerning the polarization measurements [4] and the multispectral measurements [5] introduced in 2007 and 2008 respectively. Very high angular resolution systems have been developed in 2009 for specific applications like 3D autostereoscopic displays [6]. The integration of a sample illumination across the OFT optics makes also possible measurements of the reflective properties of surface [7] which leads to various application in the field of displays and outside it. Recent developments for the characterization of NIR light sources for 3D imaging [8], will be also discussed and future systems with extended capacities for advanced characterization of light sources will be discussed.

3. References

[1] G. Barna, "Apparatus for optical characterization of displays," Rev. Sci. Instrum. 47, 10, 1258, 1976

[2] T. Leroux, "Fast contrast vs. viewing angle measurements for LCDs," Proc. 13th Int. Display Research Conf. (Eurodisplay 93), 447, 1993

[3] P. Boher, "ELDIM's Fourier optics enhance characterization of large LCDs", Display Devices, Summer (2006)

[4] P. Boher, T. Bignon, T. Leroux, "Angle of View Polarization Characterization of Liquid Crystal Displays and Their Components, Journal of Information Display, vol.8, n°4, 10, 2007

[5] P. Boher, T. Leroux, T. Bignon, D. Glinel, "New multispectral Fourier optics viewing angle instrument for full characterization of LCDs and their components", SID, Los Angeles, USA, May 18-23, P89, 2008

[6] T. Leroux, P. Boher, T. Bignon, D. Glinel, "VCMaster3D: a new Fourier optics viewing angle instrument for characterization of auto-stereoscopic 3D displays", SID, San Antonio, USA, June 2-5, 11.2, 2009

[7] P. Boher, T. Leroux, T. Bignon, "Spectral BRDF of color shifting paints and e-papers using multispectral Fourier optics instrument", Eurodisplay, 7.4, 2011

[8] P. Boher, T. Leroux, "High resolution optical characterization of NIR light sources for 3D imaging", Display Week, San Francisco, May, 2019

Modular imaging measurement systems to cover automotive applications

C.Fatho[1], M.Zorn[1], M.Scholz[2]
[1]Konica Minolta Sensing Europe B.V., Germany
[2]Radiant Vision Systems, USA

1. Introduction

Display and ambient lighting applications are becoming more and more prevalent in today's cars. At the same time, customer's expectations for the quality of these devices is increasing, based on their experience with smartphones and other consumer electronics. In order to assure the quality of displays within the car, measurement systems that characterize them are necessary. Here, imaging systems provide an advantage compared to spot-based systems, as they can measure entire displays in one shot, which allows capturing features such as uniformity or pixel defects in addition to luminance and color. Still, the large variety of display types ranging from head up displays all the way to VR applications, requires very different measurement setups and different optics. This talk will highlight the various needs of different applications, and show how a modular measurement setup can cover many of them in a single system.

2. Imaging System Requirements

Imaging colorimeters allow contextual evaluation, such as identifying defects or blemishes, however, in order to do so properly, they must fulfil some basic requirements, ranging from cooling of the CCD chip in order to achieve a good signal to noise ratio, all the way to various calibrations (e.g. CCD response, vignetting, color of the source). These necessary requirements, along with further beneficial features (such as electronically controlled components) will be discussed.

3. Demands and Recommendations for Specific Automotive Display Applications

The various display applications within the car set different demands for the measurement system intended to characterize them. For instance, head-up displays (HUD) require high resolution imaging systems, which frequently need to be used at much longer than typical working distances in order to focus on virtual images, in particular in AR HUDs. They also need to be evaluated for different criteria, such as ghosting and distortion, which are not commonly of interest in traditional devices. In contrast, augmented and virtual reality devices share some of the same evaluation criteria with HUDs, but again have different requirements for the optics, such as objectives with close to eye distances. This talk will detail the demands of, as well as the optics recommended for various applications, such as HUDs, AR/VR devices, digital mirrors/camera monitor systems, facial recognition and infotainment displays.

4. Advantageous Software Features

Finally, in addition to requirements placed on the measurement hardware, it can be very beneficial to control measurement and analysis via an automated software. This also opens up several possibilities that can make it easier to obtain results, or even improve their quality. In this context, this talk will detail the benefits of having a software that can automatically register the active display area within the obtained image so that evaluation can be limited to only that part of the image, which improves processing time, and for some measurements, such as uniformity, is absolutely mandatory. Additionally, the benefit of an automated Moiré removal calculation will be highlighted. Such a functionality allows removing aliasing effects from the measurement that would hinder evaluation, without requiring the measurement to be defocused. This preserves information such as pixel level defects that would otherwise be impossible to find as much of their contrast would be lost if the image was not in focus.

5. References

[1] "How to Use Imaging Colorimeters for Automated Visual Inspection of Displays" (https://www.radiantvisionsystems.com/learn/white-papers/how-use-imaging-colorimeters-automated-visual-inspection-displays)

[2] D. Kreysar, E. Eisenberg, "Optics Replicate Human Vision in AR/VR display testing", Laser Focus World, Vol. 55, No. 6, pp. 76-78, June 2019.

[3] "Automated Solutions for SAE Standard HUD Measurement" (https://www.radiantvisionsystems.com/learn/white-papers/automated-solutions-sae-standard-hud-measurement)

Ultra high resolution imaging light measurement device for subpixel metrology of micro-LEDs and OLEDs

T.Steinel, J.Blanke, M.Wolf
Instrument Systems GmbH, Germany

1. Introduction

More pixels! This is a major trend in the display industry. More (i.e. smaller) pixels with higher fill factors are urgently needed for near-eye applications such as VR goggles (using, e.g., microdisplays or µ-LED displays). With the displays so close to the observer's eye, screen-door effects and pixel non-uniformities are easily visible and disturbing for the consumer. Micro-LEDs or Micro-OLED displays feature pixel sizes < 10 µm and equally small pixel pitches. For both technologies each single subpixel is a light source itself. Luminance and color variations between the pixels are thus likely and strongly influence the visual quality of the display. This means quality control and subsequent calibration of the displays is crucial. Tests on subpixel level under the constraints of a production environment (esp. tact times), become necessary and are challenging.

2. Ultra High Resolution ILMD

Here we present measurements of OLED displays performed with an innovative ultra-high resolution ILMD ("LumiTop X150") especially designed for display subpixel metrology in production lines. The innovative concept of the device merges a 150 megapixel RGB CMOS camera with the high-end spectroradiometer CAS 140D[1]. This concept guarantees spectroradiometric test accuracy across the whole image of the camera [2]. The very high resolution of 150 megapixels thereby allows subpixel level analysis of complete displays in one single shot. Therefore, this device provides very fast and very accurate quality control and pixel calibration of OLEDs or Micro-LED displays in production lines and in-depth analysis in the laboratory. An integrated pixel shift mechanism allows to even increase the resolution to effectively 600 megapixels.

3. Experimental Results

3.1 Micro-OLED Display

A 1" Micro-OLED display with an RGBW pixel scheme by Fraunhofer FEP [3] was investigated. The display resolution is 1920x1200 pixels at 2300ppi, which translates into a 5.5µm sub-pixel pitch. Figure 1 shows zoomed pictures of full display image measurements using an internal 4x4 pixel shifter. All sub-pixels are switched on in a white image (left). Green sub-pixels are displayed at a different zoom level (right). Sub-pixels are fully resolved in both cases and allow for further quantitative analysis.

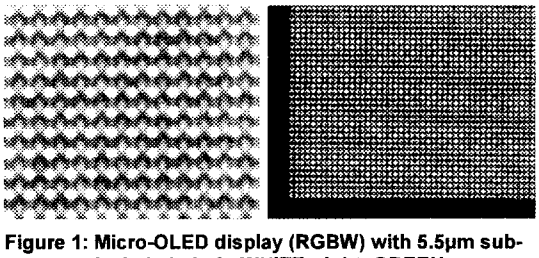

Figure 1: Micro-OLED display (RGBW) with 5.5µm sub-pixel pitch. Left: WHITE, right: GREEN

3.2 Defect Pixel Detection on OLED Display

Images of the full display of a 570ppi phone were taken with each pixel being fully resolved. Specific algorithms allow to derive pixel intensity (also: L, x, y etc.) maps for each display pixel as shown in Figure 2 for a part of the display. Another algorithm detects defect pixels according to user-defined criteria.

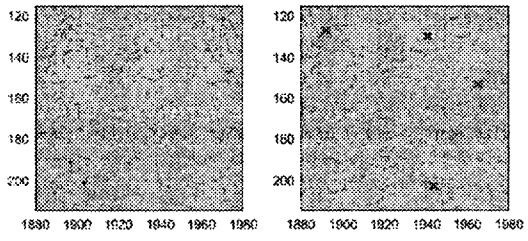

Figure 2: Intensity map and defect pixel detection

3.3 Conclusion

The ultra-high resolution data obtained by our device allows for the fast evaluation of luminance and color uniformity on a subpixel level. Using appropriate algorithms, luminance and color maps of the display are obtained to determine defect pixels and/or to calibrate OLED and µ-LED displays in-line.

4. Acknowledgements

We gratefully acknowledge the provision of the micro-display by Fraunhofer FEP.

5. References

[1] https://www.instrumentsystems.com//fileadmin/editors/downloads/Products/LumiTop2700_4000_e.pdf

[2] Spectrometer-Enhanced Imaging Colorimetry M. E. Becker, J. Neumeier, and M. Wolf, SID Symposium Digest of Technical Papers, **48** (2017)

[3] P. Wartenberg, M. Buljan, B. Richter, G. Haas, S. Brenner, M. Thieme, U. Vogel, P. Benitez, "High Frame-Rate 1" WUXGA OLED Microdisplay and Advanced Free-Form Optics for Ultra-Compact VR Headsets" SID symposium Digest of Technical Papers, Vol.**49**, pp. 514-517, 2018.

O-44

Color and spectral characteristics of white LEDs and their variation during aging

M. Masheda[2], A. Gurskii[1]
[1]Belarusian state university of informatics and radioelectronics, Belarus,
[2]BELLIS Testing and Certification of Home Appliances and Industrial Products, Belarus

White LEDs are widely used for LCD display backlighting, including low cost color displays. It is essential for these LEDs to provide stable characteristics through life cycle, especially chromaticity and color rendering. Therefore, care shall be taken for LED aging (including degradation of luminophor coating), because intense degradation will cause invalid color perception, especially when using bichromatic LEDs as backlight source.

Currently, there is not any unified approach for measurement of LEDs photometric and life characteristics. For example, there is international standard for performance requirements of LED modules [1], at the same time, Europe adopted standard [2] and Illuminating Engineering Society developed for United States a separate standard [3]. In this work, the change of colorimetric and spectral parameters during aging of some white LEDs were investigated.

This paper describes experimental results and analysis of LED chips characteristic drift within time and under stress.

For experiment, a set of Philips white LED chips was used and several accelerating factors applied, namely aging in normal work regime for 6000 h; normal work at 50 °C for 1000 h; switching cycles of power supply (70000 cycles of 10 seconds).

Within these tests, several parameters were measured, namely total luminous flux (TLF); chromaticity coordinates; correlated color temperature (CCT); color rendering index (CRI) and the luminescence spectra of LEDs under study. Measurements were made using Bentham Integrating sphere IS1800 with Bentham IDR300-PSL spectroradiometer. LEDs under study were supplied using stabilized power source Extech 6720 and controlled with power analyzer Yokogawa WT210.

All types of tests yield clear tendency of decreasing TLF and increasing CCT and CRI during aging. As an example, chromaticity coordinates drift after 6000 h is shown in Figure 1. It was shown that chromaticity coordinates have drift, but still within 6 step Mac-Adam ellipse. The time dependencies of these parameters have some peculiarities depending on accelerating factor used.

TLF was decreased for 15,7 % over 6000 h aging in normal regime, CCT increased for 1,5 % and CRI increased for 1,2 %. The highest impact on LED chip characteristic was shown under normal work at 50 °C for 1000 h: TLF decreased for 4,1 %, CCT increased for 0,8 % and CRI increased for 0,2 %. Therefore, it will investigated how combination of stress factors (ambient temperature and switching of power supply) will change color and spectral characteristics of white LEDs.

The analysis of luminescence spectra of investigated LEDs show the change of intensity

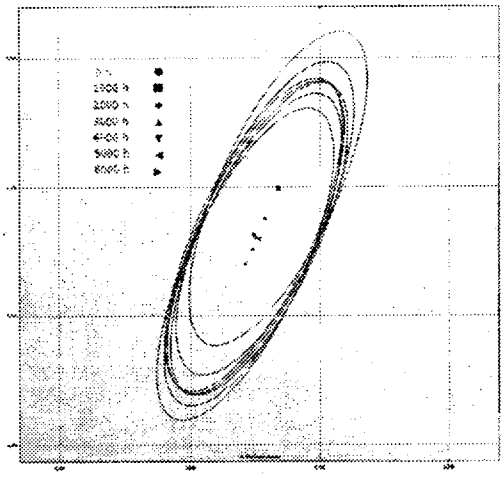

Figure 1: Chromaticity coordinates drift during aging

relation between blue and yellow bands of LED spectrum. Since the blue band originates from diode heterostructure, and the yellow band from the luminophor coating, one may conclude that investigated white LEDs are degraded with lumen output due to faster luminophor degradation that LED chip itself. Blue light component become prevail in overall emission, resulting in invalid color perception if these LEDs are used as backlight sources of color displays.

The relationships between color and spectral characteristics of investigated LEDs as well as pecularities of time dependencies of LED parameters under different aging conditions are discussed in detail.

References

[1] IEC 62717:2014+AMD1:2015+AMD2:2019 LED modules for general lighting - Performance requirements.

[2] EN 13032-4 Light and lighting - Light and lighting - Measurement and presentation of photometric data of lamps and luminaires - Part 4: LED lamps, modules and luminaires.

[3] LM-80-15 Measuring Luminous Flux and Color Maintenance of LED Packages, Arrays and Modules.

Human visual system for evaluation of holographic image quality

J.Nam, M.Park, S.Shin
Electronics and Telecommunications Research Institute (ETRI), KOREA

1. Introduction

In this paper, we present a unified framework for evaluating the visual quality of holographic images based on *Human Visual System (HVS)*. Analyzing what holographic image and its three-dimensional features really look like to the human eye is the purpose of this study. By exploiting schematic eye based on HVS, we focus on the tracing of lights that is emitted from holographically reconstructed image and propagates through intraocular structure of the human eye. In particular, we perform, based on wave theory, numerical simulation that aims at complex wave-field distribution of intraocular lights, to effectively deal with holographic properties.

2. Holographic Image Quality

Holographic display system optically reconstructs 3D image with a set of real volume pixels (voxels) distributed in space. The *wave-optics* properties of holography, such as diffraction and interference, are able to represent an optical image point where light from the holographic display converges to [1]. Holographic image provides the *depth* and *parallax* in space as 3D features, by modulating the intensity or phase of the planar wave emitted from a coherent light source using a spatial light modulator (SLM), according to a fringe pattern (hologram). These optical procedures can be well simulated by numerical reconstruction algorithms [1]. However, such a reconstructed image is just ideally computer-simulated result, not the image that human observer really see. At this point, we need to consider HVS model to figure out what holographic 3D image really looks like. Moreover, the emergence of near-eyed holographic display in [2] confirms the necessity of this study for eye safety as well as quality evaluation.

3. Human Visual System Model

3.1 Eye Model

Many different types of schematic eye have been reported in the literature over the past few decades. In this study, we use the eye models of different levels, from the simplest reduced eye with only one refraction surface, to more sophisticated model [3]. Finite schematic eye has aspherical surfaces for cornea and crystalline lens, the decentration and tilt of pupil, and wide-viewing field of curved retina, all of which aims to model and evaluate the optical effects of various ocular aberrations due to refraction anomalies, astigmatism, and high-order aberration.

3.2 Wave Optics Analysis

Optical analysis methods for almost all eye models have performed based on geometrical optics by ray tracing. However, in addition to simple refraction anomalies and astigmatism, many complex ocular wave aberrations need more effective analysis schemes. Also, considering the optical properties of holography, we make use of optical analysis for HVS based on wave theory. Particularly, for intraocular propagation we design a *cascaded* propagation scheme that consists of a series of *angular spectrums* for precise analysis and evaluation.

4. Experimental Results

Numerical simulation using schematic eyes with holographic image are performed and experimental results are analyzed for evaluating the retinal image quality of holographically reconstructed 3D object.

5. Acknowledgements

This work was supported by IITP grant funded by the Korea government (MSIP) (No.2017-0-00417, Openholo library technology development for digital holographic contents and simulation).

6. References

[1] S. A. Benton *et al*, "Holographic Imaging," 2008.
[2] A. Maimone *et al.*, "Holographic Near-Eye Displays for Virtual and Augmented Reality," ACM Trans. Graphics, Vol. 36, No. 4, 2017.
[3] D. A. Atchison and G. Smith, "Optics of the Human Eye," Butterworth-Heinemann, 2000.

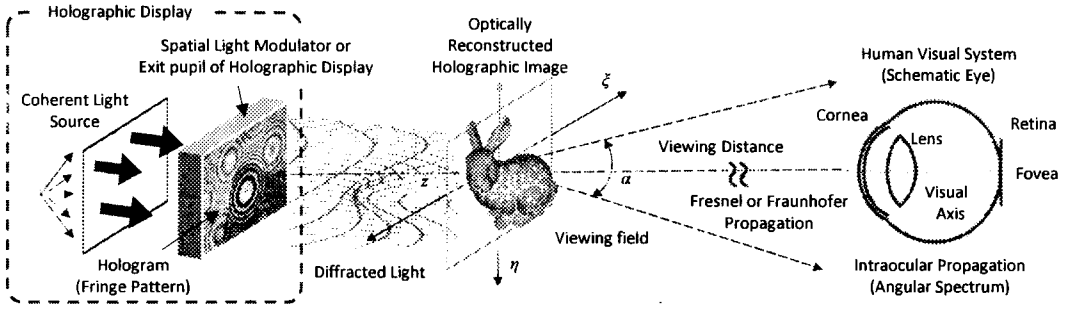

Figure 1: Human visual system model for quality evaluation of holographic image

Session 8. Thin film transistors

Chairman: Dr. Vladimir Shiripov

Memory-in-pixel circuit with low temperature poly-Si and oxide TFTs

Jongbin Kim[1], Hoon-Ju Chung[2], Seung-Woo Lee[1]
[1]Dept. of Information Display, Kyung Hee University, Seoul, South Korea
[2]School of Electronic Engineering, Kumoh National Institute of Technology, Gumi, Gyeongbuk, South Korea

1. Introduction

Memory-in-pixel (MIP) circuit has been studied for years to reduce power consumption of display products. Displays with MIP circuit can reduce power consumption because of their much lower frame rate than that of conventional displays using memory characteristics. Meanwhile, commercial display products have begun to introduce display circuits using low temperature poly-silicon and oxide (LTPO) TFTs to improve the performance and to use an advantage of extremely low leakage current of oxide TFTs. In this paper, we propose a new MIP circuit to achieve low power consumption as well as high reliability using LTPO TFTs.

2. Proposed Pixel Circuit

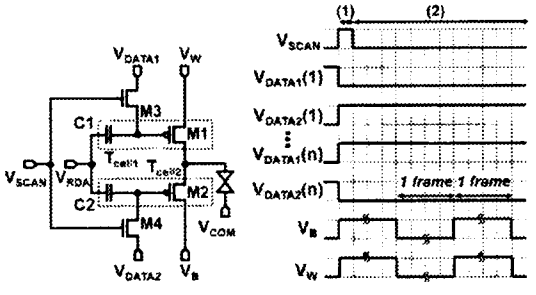

Figure 1: Proposed circuit and its driving signals

Figure 1 shows the proposed MIP circuit. M1 and M2 are driving TFTs using p-type LTPS TFTs, which drive the pixel with black (V_B) and white voltage (V_W), respectively. M3 and M4 are switching TFTs to program voltages to the gate nodes of M1 and M2, respectively. They are n-type oxide TFTs. T_{cell1} comprises M1 and C1. T_{cell2} is composed of M2 and C2. Each one acts like a memory cell. During (1), V_{DATA1} and V_{DATA2} can be applied to the gate nodes of the driving TFTs when V_{SCAN} turns on the oxide TFTs, M3 and M4. During (2), the oxide TFTs maintain the gate voltages of M1 and M2 until next program time.

3. Result and Discussion

Figure 2 shows transfer characteristics of a p-type low temperature poly-silicon (LTPS) TFT and an n-type oxide TFT. The proposed MIP circuit was verified with Spice simulation by using the fabricated LTPO TFTs as shown in Figure 3. At the 1st program, V_{DATA1} and V_{DATA2} were -10 V and 6 V, respectively. Thus, threshold voltage (V_{TH}) of T_{cell1} was shifted in the positive direction. On the contrary, V_{TH} of T_{cell2} was negatively shifted. We could observe that the pixel voltage reached V_W (5 V) at the 1st program and

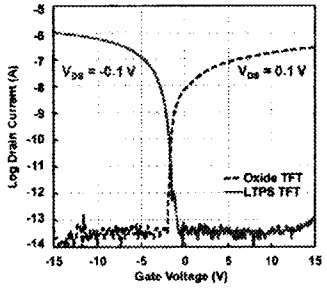

Figure 2: Transfer characteristics of LTPO TFTs

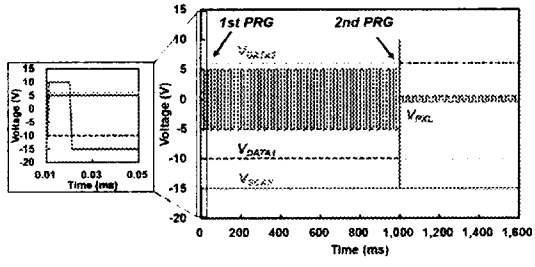

Figure 3: Simulation results of the MIP circuit

the polarity inversion was performed until the 2nd program. The oxide TFTs can maintain the programmed voltages for a long time due to extremely low leakage current. Thus, the frame rate can be quite reduced than that of conventional displays. As shown in Figure 3, we have successfully verified the operation at the low frame rate of 1 Hz. Furthermore, the driving TFTs use LTPS TFTs showing high reliability. They are stable under high voltages for a long period of time. Therefore, we expect that our proposed MIP circuits will contribute to high performance displays featuring low power consumption as well as good reliability. We will present the measurement results later.

4. Acknowledgements

This work was supported by the BK21 Plus Program through NRF under Grant 21A20130000018, and the Basic Science Research Program through NRF under Grant NRF-2017R1D1A3B03035455.

5. References

[1] S.-H. Lee, B.-C. Yu, H.-J. Chung, and S.-W. Lee, "Memory-In-Pixel Circuit for Low-Power LCDs Comprising Oxide TFTs," IEEE EDL, Vol. 11, No. 11, pp. 1551-1554, 2017.

[2] S. Kim, S.-H. Lee, H.-J. Chung, and S.-W. Lee, "Multi-Level Memory Comprising Only Amorphous Oxide TFTs," IEEE J-EDS, Vol. 7, pp. 575-580, 2019.

O-47

A stable FHD display device based on BCE IGZO TFTs

G.Wan[1], S.Ge[1], S.Li[2], C.Gong[2], X.Lin[1]

[1] School of Electronic and Computer Engineering, Peking University, Shenzhen, China 518055
[2] China Star Optoelectronics Semiconductor Display Technology Co., Ltd, Shenzhen, China 518132

Abstract

In this work, the impact of the deposition process of the SiOx passivation layer on the electrical properties of the BCE IGZO TFTs has been studied. The ΔVth of the TFTs are 2.52 and -1.67 V under PBTS (60°C, 30 V) and NBITS (60°C, -30 V, 4500 nit) after 1 hour, respectively. The stability of these TFTs is verified in 32in FHD display devices, which still could display the picture properly after the 500-hour aging test at 60°C and 90% humidity. A stable FHD display device based on BCE IGZO TFTs was achieved.

1. Introduction

In recent years, the need for thin-film transistors (TFTs) with high performance has been increasing on account of the demand for ultra high definition display, low energy consumption and interactive functionality [1, 2]. A variety of technical solutions have been tried to meet these requirements. Amorphous metal oxide semiconductors (AOSs), such as Indium-Gallium-Zinc-Oxide (IGZO), Indium-Hafnium-Zinc-Oxide (IHZO) and Indium-Gallium-Tin-Oxide (IGTO), have attained great attention due to their excellent performance in cost-effective manufacturing process, good uniformity and reasonable low off-current [3-5]. Among them, IGZO has become an industry-standard channel layer because of its desirable mobility, high Ion/Ioff ratio and good long-time stability.

Numerous studies were performed to improve the performance of the IGZO TFTs. The back-channel etch (BCE) IGZO TFTs were prepared to reduce parasitic capacitance and production costs [6-8]. The effect of hot carriers on the IGZO lattice under high field strength has been studied [9]. The source/drain/active layer was split to improve TFT robustness under mechanical bending strain [10]. However, there are few reports on the influence of the deposition process of passivation layers on performance of IGZO TFTs.

In this paper, the deposition process of the SiOx passivation layer was studied to improve the stability of BCE IGZO TFTs. The TFTs were used in 32in full high definition (FHD) display devices. The stability of these devices was verified by an aging test in a high temperature and high humidity environment.

References

[1] T. Hirao, M. Furuta, H. Furuta, T. Matsuda, T. Hiramatsu, H. Hokari, M. Yoshida, H. Ishii, M. Kakegawa, Novel top-gate zinc oxide thin-film transistors (ZnO TFTs) for AMLCDs, Journal of the Society for Information Display, 15 (2007) 17-22.

[2] P. Barquinha, A. Pimentel, A. Marques, L. Pereira, R. Martins, E. Fortunato, Influence of the semiconductor thickness on the electrical properties of transparent TFTs based on indium zinc oxide, Journal of non-crystalline solids, 352 (2006) 1749-1752.

[3] S.J. Park, D.-Y. Jeon, S.-E. Ahn, S. Jeon, L. Montès, G.-T. Kim, G. Ghibaudo, Static electrical characterization and low frequency noise of a-InHfZnO thin film transistors, Thin Solid Films, 548 (2013) 560-565.

[4] X. Ding, C. Qin, J. Song, J. Zhang, X. Jiang, Z. Zhang, The influence of hafnium doping on density of states in zinc oxide thin-film transistors deposited via atomic layer deposition, Nanoscale research letters, 12 (2017) 63.

[5] T. Kamiya, K. Nomura, H. Hosono, Origins of high mobility and low operation voltage of amorphous oxide TFTs: Electronic structure, electron transport, defects and doping, Journal of display Technology, 5 (2009) 468-483.

[6] S.-M. Ge, S. Li, S.-J. Chen, X.-Y. Kong, Y.-H. Meng, W. Shi, L.-Q. Shi, W. Wu, X. Liu, Q.-M. Gan, Y. Zhao, C. Zhang, C.-Y. Chiu, C.-Y. Lee, 42-1: Development of Cu BCE-Structure IGZO TFT for a High-ppi 31-in. 8K × 4K GOA LCD, SID Symposium Digest of Technical Papers, 48 (2017) 592-595.

[7] M. Nag, M. Rockele, S. Steudel, A. Chasin, K. Myny, A. Bhoolokam, M. Willegems, S. Smout, P. Vicca, M. Ameys, Novel back - channel - etch process flow based a - IGZO TFTs for circuit and display applications on PEN foil, Journal of the Society for Information Display, 21 (2013) 369-375.

[8] H. Ohara, T. Sasaki, K. Noda, S. Ito, M. Sasaki, Y. Endo, S. Yoshitomi, J. Sakata, T. Serikawa, S. Yamazaki, 4.0-inch active-matrix organic light-emitting diode display integrated with driver circuits using amorphous In–Ga–Zn-Oxide thin-film transistors with suppressed variation, Japanese Journal of Applied Physics, 49 (2010) 03CD02.

[9] H.-W. Park, J. Bae, H. Kang, D.H. Kim, P. Jung, H. Park, S. Lee, J.U. Bae, S.Y. Yoon, I. Kang, P-3: A Study on the Hot Carrier Effect in InGaZnO

Thin Film Transistors, SID Symposium Digest of Technical Papers, 50 (2019) 1222-1225.

[10] S. Lee, Y. Chen, H. Kim, J. Kim, J. Jang, P-14: Highly Robust Oxide TFT with Bulk Accumulation and Source/Drain/Active Layer Splitting, SID Symposium Digest of Technical Papers, 50 (2019) 1263-1266.

Table and Figure captions

Table 1 Electrical parameters of the BCE IGZO TFTs with a sputtering power of B KW, a SiH4 flow rate at M sccm and a flow ratio of N2O to SiH4 at W.

Fig. 1 Cross-sectional schematic of the BCE IGZO TFTs.

Fig. 2 Transfer characteristic curves of the BCE IGZO TFTs with a SiOx passivation layer deposited by different (a) sputtering power (b) SiH4 flow rate and (c) flow ratio of N2O to SiH4.

Fig. 3 Output characteristic curves of the BCE IGZO TFT with a SiOx passivation layer deposited with a sputtering power at B KW, a SiH4 flow at M sccm and a flow ratio of N2O to SiH4 at W.

Fig. 4 (a) PBTS @ Vg=+30 V, T=60°C and (b) NBITS @ Vg=-30 V, T=60°C, I=4500 nit of the BCE IGZO TFT with a SiOx passivation layer deposited with a sputtering power at B KW, a SiH4 flow at M sccm and a flow ratio of N2O to SiH4 at W.

Fig. 5 The circuit schematic of the gate-driver on array substrates.

Fig. 6 The photograph of the display device passed the 500-hour aging test at 60°C and 90% humidity.

Table 1

Parameter	Unit	Data
V_{th}	V	1.31
SS	V/decade	0.99
I_{on}/I_{off}		4.60×10^{7}
μ_{fe}	cm^2/Vs	7.54

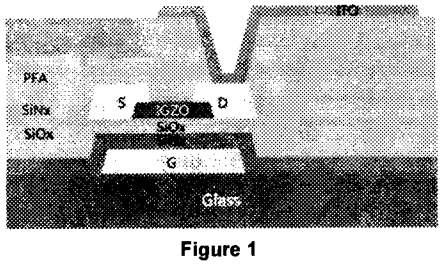

Figure 1

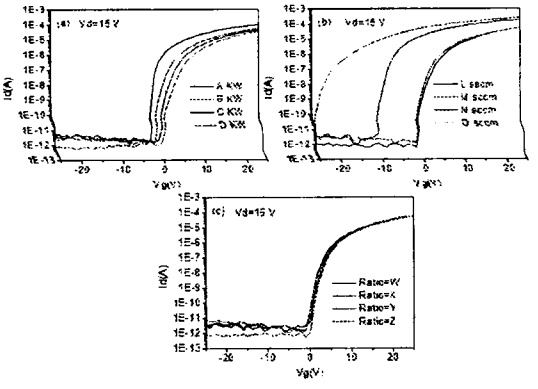

Figure 2

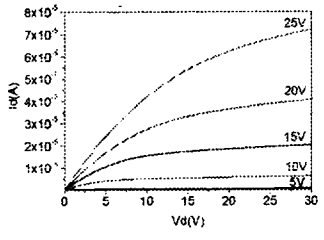

Figure 3

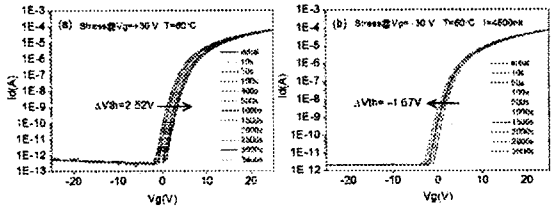

Figure 4

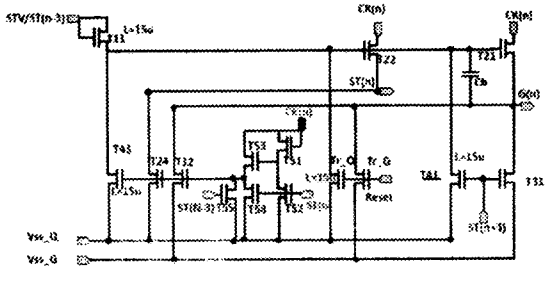

Figure 5

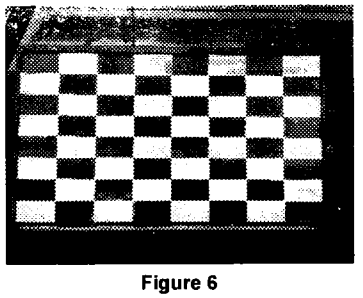

Figure 6

Robust performance and stability of In_2O_3 thin-film transistors with atomic-layer-deposited channels

Qian Ma, Letao Zhang, Shengdong Zhang
Shenzhen Graduate School,Peking University,Shenzhen, PR China

Abstract

Atomic-layer-deposition (ALD) In_2O_3 thin-film transistors (TFTs) were fabricated under a maximum processing temperature of 200 °C. In order to reduce the concentration of oxygen vacancies in the In_2O_3 channel, O_2 plasma treatment was carried out on the TFTs by plasma-enhanced chemical vapor deposited (PECVD). The In_2O_3 TFT treated at 200 °C for 240s exhibited good performance such as a field-effect mobility of 11cm²/V·s, a threshold voltage (V_{th}) of 0.9 V, a subthreshold swing of 0.38 V/dec, and an on/off current ratio of 10^7. In addition, the device exhibits a small negative threshold voltage shift (ΔV_{th}) during negative gate bias stress. However, it showed a more pronounced ΔV_{th} under positive bias stress with a characteristic turnaround behavior from a positive ΔV_{th} to a negative ΔV_{th}. The positive ΔV_{th} is attributed to the charge trapping effect, and the abnormal negative ΔV_{th} should due to the hydrogen incorporated into the film.

Results

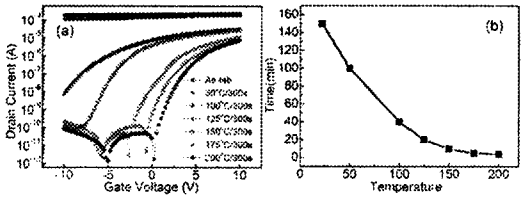

Figure 1a: Transfer characteristics of In_2O_3 TFTs annealed at 300°C for different time in air
Figure 1b: Dependence of the treatment time of the optimized In_2O_3 TFT on treatment

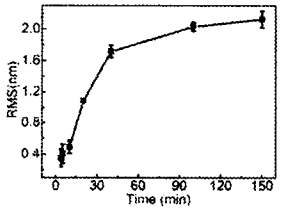

Figure 2: RMS roughness of In2O3 surface measured by AFM as a function of O2 plasma treatment time

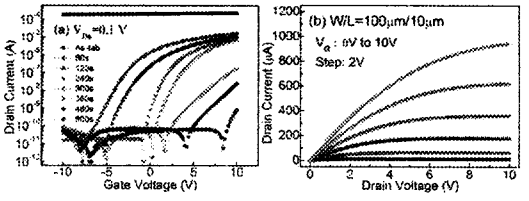

Figure 3a: Transfer characteristics of the In_2O_3 TFT treated by O_2 plasma at 200°C for different times

Figure 3b: Output characteristics of the In_2O_3 TFT treated at 200°C for 240s

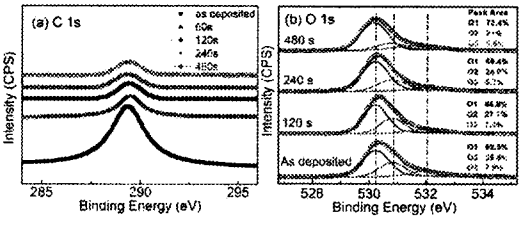

Figure 4: High resolution (a) C 1s and (b) O 1s XPS spectra of the In_2O_3 films treated by O_2 plasma for different time, respectively. To remove adventitious surface contaminants, all the samples were etched with in-situ Ar ion bombardment for 3 min before signal collection

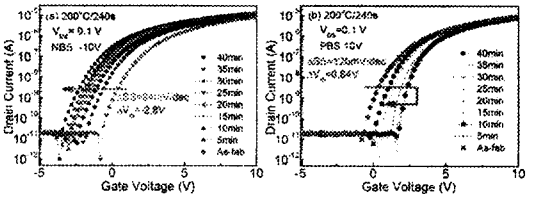

Figure 5: Typical stress time-dependent transfer curves of the In_2O_3 TFT treated by O_2 plasma at 200°C for 240s, under (a) negative gate bias stress (V_G= -10V) and (b) positive gate bias stress (V_G=10V), respectively

InGaZnO based TFT structures for active matrix addressing

B.Kazarkin[1], A. Stepanov[1], A. Smirnov[1], V. Shiripov[2], E. Khokhlov[2], A.Ksendzov[2]
[1]Belarusian State University of Informatics and RadioElectronics, Belarus
[2]IZOVAC Technologies, Belarus

1. Introduction

We present the results on a TFT active-matrix structure based on the InGaZnO (IGZO) semiconductor compound formed by the magnetron plasma-chemical deposition method. Their structural, morphological and electro physical properties were studied.

InGaZnO is an amorphous n-type transparent conductive oxide. The main advantage of IGZO over organic semiconductors is the stability of their properties and the significantly higher mobility of charge carriers.

Thus, the balance of the required properties inherent in IGZO makes it a promising material for optoelectronics, photonics and display technology.

2. Test structures

Arrays of TFT test structures differing in the thickness of an active IGZO layer, width and length of a gate were formed on a 60.0x48.0x1.1 mm glass substrate. First, a 100 nm buffer Si_3N_4 layer was deposited by plasma chemical deposition from the gas phase (PCO). Next, a 200 nm Mo gate was formed by magnetron deposition. The gate dielectric SiO_2 with a thickness of 100 nm was formed by PHO method. The 75 and 150 nm IGZO layers were magnetron sputtered. The 200 nm thick drain / source regions were formed by magnetron sputtering as well. Finally a 500 nm passivating SiO_2 layer was formed using PEC method. Contact windows were opened using "dry" reactive ion etching.

Figure 1 shows a view of a TFT test structure in a section.

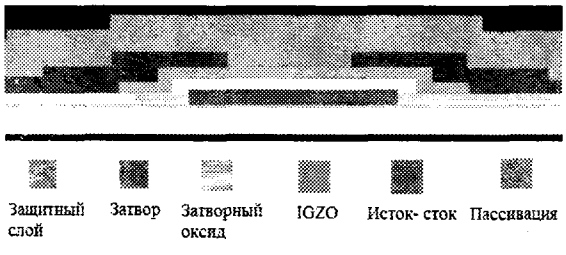

Figure 1: Schematic view of a test TFT structure

3 Experimental results

Figure 2 shows typical current-voltage characteristics of a test sample.

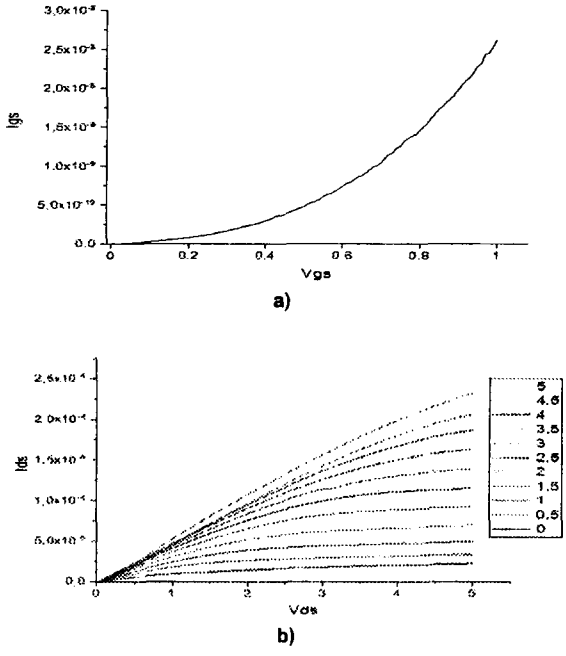

Figure 2: Current-voltage characteristics of TFT test structures with an IGZO layer: a - drain-gate characteristic; b - stock characteristics at different voltages on the gate

Mobility of IGZO material was determined by four probe method using Hall Ecopia Hall Effect Measurement Systems HMS-5000. Typical values of carrier mobility in the active layer of TFT test structures were in the range 4–5 cm^2 / V s.

Thus, obtained layers were characterized by high mobility of the charge carriers and transparency, which allow to use them for manufacturing of new generation of LCD and OLED displays.

4. Acknowledgements

This work was done as the part of task 4.03 GNPI "Convergence".

5. References

[1] Hosono H., et al. Transparent Amorphous Oxide Semiconductors for High Performance TПТ, SID'07, Dig., 2007. pp.1830.

[2] Nomura K., et al. Origins of threshold voltage shifts in room-temperature deposited and annealed a-In–Ga–Zn–O thin-film transistors. Applied Physics Letters, 95, 013502, 2009.

Session 9. OLED displays

Chairman: Prof. Vladimir Chigrinov

O-50

High efficient all-solution OLEDs and their transient electroluminescence

Suling Zhao, Dandan Song, Bo Qiao, Zheng Xu
Key Laboratory of Luminescence and Optical Information (Beijing Jiaotong University), Ministry of Education, Beijing 100044, China
Institute of Optoelectronics Technology, Beijing Jiaotong University, Beijing 100044, China

Solution-processed OLEDs have always been the hot topic in the research of OLEDs. The electron-hole evolution in all solution processed OLEDs involves the carrier transportation, the exciton recombination and dissociation.The dynamic of excitons plays a crucial role in governing the ultimate device performance. Therefore, the fundamental understanding of the evolution of excitons is essential to achieve high emission performance with simple structured OLEDs. A series of devices, polymer light-emitting diodes (PLEDs), thermally activated delayed fluorescent devices (TADF) and phosphorescent devices (PhOLEDs), were prepared by solution method. We systemically investigated the dynamics of excitons by using transient photoluminescence measurements combining with transient electroluminescence measurements on the prepared different OLEDs. The dynamic properties of excitons upon both photo-excitation and electro-excitation offer in-depth insight to the fundamental mechanisms driving its decay pathways, and by studying the electric-field dependent motion, we can explore their emission evolution and the underlying reason for the efficiency roll-off of OLEDs.

O-51

Large-scale patterned quantum dots as color conversion layer for organic light emitting diode by inkjet printing

Zhiping Hu[1,2], Yongwei Wu[1,2], Wenxiang Peng[2], Shijie Zhang[2], Dongze Li[2], Yuanyuan Li[2], Shibo Jiao[2], Shu-jhih Chen[2], Chia-Yu Lee[2], Hang Zhou[1]

[1] School of Electronic and Computer Engineering, Peking University Shenzhen Graduate School, China
[2] Shenzhen China Star Optoelectronics Semiconductor Display Technology Co., Ltd., China

Abstract

In this work, we fabricated 6.6-inch QD display panel by inkjet printing technology, being cooperated with active matrix organic light emitting diodes (AMOLEDs). Here 3-stack blue OLEDs (BOLEDs) with top-emission structure acted as backlight and red QD layer acted as converted materials, which exhibited high quantum efficiency, high luminance, high color purity and improved wide viewing angle of output emission. We believe that inkjet-printed QD display with AMOLEDs would be promising candidate for the next generation display and lighting in the near future.

1. Introduction

Recently, quantum dots (QDs) have shown great potential for next generation displays owing to their solution process, color tunability, narrow emission, and high luminescence efficiency[1-3] . Since the excellent physical and optical properties of QDs, QDs can not only act as self-emitting layers in electroluminescence device quantum dot light-emitting diodes (QLEDs), but also can be color converted layer for liquid crystal display (LCD) or LED due to the photoluminescence of QDs[3-5] . So far, most of the application of QDs in display device are QD-enhanced film (QDEF) equipped in backlight, offers an alternative approach to extend the color gamut and improve the optical efficiency of the LCDs [4-6]. For LCDs using conventional phosphors as down-converters, the color gamut is ~72% of the National Television Systems Committee (NTSC) standard. [12] In comparison with phosphors, QDs are semiconductor particles with nanoscale in size, whose bandwidth of spectrum is narrower resulting in better color purity. Eunjoo Jang have reported that they used green- and red-light-emitting QDs as color converter and successfully fabricated a 46 inch LCD panel using white QD-LED backlight as the first time, which showed more than 100% color reproducibility compared to the NTSC standard in the Commission Internationale de l'Eclairage (CIE) 1931 color space [4]. Chen proposed a new backlight system using a blue LED to pump green perovskite polymer film and red quantum dots, which achieved 95.8%Rec. 2020 in CIE 1931 color space with commercial high-efficiency color filters [7].

3. Results and discussion

In our work, we realized colorful display by cooperating OLED with QD, in which blue OLED act as excited light pumping green and red QDs, QDs act as color conversion materials. The structure diagram is showed in Figure 1a and b. In comparison with the structure of withe OLED with RGB CF, this method is easier and exhibit better optical performances. Moreover, the patterned QDs layer were prepared by solution ink-jet printing process (Figure 1c and d), which was low-cost and could use nanomaterials completely. We also used special design to reduce the cross-talk between sub-pixel. Based on this structure, we prepared a colorful display panel with size of 6.6 inch successfully.

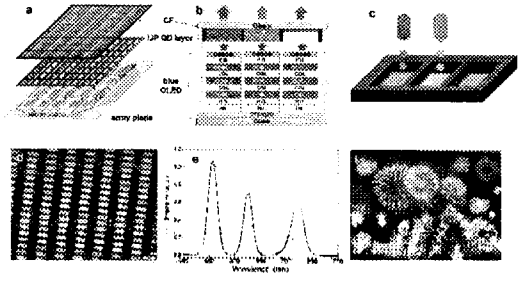

Figure 1a, 1b: The structure diagram of QD- OLED
Figure 1c: Inkjet printing process of QD in black bank
Figure 1d: Microscope image of colorful QDCF
Figure 1e: PL spectrumofwhitelightofQD-OLED
Figure1f:Photographof 6.6-inch QD-OLED display panel

Figure 1e and f show the photoluminance spectrum of white light the image of QD-OLED, respectively. These results express that the cooperation of QD and OLED can realize colorful display and QD can widen the color gamut and the view angle of OLED. This work would extend the application of QD in display technology in the future.

4. Acknowledgements

This work was supported by China Postdoctoral Science Foundation 2019M650331.

5. References

[1] S. Coe, W. K. Woo, M. Bawendi, V. Bulović, "Electroluminescence from single monolayers of nanocrystals in molecular organic devices" *Nature*, Vol. **420**, pp. 800, 2002.

[2] J. Lim, S. Jun, E. Jang, H. Baik, H. Kim, J. Cho, "Preparation of highly luminescent nanocrystals and their application to light-emitting diodes" *Advanced Materials*, Vol. **19**, pp. 1927-1932, 2007.

[3] M. A. Schreuder, K. Xiao, I. N. Ivanov, S. M. Weiss, S. J. Rosenthal, "White light-emitting diodes based on ultrasmall CdSe nanocrystal electroluminescence" Nano letters, Vol. **10**, pp. 573-576, 2010.

[4] E. Jang, S. Jun, H. Jang, J. Lim, B. Kim, Y. Kim, "White-light-emitting diodes with quantum dot color converters for display backlights" *Advanced materials*, Vol. **22**, pp. 3076-3080, 2010.

[5] Z. Y. Luo, D. M. Xu, S. T. Wu, "Emerging quantum-dots-enhanced LCDs" J. Display Technol., Vol. **10**, no. 7, pp. 526-539, 2014.

[6] R. Zhu, Z. Luo, H. Chen, Y. Dong, and S.-T. Wu, "Realizing Rec. 2020 color gamut with quantum dot displays" Opt. Exp., Vol. 23, pp. 23680-23693, 2015.

[7] H. W. Chen, R. D. Zhu, J. He, W. Duan, W. Hu, Y. Q. Lu, S. T. Wu, "Going beyond the limit of an LCD's color gamut" *Light: Science & Applications*, Vol. **6**, pp. 17043, 2017.

O-52

High-performance near-infrared organic light-emitting materials and devices

Juan Qiao
Key Lab of Organic Optoelectronics and Molecular Engineering of Ministry of Education, Department of Chemistry, Tsinghua University, Beijing 100084, P. R. China
Center for Flexible Electronics Technology, Tsinghua University, Beijing 100084, P. R. China

1. Introduction

As the extension of visible light, near-infrared (NIR) emitting materials have aroused growing interests due to their great potential for applications spanning from military night-vision displays and information-secured devices to civilian medical diagnostics and phototherapy [1]. However, the development of highly efficient, stable, and low-cost organic NIR-emitting materials is still a formidable challenge according to the energy-gap law. We have developed two classes of novel organic NIR-emitting materials including Ir(III) complexes with extensively π-conjugated ligands and purely organic NIR dyes with high quantum yields.

2. NIR-emitting Ir(III) complexes

Since 2009, we have designed and synthesized series of NIR-emitting Ir(III) complexes based on highly conjugated benzo[g]quinoline, benzo[g]quinoxaline and benzo[g]phthalazine ligands and the NIR-OLEDs based on those Ir(III) complexes demonstrated maximum EQEs up to 4.5% and small efficiency roll-off in the range of 700–900 nm [2,3]. Most notably, the use of benzo[g]-phthalazine derivatives as cyclometalated ligands can allow facile synthesis of homoleptic facial NIR-emitting Ir(III) complexes under mild conditions, thus enabling the successful fabrication of high-performance NIR-OLEDs bearing a peak emission at 760 nm, maximum EQE up to 4.5% with small efficiency roll-off, and high NIR radiance of 4.5 mW/cm^2, which are amongst the most efficient values for NIR-OLEDs over 750 nm. Importantly, the content percentages of the noble metal in our Ir complexes (~10% Ir) are markedly lowered by about two-thirds than that of typical green-emitting tris(2-phenylpyridine) iridium (~30% Ir)[3].

3. NIR-emitting purely organic materials

Given that the price and rarity of noble metals would limit their mass production and future application, approaches to utilize the 75% triplet excitons of organic fluorescent materials are highly desirable to enable highly efficient NIR-OLEDs with cost advantage. Recently, we realized high-efficiency and low efficiency roll-off fluorescent NIR-OLEDs through efficient triplet fusion of a bipolar host with a special naphthoselenadiazole (NSeD) emitter [4]. By using a thermally activated delayed fluorescence (TADF) material as the sensitizing host and a novel NIR dye TPANSeD, we further improved the device performances with EQE of up to 2.65% at 730 nm [5]. More recently, we proposed and confirmed a novel design strategy for realizing highly efficient TADF materials via J-aggregates with strong intermolecular charge transfer [6]. These OLEDs exhibit EQE of 15.8% for red emission and 14.1% for NIR emission, which are amongst the best results for NIR-OLEDs based on TADF materials. These findings would open a new avenue for the development of high-efficiency organic emissive materials and devices based on molecular aggregates.

4. Acknowledgements

We thank the financial support from the National Key R&D Program of China (2016YFB0401003), and National Natural Science Foundation of China (51773109, 51473086).

5 References and Citations

[1] G. Qian, Z. Y. Wang," Near-Infrared Organic Compounds and Emerging Applications" Chem.–Asian. J, 2010, **5**, 1006.

[2] J. Qiao, L. Duan, L. Tang, L. He, L. D. Wang, Y. Qiu, "High-efficiency orange to near-infrared emissions from bis-cyclometalated iridium complexes with phenyl-benzoquinoline isomers as ligands" J. Mater. Chem. 2009, **19**, 6573.

[3] J. Xue, L. Xin, J. Hou, L. Duan, R. Wang, Y. Wei, J. Qiao, "Homoleptic facial Ir(III) complexes via facile synthesis for high-efficiency and low-roll-off near-infrared organic light-emitting diodes over 750 nm" Chem. Mater. 2017, **29**: 4775.

[4] J. Xue, C. Li, L. Xin, L. Duan, J. Qiao, "High-efficiency and low efficiency roll-off near-infrared fluorescent OLEDs through triplet fusion" Chem. Sci., 2016, **7**(4), 2888.

[5] J. Xue, Q. Liang, Y. Zhang, R. Zhang, L. Duan, J. Qiao, "High-Efficiency near-infrared fluorescent organic light-emitting diodes with small efficiency roll-off: a combined design from emitters to device" Adv. Funct. Mater., 2017, **27**(45), 1703283.

[6] J. Xue, Q. Liang, R. Wang, J. Hou, W. Li, Q. Peng, Z. Shuai, J. Qiao, "Highly efficient thermally activated delayed fluorescence via J-aggregates with strong intermolecular charge-transfer", Adv. Mater. 2019, 1808242.

O-53

Al_2O_3 electron suppressing layer for brighter infra-red quantum dot-based light-emitting diode

Mikita Marus[1], Yong Xia[2], Kang Wang[2], Huaying Zhong[1], Depeng Li[1], Jianbing Zhang[2], Xiao Wei Sun[1]

[1]Guangdong University Key Lab for Advanced Quantum Dot Displays and Lighting, Shenzhen Key Laboratory for Advanced Quantum Dot Displays and Lighting, Department of Electrical & Electronic Engineering, Southern University of Science and Technology, Shenzhen 518055, China

[2]School of Optical and Electronic Information, Huazhong University of Science and Technology, Wuhan 430074, China

1. Introduction

Colloidal quantum dots (QDs) are promising materials for making near infrared light emitting diodes (NIR QLEDs) thanks to the tunable wavelength of emitted light, high quantum efficiency and full integration with solution processing technique. However, the charge imbalance resulting in leakage currents and exciton quenching, strongly limit the performance of NIR QLEDs [1]. Here, we employ 1.5 nm thin Al_2O_3 electron suppressing layer, which allowed to reach an impressive 7.42 W/sr/m^2 brightness at 1.3 μm wavelength, which is among the highest values reported for NIR QLED in the literature [2].

2. Discussion

Figure 1 shows the radiance-voltage characteristics of fabricated NIR QLED devices. The inset shows the device configuration. ZnO nanoparticle (NP) electron transporting layer was spin-coated over ITO cathode, followed by atomic layer depositing (ALD) of Al_2O_3 electron suppressing layer, spin-coating of PbS-halide emitting layer, thermal evaporating of 4,4'-Bis

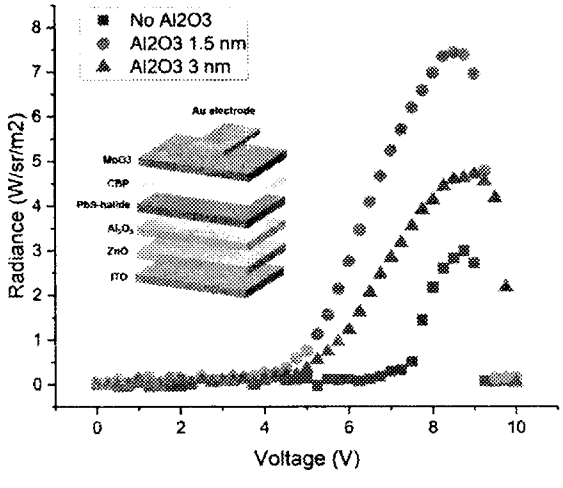

Figure 1: Radiance-voltage characteristics of NIR QLED devices. The inset shows the device configuration.

(9-carbazolyl)-1,1'-biphenyl (CBP) hole transporting layer (HTL), MoO_3 hole injecting layer (HIL) and Au anode. The device with reference inverse configuration reached maximum of 2.99 W/sr/m^2 radiance, while devices with 1.5 and 3.0 nm Al_2O_3 electron suppressing layers reached 7.42 and 4.69 W/sr/m2 maximum radiance. Moreover, the device turn on voltage (set at 0.2 W/sr/m2, limitation of measurement setup) was improved to 3.75 V compared to 6.5 V of the reference configuration.

3. Summary

Al_2O_3 deposited by ALD had been employed to strongly improve the maximum radiance of the NIR QLED through effective electron suppressing to achieve the charge balance in the emitting layer. The maximum radiance achieved by the device with inverse configuration was 7.42 W/sr/m^2 at 1.3 μm wavelength, which is among the highest reported in literature.

4. Acknowledgements

This material is based upon work supported by National Key Research and Development Program of China, which is administrated by the Ministry of Science and Technology of China (No. 2016YFB0401702), National Natural Science Foundation of China (No. 61674074 and 61405089), Development and Reform Commission of Shenzhen Project (No. [2017]1395), Shenzhen Peacock Team Project (No. KQTD2016030111203005), Shenzhen Key Laboratory for Advanced quantum dot Displays and Lighting (No.ZDSYS201707281632549), Guangdong University Key Laboratory for Advanced Quantum Dot Displays and Lighting (No. 2017KSYS007), Distinguished Young Scholar of National Natural Science Foundation of Guangdong (No. 2017B030306010). We thank the start-up fund from Southern University of Science and Technology, Shenzhen, China.

5. References

[1] J. Pan, C. Wei, L. Wang, J. Zhuang, Q. Huang, W. Su, Z. Cui, A. Nathan, W. Lei, and J. Chen, "Boosting the efficiency of inverted quantum dot light-emitting diodes by balancing charge densities and suppressing exciton quenching through band alignment," Nanoscale 10 (2), 2018.

[2] L. Sun, J. J. Choi, D. Stachnik, A. C. Bartnik, B.-R. Hyun, G. G. Malliaras, T. Hanrath, and F. W. Wise, "Bright infrared quantum-dot light-emitting diodes through inter-dot spacing control," Nat. Nanotechnol. 7 (6), 2012.

Solution-processed quasi-two-dimensional perovskite light-emitting diodes using organic small molecular electron transporting layer

Yongwei Wu[1,2], Zhiping Hu[1,2], Miao Duan[2], Pei Jiang[2], Dongze Li[2], Chia-Yu Lee[2], Shengdong Zhang[1]
[1]Peking University, Shenzhen Graduate School, Shenzhen 515800, China
[2]Shenzhen China Star Optoelectronics Technology Co., Ltd, Shenzhen 518132, China

Abstract
In this paper, all-solution-processed LEDs using quasi-two-dimensional perovskites with organic small molecular electron transporting materials (ETMs) are successfully fabricated. The obtained LEDs exhibit high efficiency and narrow emission (FWHM = 22 nm), in which the one with TPBi as ETMs record a peak current efficiency and maximum brightness of 11.9 cd/A and 3 × 10^3 cd/m^2 respectively.

1. Introduction

Beneficial to their intriguing optoelectronic properties, metal halide perovskites (MHPs) are recently emerging as a promising candidate for a series of applications such as solar cells, light-emitting diodes (LEDs), photodetectors, and lasers. In particular, due to their high photoluminescence quantum yield (PLQY), facile color tunability, solution processability, and sharp emission, perovskite light-emitting diodes (PeLEDs) have attracted significant attention[1-2].

Generally, for a high efficiency, the devices of light-emitting diodes based on MHPs adopt multilayer thin-film structure, in which electron or hole transporting materials were subtly inserted between MHPs and cathode or anode. 2,2',2''-(1,3,5-benzinetriyl)-*tris*(1-phenyl-1-*H*-benzimiazole) (TPBi) and 2,9-dimethyl-4,7-biphenyl-1,10-phenanthroline (BCP), which are two commonly used commercial ETMs since of their high electron mobility (10^{-4} to 10^{-3} cm^2 V^{-1} s^{-1}), deep LUMO (~ –2.7, –3.0 eV) and HOMO (–6.2 eV, –6.4 eV) energy levels, are widely used in optoelectronic devices such as OLEDs and QLEDs. However, TPBi and BCP are generally thermally evaporated during device fabrication, which not only requires expensive equipment, but also inevitably accompanies serious material waste and quite complicated fabrication process. Therefore, a substantial increase in cost is generated. On the contrary, with almost no waste of materials, low equipment dependence and simple fabrication process, solution processing is commonly recognized as an efficient solution for industrial production. Therefore, since the hole transporting layer and perovskite layer are usually fabricated via solution process, development of solution process as well for ETMs, is of great significance for the practical applications of PeLEDs and other perovskite optoelectronic devices.

2. Results and Disscussions

In this work, $PEA_2(FAPbBr_3)_2PbBr_4$ is applied as the emitting layer for quasi-2D perovskite LEDs, where PEA and FA are phenylethylammonium ($C_6H_5C_2H_4NH_3^+$) and formamidinium ($HC(NH_2)_2^+$), respectively. As can be seen from Fig. 1 (a), the solution-processed film shows consecutive and full coverage, along with brilliant green emission. Then, PeLED devices were fabricated with a device structure shown in Fig. 1 (b), in which the HTMs, ETMs and perovskite layers are all formed via solution process. Both two devices taking TPBi and BCP as ETMs gave strong luminescence with narrow bandwidth, in which the one with TPBi as ETMs record a peak current efficiency and maximum brightness of 11.9 cd/A and 3 × 10^3 cd/m^2 respectively [Fig. 1 (c) and (d)].

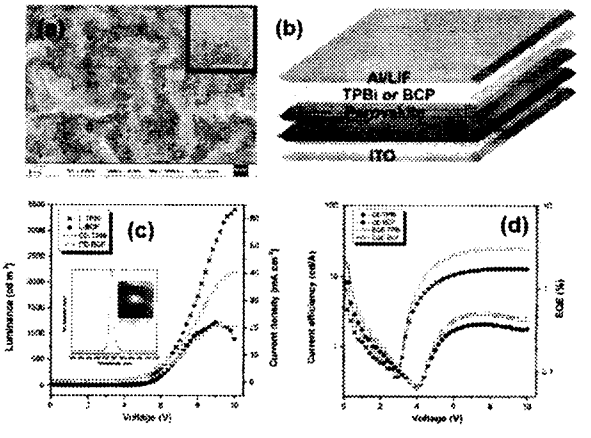

Figure 1a: Top-view SEM image of the perovskite layer, Inset: Photoluminescence photo of the perovskite film

Figure 1b: Device structure of the PeLEDs

Figure 1c: *J-V-L* characteristics

Figure 1d: *CE-V-EQE* curves of the PeLEDs. Inset: EL spectra of PeLEDs and electroluminescence photo of PeLED

3. References

[1] Z. K. Tan, R. H. Friend et al., "Bright light-emitting diodes based on organometal halide perovskite" Nature Nanotechnology, vol. **9**. pp. 687-693, 2014.

[2] X. Yang, J. You et al., "Efficient green light-emitting diodes based on quasi-two-dimensional composition and phase engineered perovskite with surface passivation" Nature Communications, vol. **9**. pp. 570-578, 2018.

Poster Session

P-1 "Elastic properties of anisotropic elastomers"
M.T.Hovakimyan, M.L.Sargsyan, M.R.Hakobyan, R.S.Hakobyan (Yerevan State University, Armenia)

P-2 "Phototunable selective reflection of cholectric liquid crystal"
D.Chepeleva, A.Yakovleva, A.Murauski, I.Kukhta, A.Muravsky (Institute of Chemistry of New Materials, NASB, Belarus)

***P-3* "*Self*-organization of octa-phenyl-2, 3-naphthalocyaninato zinc floating layers"**
A.Kazak (Nanomaterials Research Institute, Ivanovo State University; Shubnikov Institute of Crystallography of Federal Scientific Research Center "Crystallography and Photonics" of RAS; Moscow Region State University, Russia)
M.Marchenkova (Shubnikov Institute of Crystallography of Federal Scientific Research Center "Crystallography and Photonics" of RAS; National Research Center "Kurchatov Institute", Russia)
A.Smirnova, N.Usol'tseva (Nanomaterials Research Institute, Ivanovo State University, Russia)
T.Dubinina (Lomonosov Moscow State University; Institiute of Physiologically Active Compounds, RAS, Russia)
A.Rogachev (National Research Center "Kurchatov Institute"; National Research University Higher School of Economics, Russia)
D.Chausov (Moscow Region State University, Russia)

P-4 "Compensation of technological variation of chromaticity coordinates of LCD displays"
D.V.Chistobaev, S.V.Gashkov, A.F.Rybakov (OJSC "Display" Design office, Belarus)

P-5 "Bistable effect with low threshold voltage on the base of viscous chiral dopants"
V.Lapanik, S.Timofeev (Institute of Applied Physics Problems, Belarus)
V.Bezborodov (Belarusian State Technological University, Belarus)

P-6 "Transmittance of polymer dispersed liquid crystal film doped with single- and multiwall carbon nanotubes"
V.A.Loiko, A.V.Konkolovich, A.A.Miskevich (Institute of Physics of NASB, Belarus)
D.Maximean, O.Danila (University Politehnica of Bucharest, Romania)
V.Circu (University of Bucharest, Romania)
A.Barar (University Politehnica of Bucharest, Romania)

P-7 "Green OLED microdisplays based on TADF materials"
O.Grachev, E.Kudryashova, N.Usov (JSC "Central Research Institute "Cyclone", Russia)

P-8 "Femtosecond laser scribing of sapphire at λ = 1040 and 520 nm"
B.A.Shulenkova, A.V.Danilchik, A.G.Vainilovich, E.V.Lutsenko (B.I. Stepanov Institute of Physics of NASB, Belarus)
A.N.Pyatlitski, Ja.A.Solovjov, M.V.Kirosirova (JSC «INTEGRAL» - «INTEGRAL» holding managing company, Belarus)

P-9 "Thermal management of LED spotlights based on aluminum PCB with anodic alumina"
V.Pham, L.Tran (Institute for Tropical Technology, VAST, Vietnam)
T.Dinh, N.Lushpa, K.Chernyakova, I.Vrublevsky (Belarusian State University of Informatics and Radioelectronics, Belarus)

P-10 "In-line sputtering coater for hydrophobic antireflection coating for sensor displays"
A.Myslivets, P,Rosel, E.Khokhlov (IZOVAC Technologies Ltd., Belarus)

P-11 "Large scale substrate processing by ion beam assisted magnetron sputter deposition"
M.Palmera, R.Diaz, V.Shekelevskiy, D.Kotov (Belarusian State University of Informatics and Radioelectronics, Belarus)

P-12 "Synthesis and optical properties of sol-gel derived $BaTiO_3/SiO_2$ multilayer coatings"
P.A.Kholov, D.A.Parafinyuk, Y.D.Karnilava, N.V.Gaponenko (Belarusian State University of Informatics and Radioelectronics, Belarus)
T.F.Raichenok (Stepanov Institute of Physics of NASB, Belarus)

P-13 "Analysis of control methods for LED backlighting of display devices"
D.V.Chistobaev, S.V.Gashkov, A.F.Rybakov (OJSC "Display" Design office, Belarus)

P-14 "Modular approach to the study of displays for electric vehicles"
I.Shpak (Belarusian State University of Informatics and Radioelectronics, Belarus)

P-15 "Formation of SiSn nanostructures and their morphology, structure and optical properties"
V.Timofeev, I.Skvortsov, V.Mashanov, A.Nikiforov, T.Gavrilova, D.Gulyaev, A.Gutakovskii (Institute of Semiconductor Physics SB RAS, Russia)
I.Chetyrin (Institute of Catalysis SB RAS, Russia)

P-16 "Synthesis and properties study of the X-ray phosphors Gd_2O_2S:Tb"
P.Ustabaev, V.Bakhmetyev (Saint-Petersburg State Institute of Technology, Russia)

P-17 "Reliability-enhanced test pattern scheme for holographic display measurement"
J.Nam, J.Kim (Electronics and Telecommunications Research Institute, Korea)

P-18 "Ammonia molecular beam epitaxy of AlGaN heterostructures on Al_2O_3 (0001) substrates"
M.V.Rzheutski, A.G.Vainilovich, I.E.Svitsiankou, E.V.Lutsenko (Institute of Physics of NAS of Belarus, Belarus)
Ja.A.Solovjov, A.N.Pyatlitski, D.V.Zhyhulin (JSC «INTEGRAL» - «INTEGRAL» holding managing company, Belarus)

P-19 "Integrated channel optical waveguides based on sintered and oxidized porous silicon"
H.Bandarenka, A.Dolgiy, S.Redko, V.Bondarenko (Belarusian State University of Informatics and Radioelectronics, Belarus)

P-20 "Concentration instability due to delocalization of electrons in the upper Hubbard band in antimony doped silicon"
S.Prischepa (Belarusian State University of Informatics and Radioelectronics, Belarus; National Research Nuclear University "MEPhI", Russia)
A.Danilyuk, A.Trafimenko (Belarusian State University of Informatics and Radioelectronics, Belarus)
A.Fedotov, I.Svito (Belarusian State University, Belarus)
C.Attanasio (Universita degli Studi di Salerno, Italy)

P-21 "Hybrid large-area transparent electrode film using AgNW and PEDOT:PSS"
Jik Kyo Jung (Korea)

P-22 "Effective shell thickness controlled InP/ZnSe/ZnSeS/ZnS quantum dots"
Jonghyuk Lee (Korea)

P-23 "Analysis of image flicker in polymer-sustained-alignment liquid crystal display"
Munan Lin (Peking University Shenzhen Graduate School, China; Shenzhen China Star Optoelectronics Technology Co., Ltd., China; Shenzhen China Star Optoelectronics Semiconductor Display Technology Co., Ltd., China)
Xia Zhan (Centre of Excellence for Advanced Materials, China)
Zhiying Shen, Fan Deng, Xiaohui Yao, Jack Kim (Shenzhen China Star Optoelectronics Semiconductor Display Technology Co., Ltd., China)
Bin Zhao, Xin Zhang (Shenzhen China Star Optoelectronics Technology Co., Ltd., China; Shenzhen China Star Optoelectronics Semiconductor Display Technology Co., Ltd., China)
Hang Zhou (Peking University Shenzhen Graduate School, China)

P-24 "Novel pixel design for transmittance and picture quality improvement"
Y.F.Zhang, Y.H.Zhang (Peking University Shenzhen Graduate School; Shenzhen China Star Optoelectronics Technology Co., Ltd., China)
W.Cao, Q.Zhang, Y.L.Lin (Shenzhen China Star Optoelectronics Technology Co., Ltd., China)
M.Zhang (Peking University Shenzhen Graduate School, China)

P-25 "Modeling of multilayer ultrathin-film photonic crystals for selective filters and optical resonators"
A.Hnitsko, L.Khoroshko, A.Baglov (Belarusian State University of Informatics and Radioelectronics, Belarus)

P-26 "Electrical properties of sputter-deposited bilayered ITO thin films"
S.Zhuk (Nanyang Technological University; Institute of Materials Research and Engineering, A'STAR, Singapore)
G.K.Dalapati (Institute of Materials Research and Engineering, A'STAR, Singapore; SRM University AP-Amaravati, India)

P-27 "Viewing angle enhancement method for holographic displays with spatial division multiplexing method using DOE"
Hyun-Eui Kim, Taeone Kim, Jinwoong Kim (Electronics and Telecommunications Research Institute, Korea)

P-28 "Short-channel TFT technology for high-performance and cost-effective liquid crystal displays"
Yani Chen (Peking University Shenzhen Graduate School, China, Shenzhen China Star Optoelectronics Technology Co., Ltd, China)
Shengdong Zhang (Peking University Shenzhen Graduate School, China)
Jiaqing Zhuang, Hongyuan Xu, Zhixiong Jiang, Tian Ou, Daobin Hu, Jinjie Wang (Shenzhen China Star Optoelectronics Technology Co., Ltd, China)

P-29 "Multi-view binary hologram compression for table-top holographic display"
Kwan-Jung Oh, Seunghyup Shin, Yongjun Lim, Seoungbae Cho, Jaehan Kim, Jinwoong Kim (Electronics and Telecommunications Research Institute, Korea)

P-30 "Managing the surface properties of materials of display technology by means of treatment in atmospheric discharge plasma"
Y.V.Zaporozhchenko, D.A.Kotov, A.V.Aksyuchits, A.N.Osipov, S.V.Paceev (Belarusian State University of Informatics and Radioelectronics, Belarus)

P-31 "Low-temperature magnetron deposition of Zn and ZnO films"
A.Abduev, A.Akhmedov, A.Asvarov (Institute of Physics, RAS, Russia)
V.Belyaev (Moscow Region State University, Russia; RUDN University, Russia)

P-32 "3D imaging with high resolution ultrasonic tomography"
V.Petrov (Saratov State University, Russia)

P-33 "Physico-chemical properties of core-shell quantum dots and composites with liquid crystals"
D.Chausov, A.Kurilov (Moscow Region State University, Russia)
V.Osipova, D.Sagdeev, Yu.Galyametdinov (Kazan National Research Technological University, Russia)

P-34 "ITO Transparent Conductive Electrode for MicroLED Applications"
Vadzim Haronin, Waqar Azeem, Jiang Fulong, Xioawei Sun, Zhaojun Liu (Southern University of Science and Technology, Shenzhen, Guangdong, China)
Alexander Smirnov(Belarusian State University of Informatics and Radioelectronics, Belarus)